Enclosure 2

IMPELL CORPORATION

SONGS-1

PRESENTATION TO THE NRC AND
NRC CONSULTANTS

ON

LOAD GENERATION FOR REACTOR BUILDING
AND TURBINE BUILDING

JULY 1, 1985

IMPELL CORPORATION

AGENDA

JULY 1, 1985

IMPELL PRESENTATION:

OVERVIEW OF LOAD GENERATION

1. GENERATION OF ARTIFICIAL TIME HISTORIES FOR FREE FIELD MOTION.

2. GENERATION OF REACTOR BUILDING FLOOR RESPONSE SPECTRA

3. GENERATION OF TURBINE BUILDING FLOOR RESPONSE SPECTRA

JULY 2, 1985

CALCULATION FILE REVIEW BY NRC

IMPELL CORPORATION

GENERATION OF ARTIFICIAL TIME HISTORIES

- SEE CALCULATION RB-Ø1 FOR DETAILS

CRITERIA

- THREE TIME HISTORIES DEVELOPED FOR REEVALUATION OF SONGS-1 REACTOR BUILDING AND TURBINE BUILDING

- DESIGN FREE FIELD SPECTRA ARE MODIFIED HOUSNER, Ø.67G HORIZONTAL, Ø.44G VERTICAL

- DURATION IS 2Ø SECONDS

- DIRECTION 1 = NORTH-SOUTH
  DIRECTION 2 = EAST-WEST
  DIRECTION 3 = VERTICAL

IMPELL CORPORATION

METHODOLOGY

- USE 3 COMPONENTS OF REAL EARTHQUAKE (EL CENTRO 1940) AS THE 3 SEEDS.

- USE FREQUENCY RAISING AND SUPPRESSING TECHNIQUE ON THE FOURIER TRANSFORMS OF THE TIME HISTORIES UNTIL A MATCH IS OBTAINED WITH THE FREE FIELD HOUSNER DESIGN SPECTRA.

- USE 75 FREQUENCY POINTS FOR RESPONSE SPECTRA GENERATION, 0.20 TO 33 HZ.

- COMPARE ENVELOP RESPONSE SPECTRA OF FINAL TIME HISTORIES WITH MODIFIED HOUSNER DESIGN SPECTRA. MEET S.R.P. 3.7.2 CRITERIA THAT NO MORE THAN 5 POINTS FALL BELOW DESIGN SPECTRA BY NO MORE THAN 10 PERCENT.

- CALCULATE CORRELATION COEFFICIENTS BETWEEN TIME HISTORIES TO ENSURE STATISTICAL INDEPENDENCE.

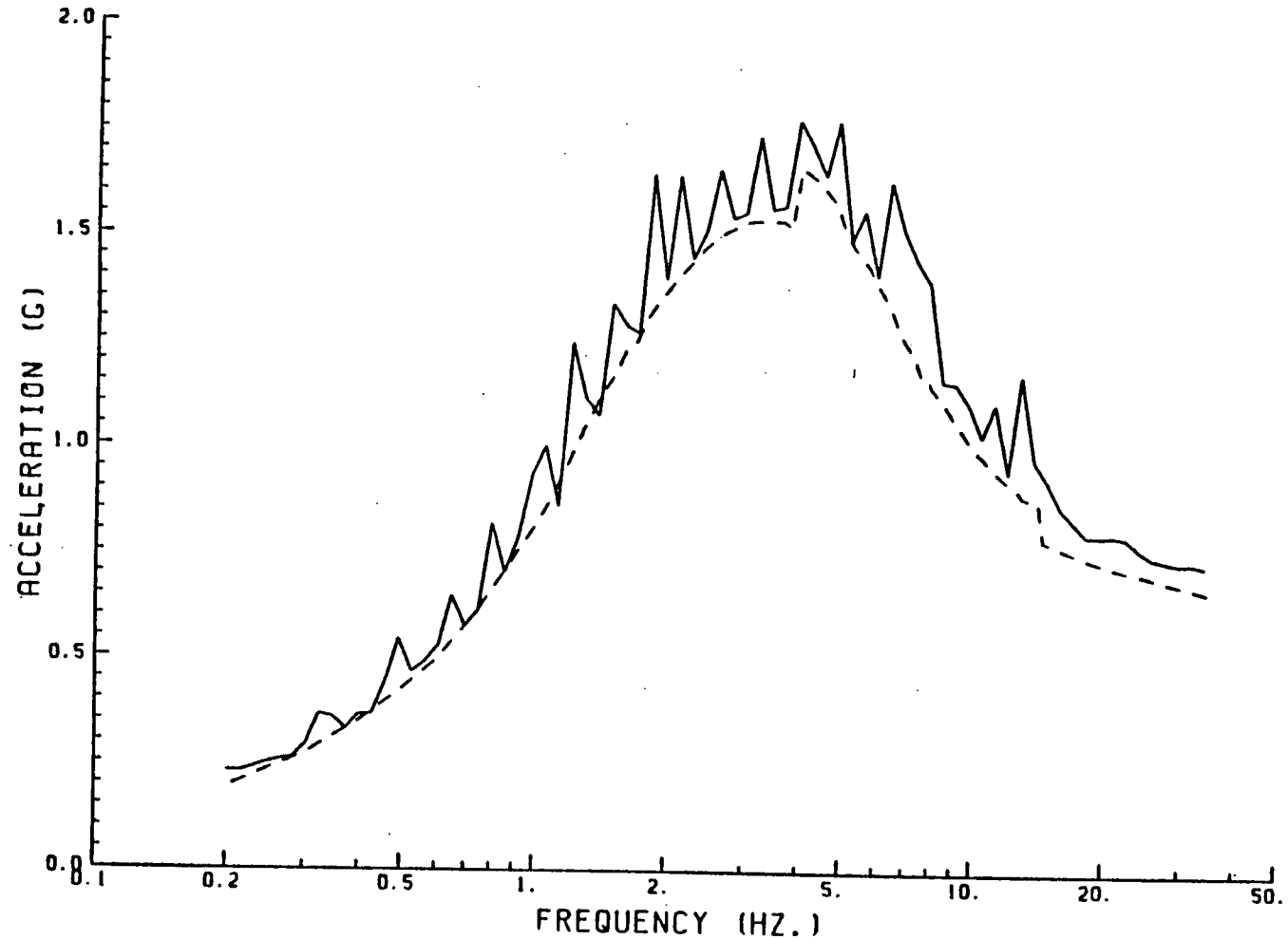

SCE-SONGS1
DESIGN (DASHED LINE) VERSUS ENVELOPE (SOLID LINE) SPECTRA
NORTH-SOUTH DIRECTION
2 PERCENT DAMPING

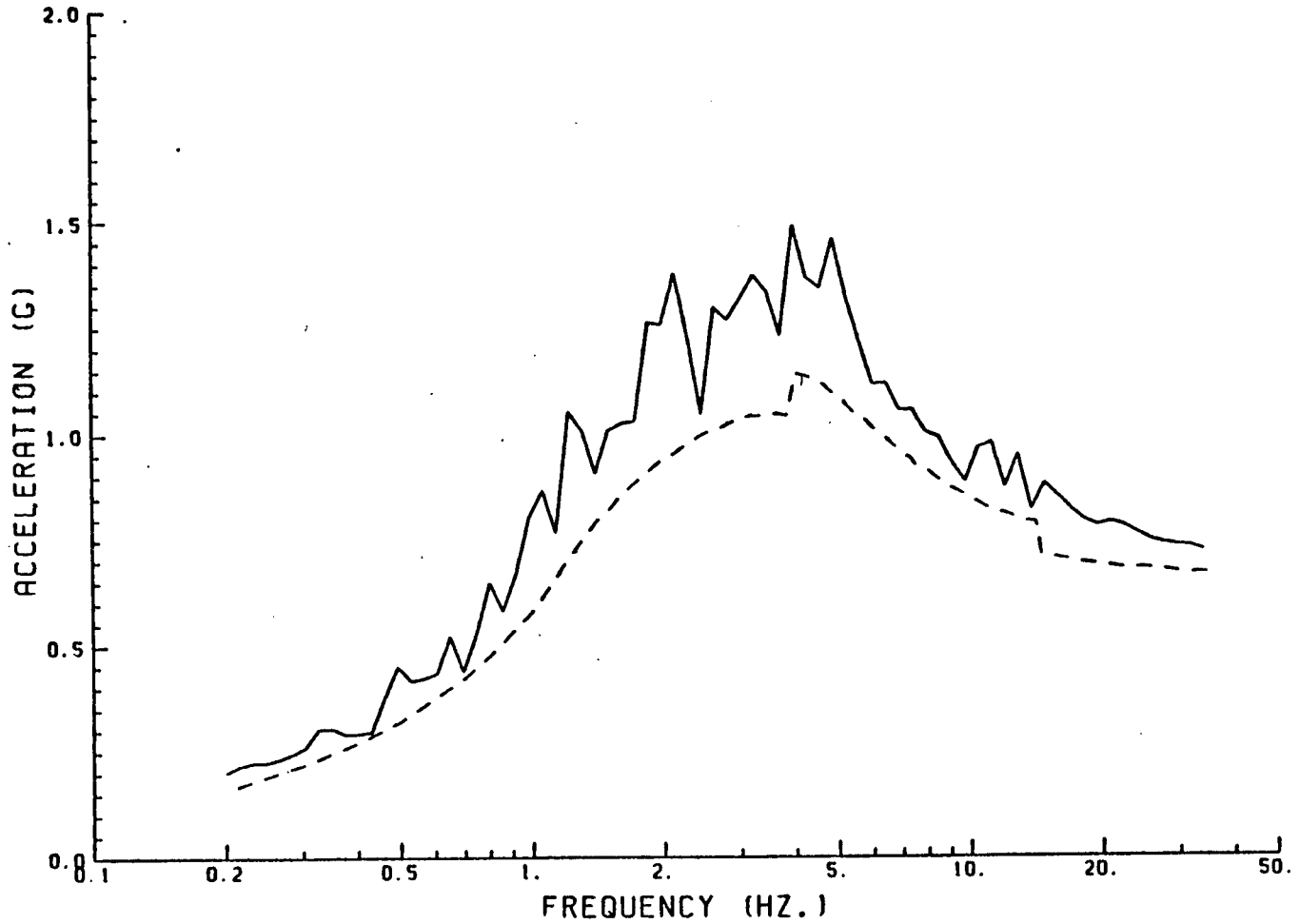

SCE-SONGS1
DESIGN (DASHED LINE) VERSUS ENVELOPE (SOLID LINE) SPECTRA
NORTH-SOUTH DIRECTION
4 PERCENT DAMPING

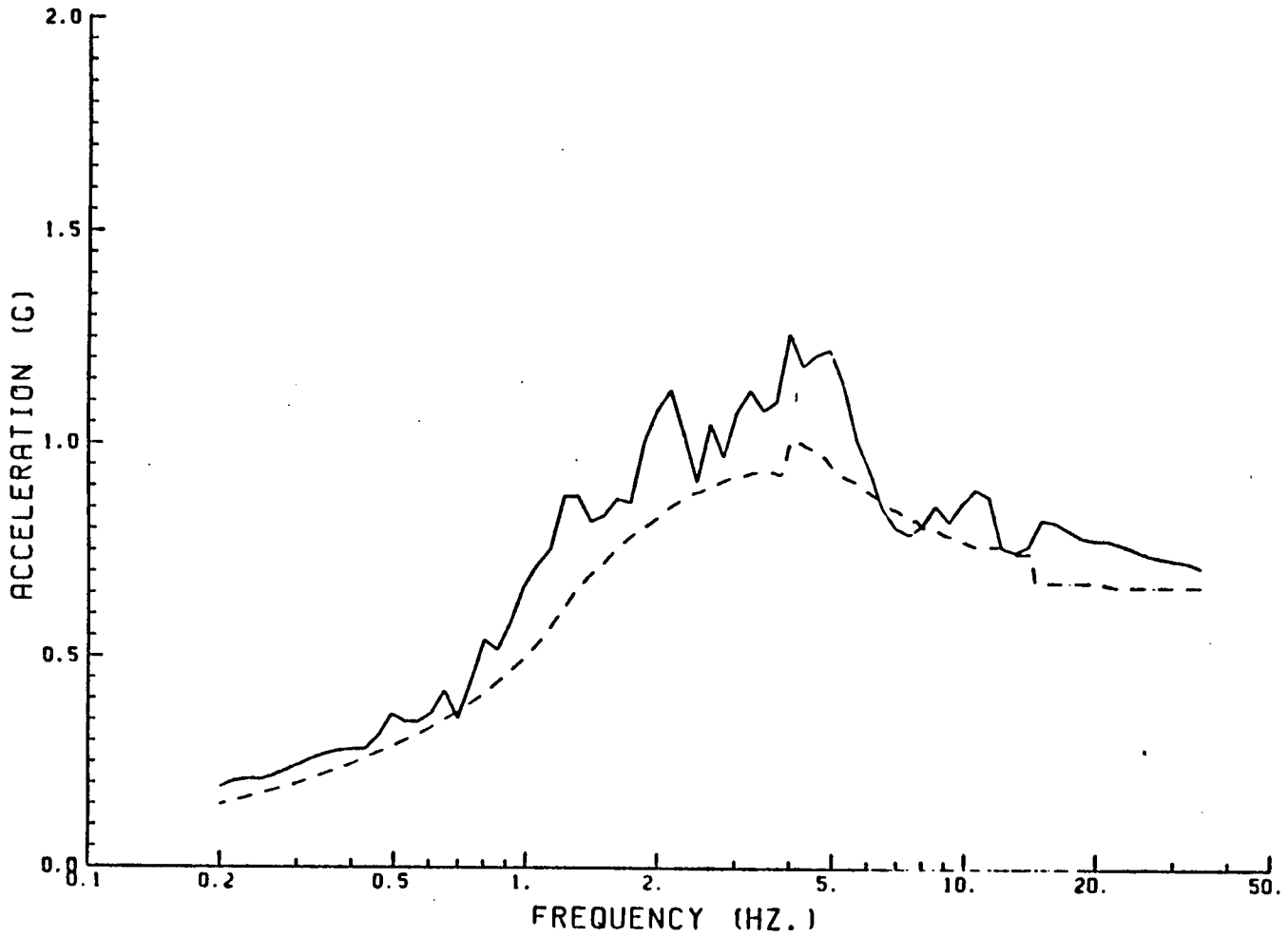

SCE-SONGS1
DESIGN (DASHED LINE) VERSUS ENVELOPE (SOLID LINE) SPECTRA
NORTH-SOUTH DIRECTION
7 PERCENT DAMPING

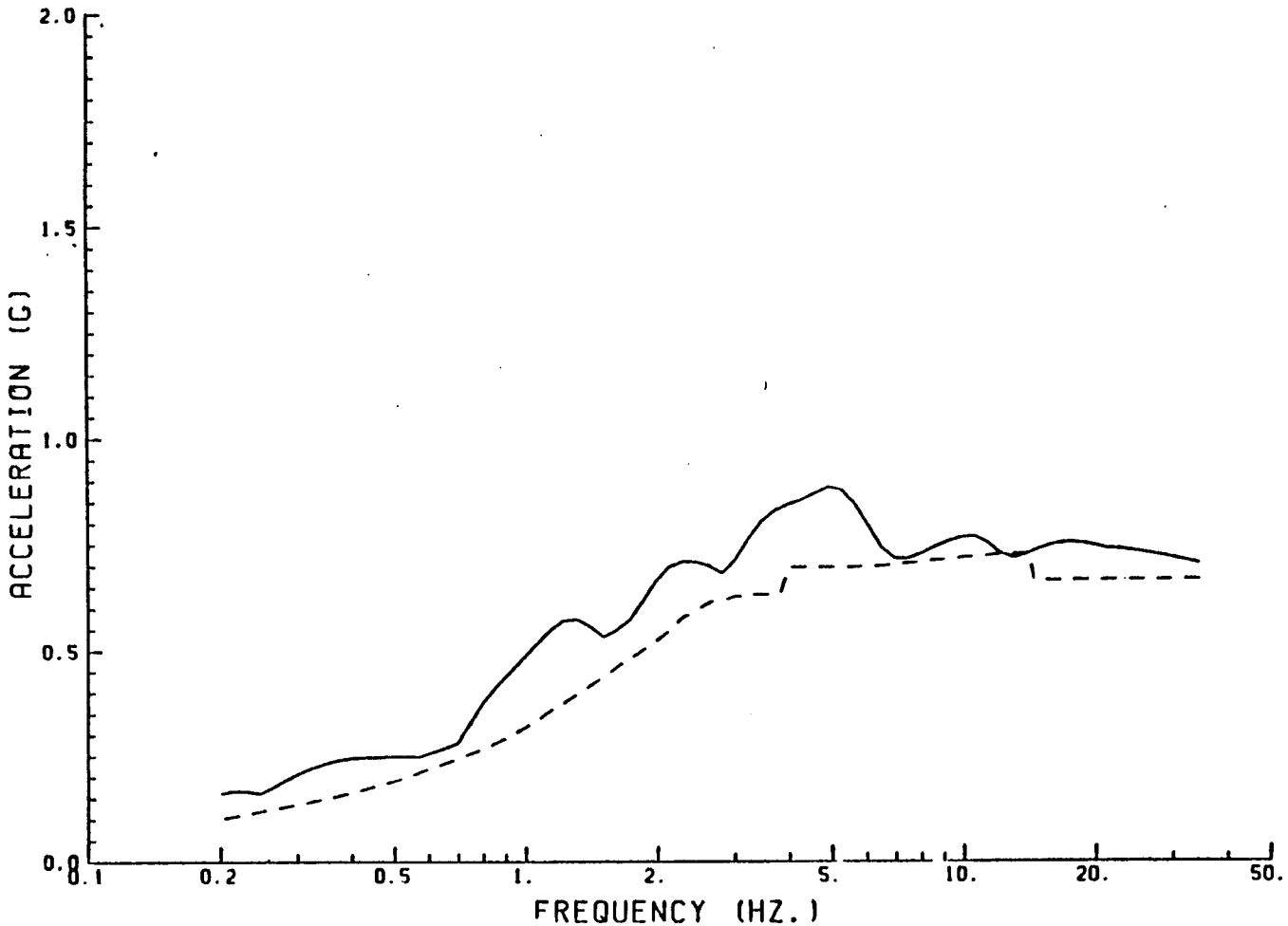

SCE-SONGS1
DESIGN (DASHED LINE) VERSUS ENVELOPE (SOLID LINE) SPECTRA
NORTH-SOUTH DIRECTION
20 PERCENT DAMPING

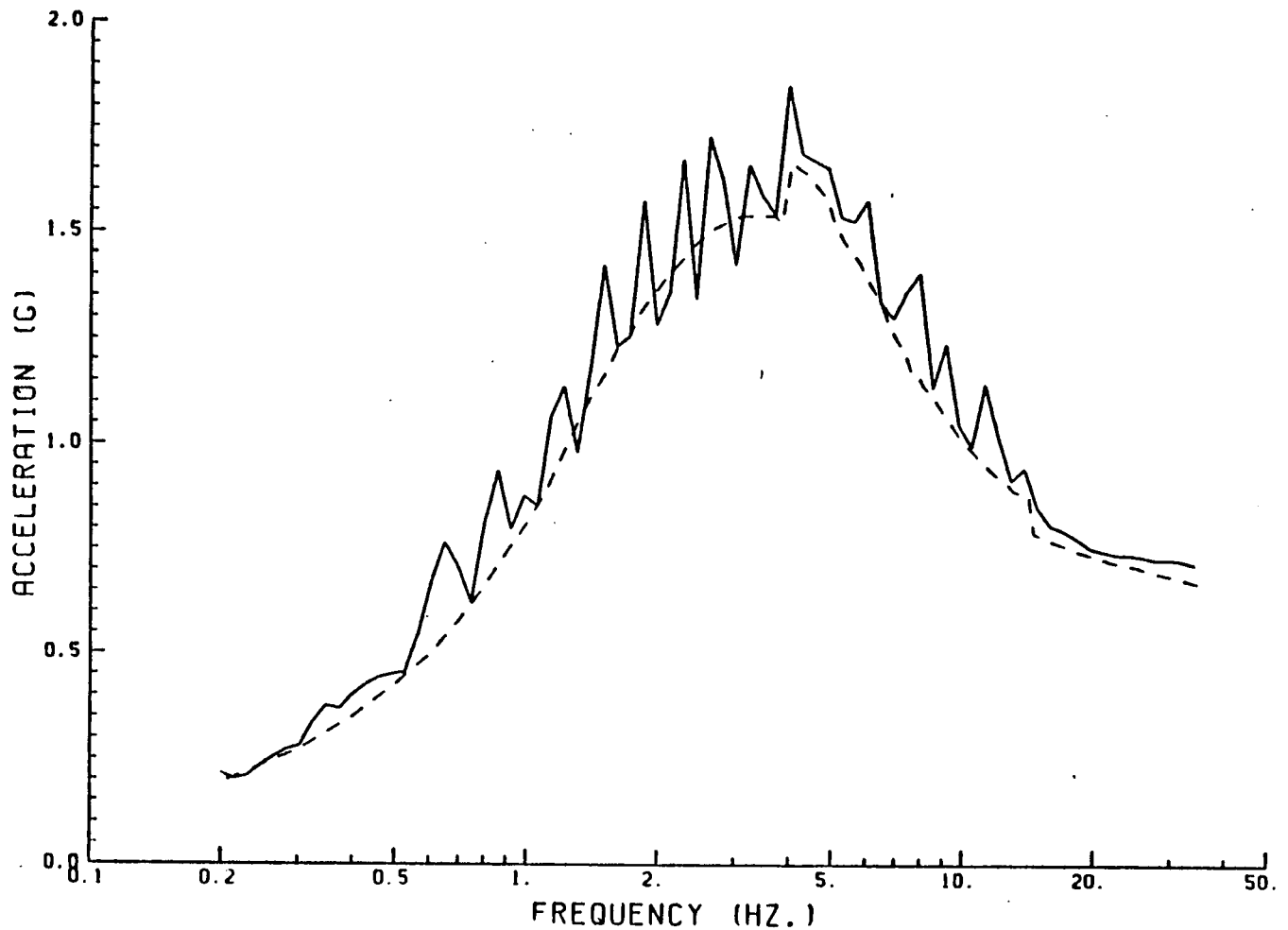

SCE-SONCS1
DESIGN (DASHED LINE) VERSUS ENVELOPE (SOLID LINE) SPECTRA
EAST-WEST DIRECTION
2 PERCENT DAMPING

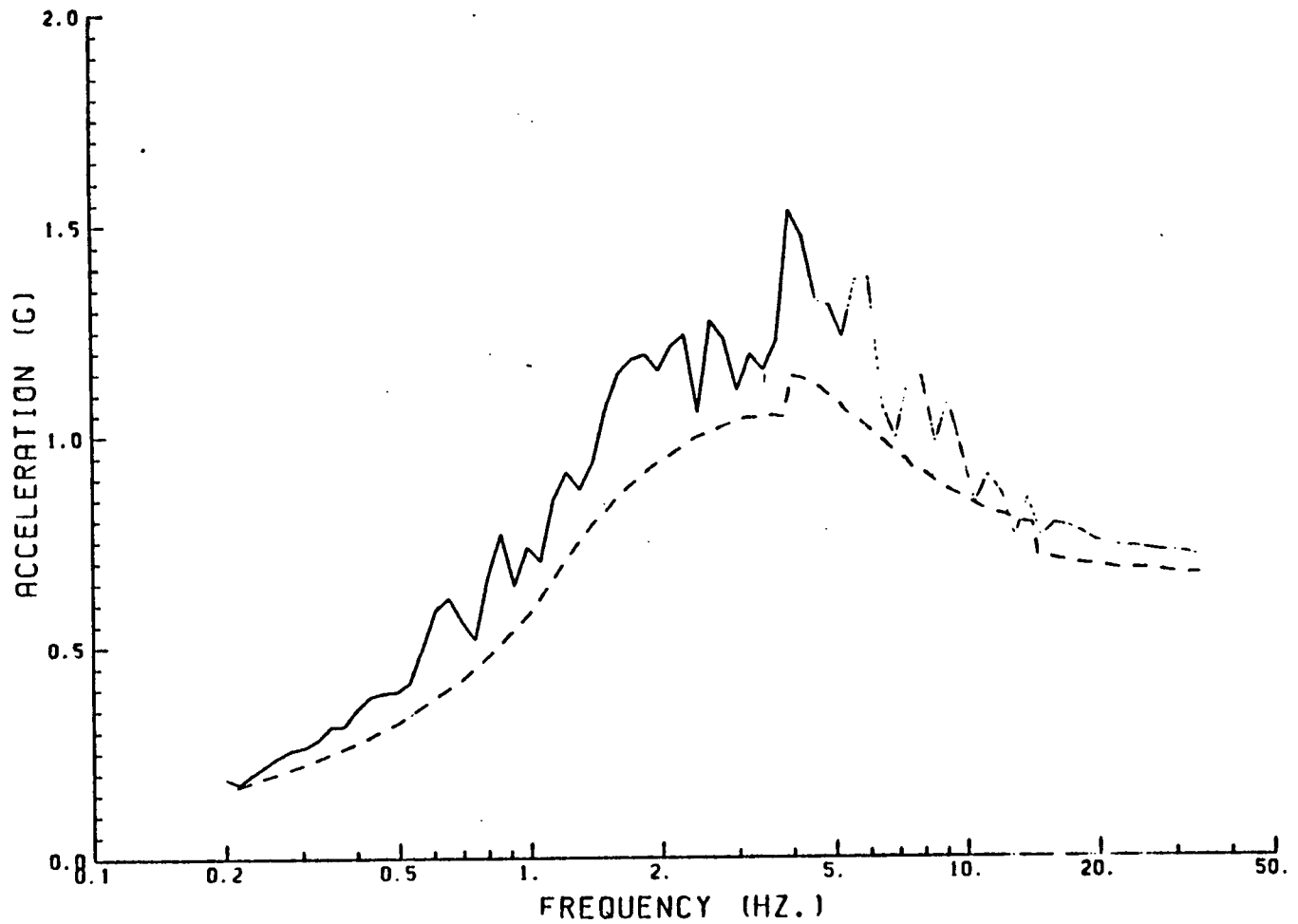

SCE-SONGS1
DESIGN (DASHED LINE) VERSUS ENVELOPE (SOLID LINE) SPECTRA
EAST-WEST DIRECTION
4 PERCENT DAMPING

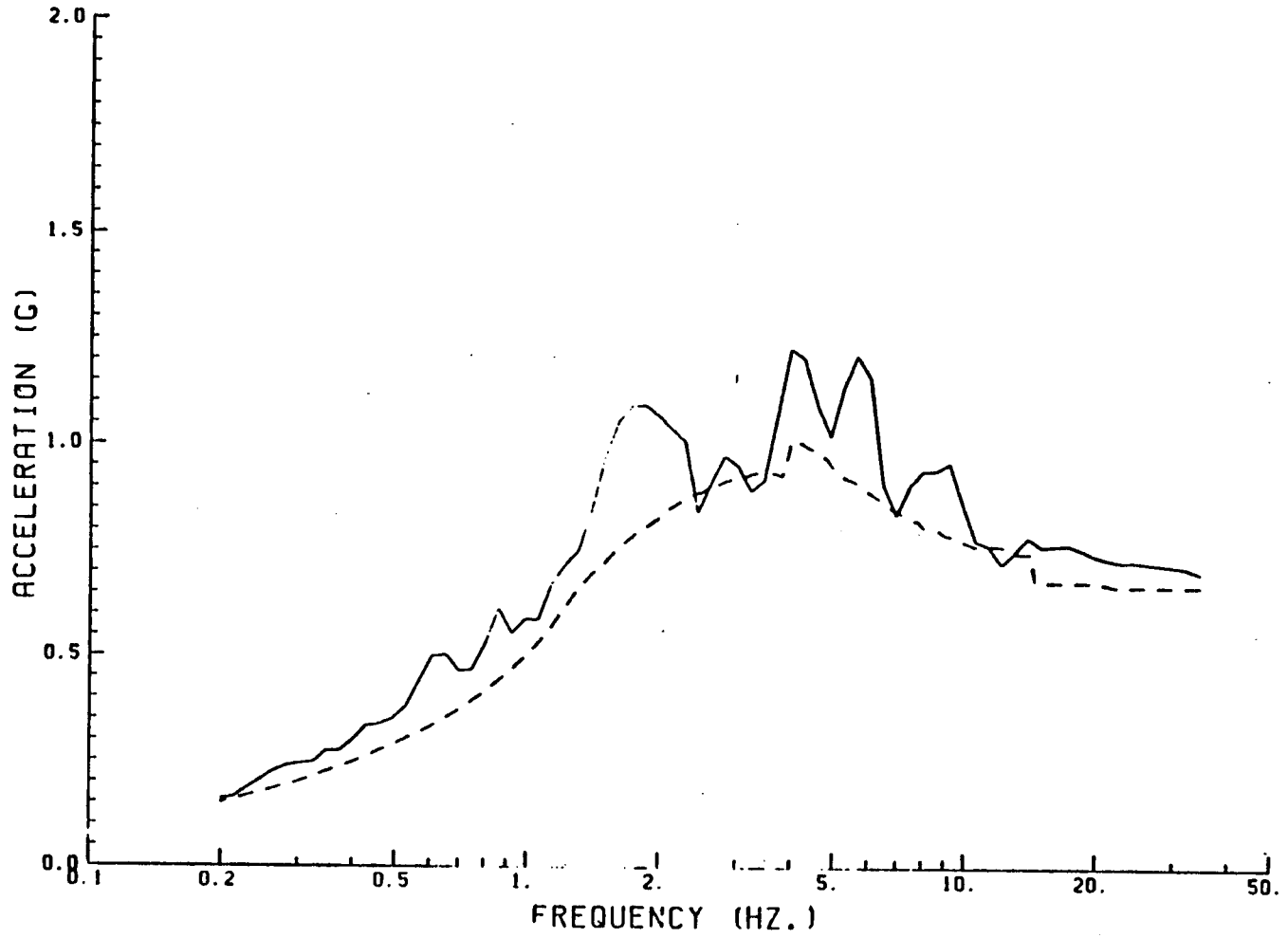

SCE-SONGS1
DESIGN (DASHED LINE) VERSUS ENVELOPE (SOLID LINE) SPECTRA
EAST-WEST DIRECTION
7 PERCENT DAMPING

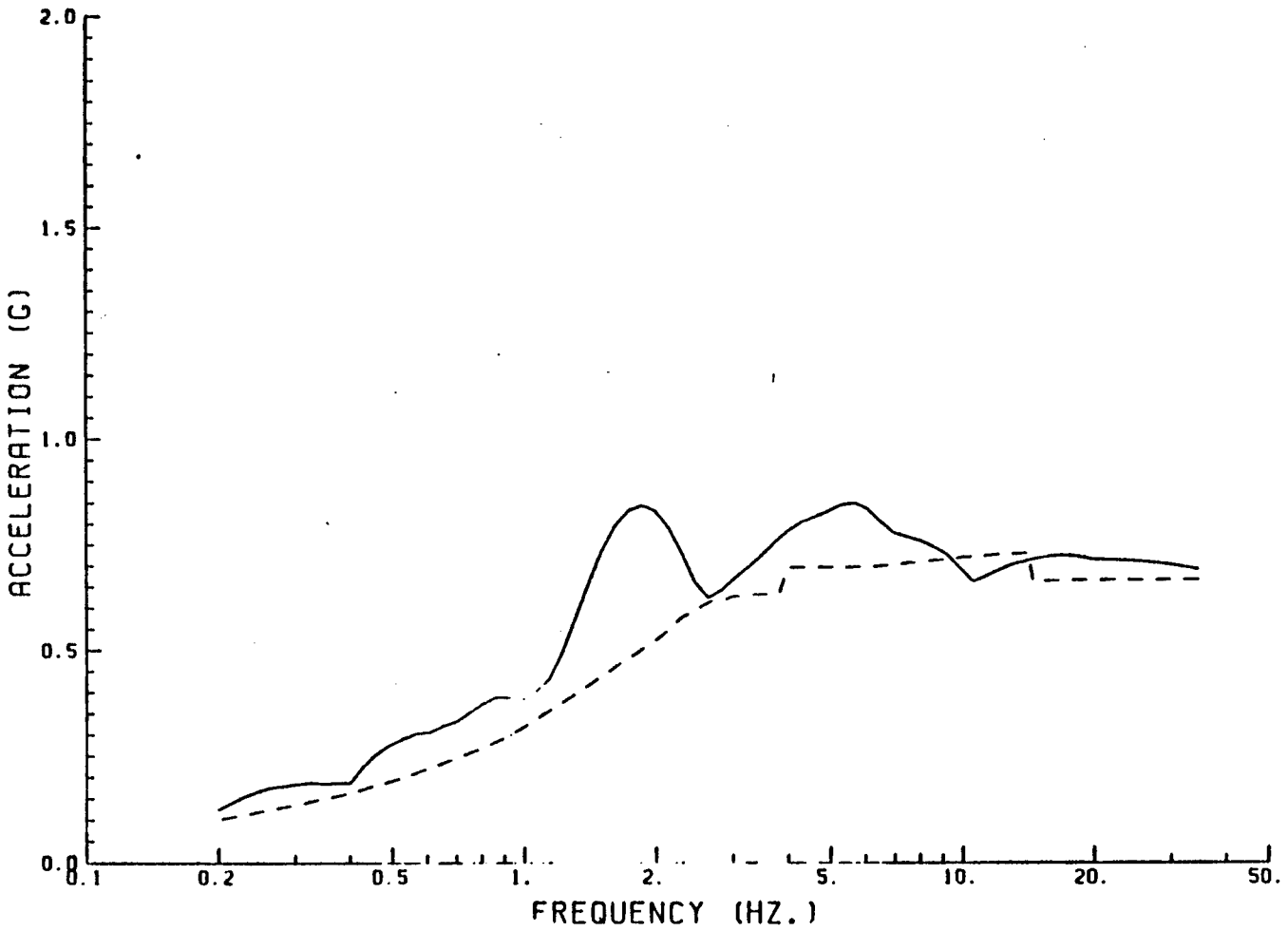

SCE-SONGS1
DESIGN (DASHED LINE) VERSUS ENVELOPE (SOLID LINE) SPECTRA
EAST-WEST DIRECTION
20 PERCENT DAMPING

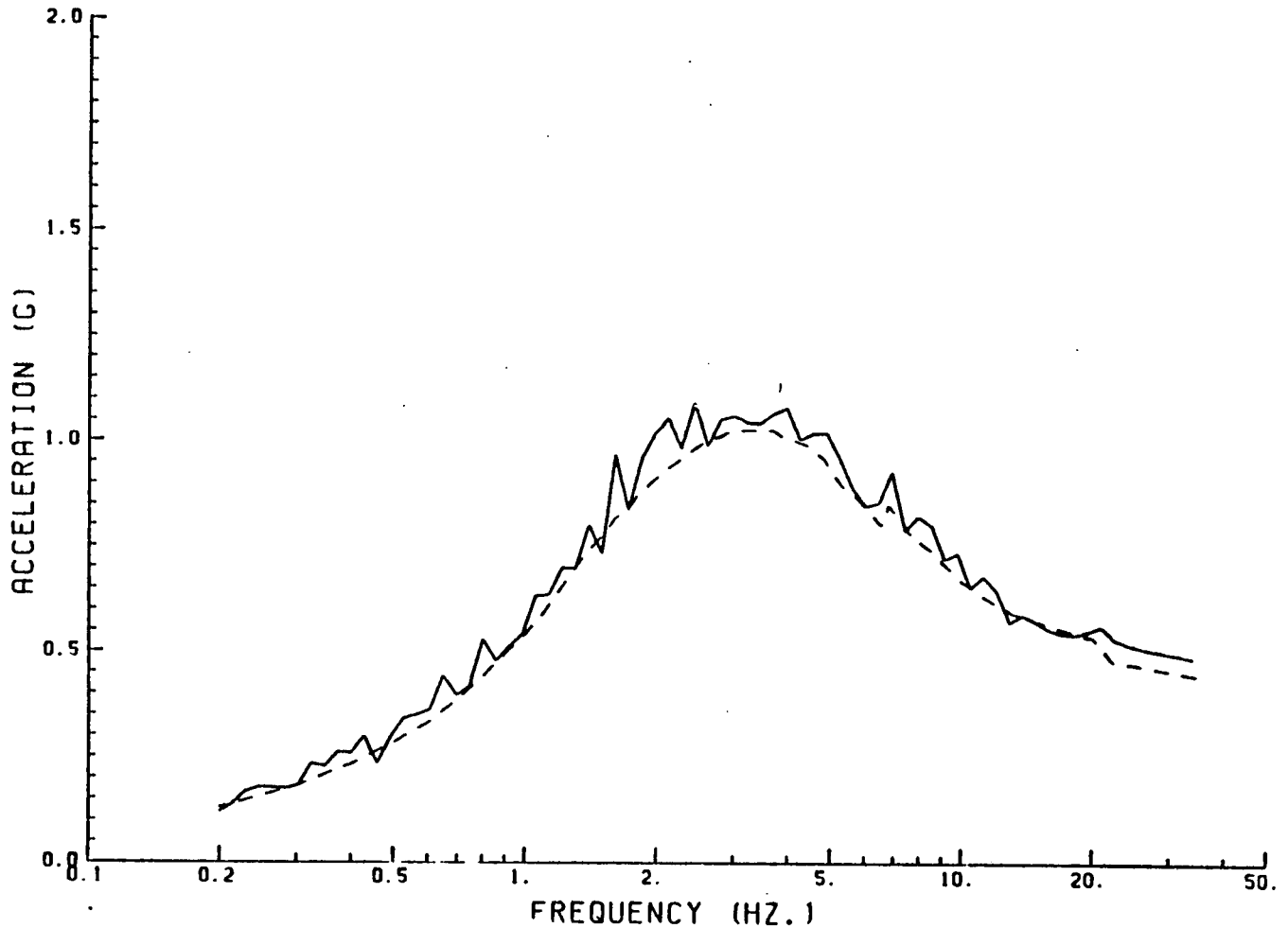

SCE-SONGS1
DESIGN (DASHED LINE) VERSUS ENVELOPE (SOLID LINE) SPECTRA
VERTICAL DIRECTION
2 PERCENT DAMPING

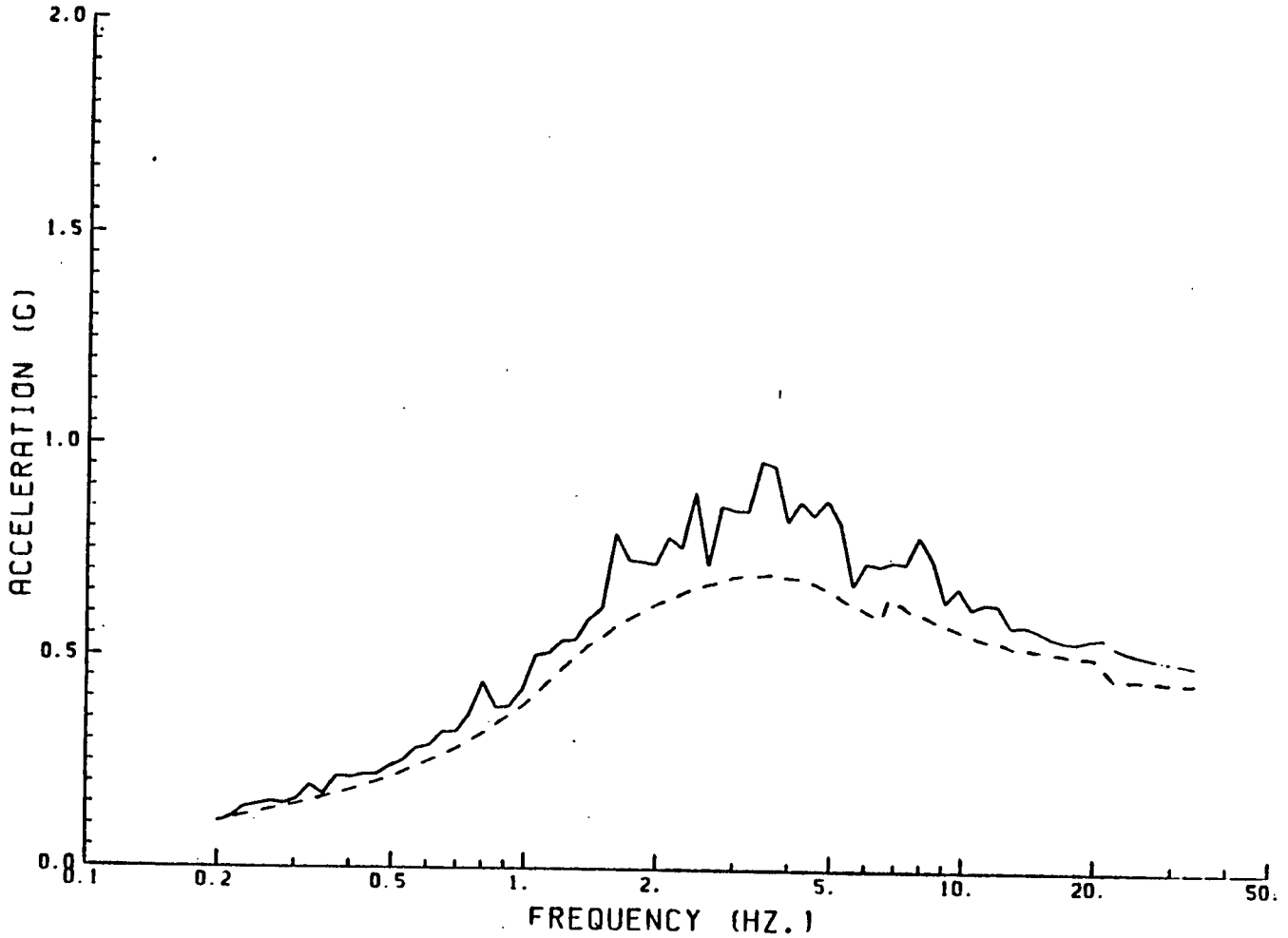

SCE-SONGS1
DESIGN (DASHED LINE) VERSUS ENVELOPE (SOLID LINE) SPECTRA
VERTICAL DIRECTION
4 PERCENT DAMPING

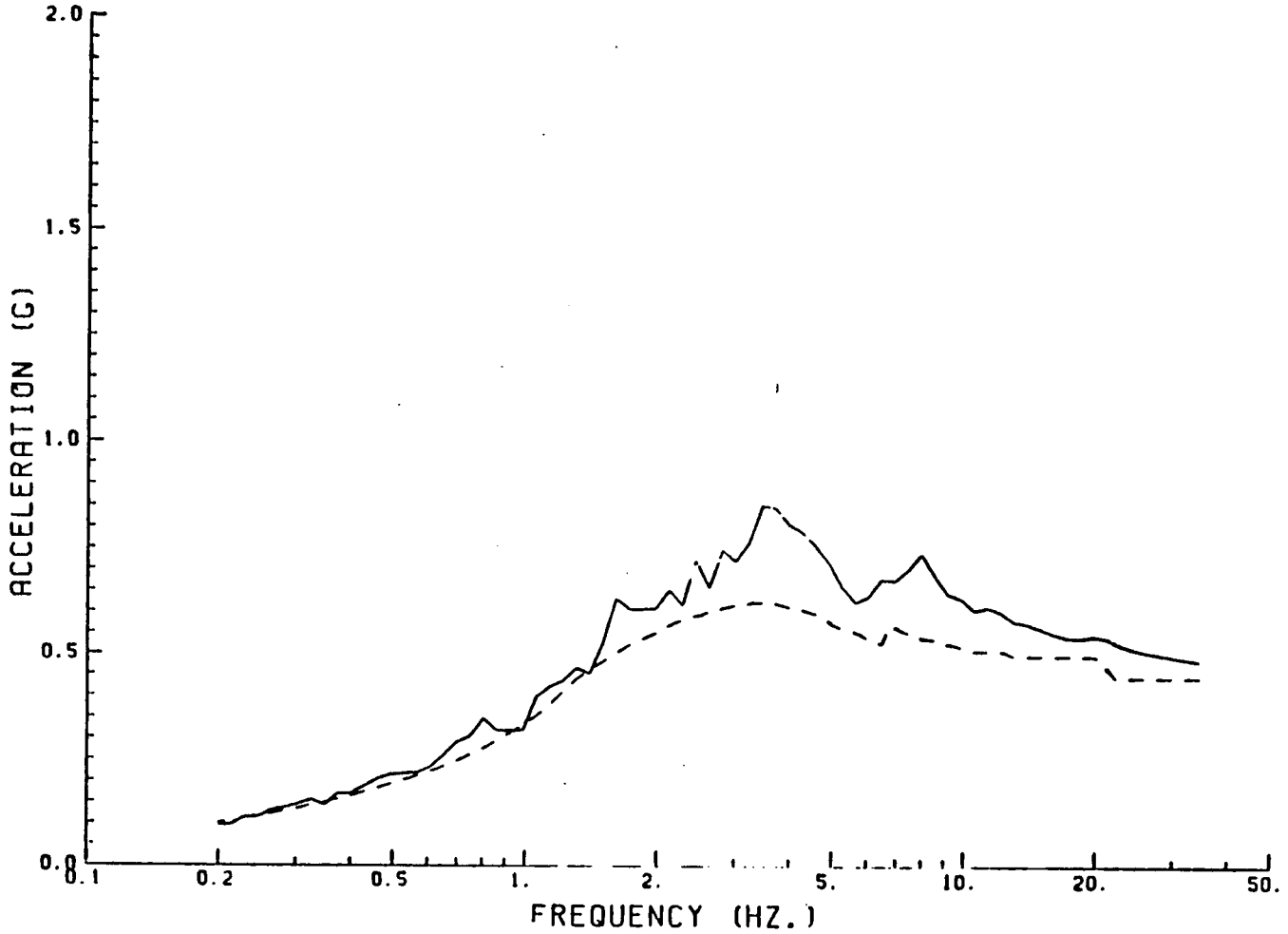

SCE-SONGS1
DESIGN (DASHED LINE) VERSUS ENVELOPE (SOLID LINE) SPECTRA
VERTICAL DIRECTION
7 PERCENT DAMPING

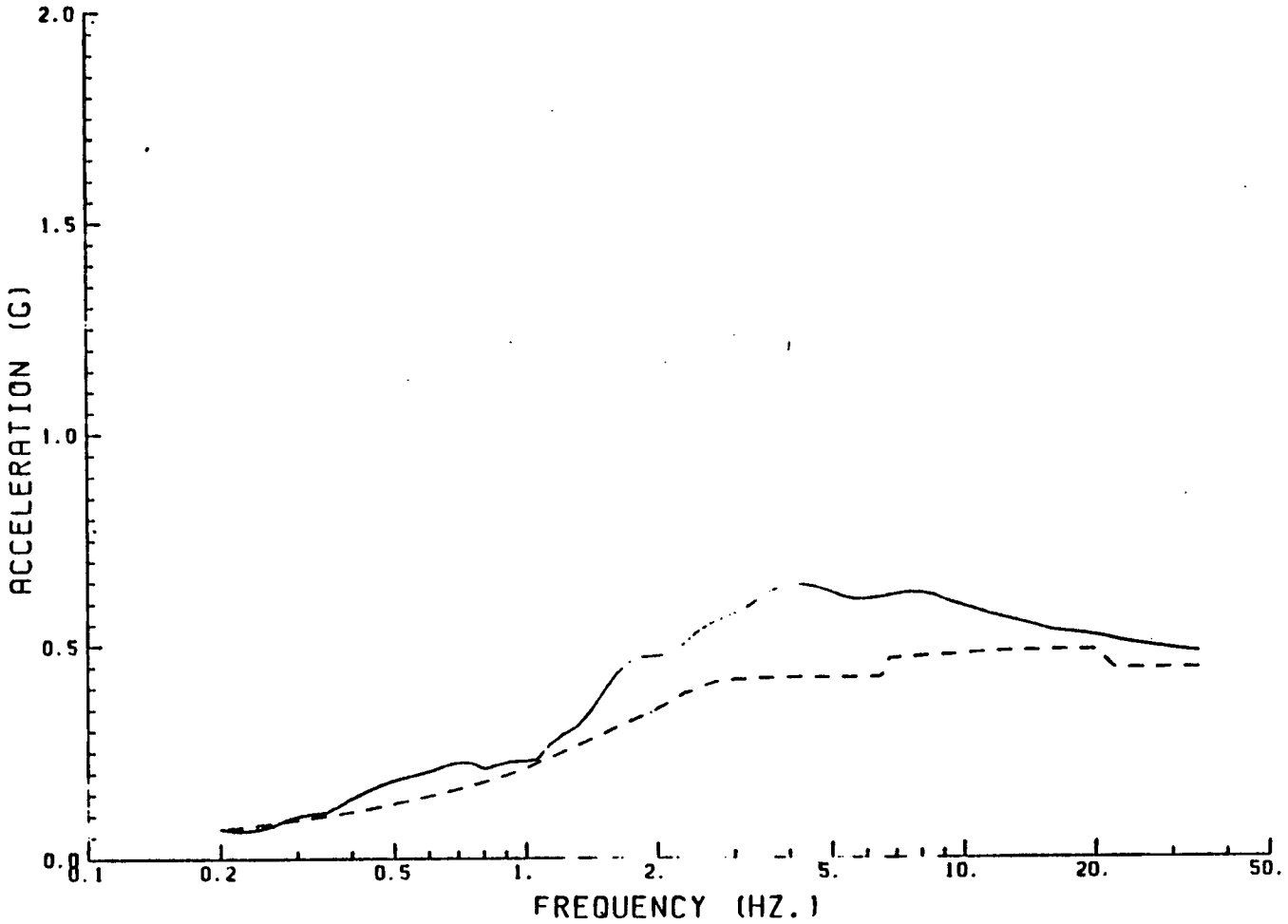

SCE-SONGS1
DESIGN (DASHED LINE) VERSUS ENVELOPE (SOLID LINE) SPECTRA
VERTICAL DIRECTION
20 PERCENT DAMPING

IMPELL CORPORATION

RESULTS

- CROSS CORRELATIONS:

	P
N-S TO E-W	-0.06
N-S TO VERTICAL	0.07
E-W TO VERTICAL	0.16

IMPELL CORPORATION

RESULTS (CONTINUED)

- COMPARISON SPECTRA TO S.R.P. 3.7.2 CRITERIA

	TOTAL NUMBER OF EXCEEDENCES	AVERAGE CONSERVATISM
NORTH-SOUTH		
2%	4	10%
4%	0	20%
7%	6 NOTE 1	17%
20%	1	25%
EAST-WEST		
2%	5	8%
4%	1	20%
7%	6 NOTE 1	16%
20%	6 NOTE 1	23%
VERTICAL		
2%	10 NOTES 1,2,3	6%
4%	1	16%
7%	3	14%
20%	4 NOTE 4	25%

NOTE 1: LESS THAN 5 EXCEEDENCES OF MORE THAN -2.5%

NOTE 2: ONE EXCEEDENCE OF -11.5% AT 0.46 HZ. NO EFFECT ON R.B. OR T.B.

NOTE 3: NO R.B. OR T.B. HAVE STRUCTURAL MODES WITH DAMPING BELOW 4%. HENCE THE 2% INPUT SPECTRA EXCEEDENCE NOT RELEVANT TO ANY ANALYSES OF R.B. OR T.B.

NOTE 4: ONE EXCEEDENCE OF -11.3% AT 0.23 HZ. NO EFFECT ON R.B. OR T.B.

IMPELL CORPORATION

- CONCLUSIONS
  - THREE MOTIONS ARE STATISTICALLY INDEPENDENT
  - MINOR VARIATION FROM S.R.P. 3.7.2 GUIDELINE
  - NO SIGNIFICANT EXCEEDENCES
  - AVERAGE CONSERVATISM (Ø.2 TO 33 HZ.) IN DAMPING RANGE OF INTEREST (4-2Ø%) IS 14 TO 26 PERCENT
  - INPUT TIME HISTORIES ARE SUITABLE FOR LOAD GENERATION

CASE # 1 DAMPING = .02

NORTH-SOUTH

$\xi = 2\%$

FREQ(HZ)	DESIGN SPECTRUM	ENVELOPE SPECT.	DIFF(PER CENT)
.2000	.19E+00	.23E+00	21.1
.2144	.20E+00	.23E+00	15.0
.2290	.21E+00	.24E+00	14.3
.2453	.23E+00	.25E+00	8.7
.2640	.24E+00	.26E+00	8.3
.2838	.26E+00	.26E+00	0.0
.3033	.27E+00	.29E+00	7.4
.3251	.27E+00	.36E+00	24.1
.3485	.31E+00	.36E+00	16.1
.3735	.33E+00	.33E+00	0.0
.4004	.35E+00	.36E+00	2.9
.4291	.37E+00	.37E+00	0.0
.4600	.39E+00	.44E+00	12.8
.4930	.42E+00	.54E+00	28.6
.5285	.44E+00	.47E+00	6.8
.5664	.47E+00	.49E+00	4.3
.6071	.50E+00	.53E+00	6.0
.6508	.54E+00	.65E+00	20.4
.6975	.57E+00	.58E+00	1.8
.7477	.62E+00	.61E+00	-1.6
.8014	.66E+00	.82E+00	24.2
.8590	.71E+00	.70E+00	-1.4
.9207	.76E+00	.79E+00	3.9
.9869	.82E+00	.90E+00	10.3
1.0578	.88E+00	.10E+01	17.6
1.1339	.94E+00	.89E+00	-5.5
1.2153	.10E+01	.12E+01	26.5
1.3027	.11E+01	.11E+01	5.7
1.3963	.11E+01	.11E+01	-3.6
1.4967	.12E+01	.13E+01	15.5
1.6042	.12E+01	.13E+01	4.9
1.7195	.13E+01	.13E+01	.9
1.8431	.13E+01	.16E+01	24.2
1.9756	.14E+01	.14E+01	2.9
2.1179	.14E+01	.16E+01	17.1
2.2697	.14E+01	.14E+01	0.0
2.4328	.15E+01	.15E+01	2.7
2.6077	.16E+01	.17E+01	10.7
2.7951	.16E+01	.16E+01	1.3
2.9960	.16E+01	.16E+01	2.0
3.2113	.16E+01	.17E+01	13.0
3.4421	.16E+01	.16E+01	1.3
3.6894	.16E+01	.16E+01	2.6
3.9545	.16E+01	.16E+01	2.6
4.2383	.16E+01	.17E+01	4.9
4.5424	.16E+01	.16E+01	1.9
4.8700	.16E+01	.14E+01	13.5
5.2200	.16E+01	.16E+01	0.0
5.5951	.14E+01	.16E+01	8.3
5.9972	.14E+01	.14E+01	1.4
6.4282	.13E+01	.16E+01	22.6
6.8902	.13E+01	.15E+01	19.3
7.3854	.12E+01	.14E+01	20.0
7.9161	.12E+01	.14E+01	20.9
8.4851	.11E+01	.12E+01	4.5
9.0949	.11E+01	.12E+01	8.5
9.7485	.10E+01	.11E+01	8.8
10.4491	.98E+00	.10E+01	5.1
11.2000	.95E+00	.11E+01	16.9
12.0050	.92E+00	.94E+00	2.2
12.8677	.89E+00	.12E+01	31.5
13.7925	.85E+00	.95E+00	11.4
14.7837	.79E+00	.94E+00	19.2
15.8462	.77E+00	.86E+00	11.7
16.9851	.73E+00	.83E+00	9.2
18.2057	.74E+00	.80E+00	8.1
19.5141	.73E+00	.80E+00	9.5
20.9156	.73E+00	.80E+00	9.5
22.4166	.72E+00	.79E+00	9.7
24.0311	.71E+00	.77E+00	8.5
25.7531	.70E+00	.75E+00	7.1
27.5993	.69E+00	.74E+00	7.2
29.5765	.69E+00	.73E+00	5.8
31.7203	.69E+00	.74E+00	7.4
34.0000	.67E+00	.73E+00	9.0

DL

CASE # 2 DAMPING = .04

NORTH-SOUTH $\xi = 4\%$

FREQ(HZ)	DESIGN SPECTRUM	ENVELOPE SPECT.	DIFF(PER CENT)
.2000	.19E+00	.20E+00	25.0
.2144	.17E+00	.22E+00	29.4
.2298	.19E+00	.23E+00	27.8
.2463	.19E+00	.23E+00	21.1
.2640	.20E+00	.23E+00	15.0
.2830	.21E+00	.25E+00	19.0
.3033	.22E+00	.25E+00	16.2
.3251	.23E+00	.30E+00	30.4
.3485	.24E+00	.31E+00	29.2
.3735	.25E+00	.29E+00	11.5
.4004	.27E+00	.29E+00	7.4
.4291	.29E+00	.30E+00	3.4
.4600	.30E+00	.38E+00	26.7
.4930	.32E+00	.45E+00	40.6
.5285	.34E+00	.42E+00	23.5
.5664	.36E+00	.42E+00	16.7
.6071	.38E+00	.44E+00	15.8
.6508	.40E+00	.52E+00	30.0
.6975	.42E+00	.44E+00	4.8
.7477	.45E+00	.53E+00	17.5
.8014	.48E+00	.65E+00	35.4
.8590	.51E+00	.58E+00	13.7
.9207	.54E+00	.67E+00	24.1
.9869	.57E+00	.81E+00	42.1
1.0578	.61E+00	.87E+00	42.6
1.1339	.66E+00	.77E+00	16.7
1.2153	.71E+00	.11E+01	47.9
1.3027	.76E+00	.10E+01	34.7
1.3963	.79E+00	.91E+00	15.2
1.4957	.82E+00	.10E+01	23.2
1.6042	.85E+00	.10E+01	19.6
1.7195	.88E+00	.10E+01	17.0
1.8431	.91E+00	.13E+01	38.5
1.9755	.94E+00	.13E+01	33.0
2.1175	.98E+00	.14E+01	44.2
2.2697	.97E+00	.12E+01	26.8
2.4328	.99E+00	.10E+01	5.1
2.6077	.10E+01	.13E+01	27.7
2.7951	.10E+01	.13E+01	23.5
2.9960	.10E+01	.13E+01	27.2
3.2113	.10E+01	.14E+01	31.7
3.4421	.10E+01	.13E+01	27.9
3.6894	.10E+01	.12E+01	16.3
3.9546	.11E+01	.13E+01	33.0
4.2388	.11E+01	.14E+01	20.4
4.5434	.11E+01	.13E+01	14.6
4.8700	.11E+01	.15E+01	33.0
5.2200	.11E+01	.13E+01	24.5
5.5951	.10E+01	.12E+01	16.3
5.9972	.10E+01	.11E+01	9.9
6.4282	.99E+00	.11E+01	13.1
6.8902	.95E+00	.11E+01	10.5
7.3854	.93E+00	.11E+01	12.9
7.9161	.91E+00	.10E+01	9.9
8.4851	.89E+00	.99E+00	11.2
9.0949	.87E+00	.93E+00	6.9
9.7485	.85E+00	.88E+00	3.5
10.4491	.83E+00	.96E+00	15.7
11.2000	.82E+00	.98E+00	19.5
12.0050	.81E+00	.87E+00	7.4
12.8677	.79E+00	.95E+00	20.3
13.7925	.77E+00	.82E+00	6.8
14.7837	.71E+00	.88E+00	23.9
15.8462	.70E+00	.85E+00	21.4
15.9851	.70E+00	.82E+00	17.1
18.2057	.69E+00	.79E+00	14.5
19.5141	.69E+00	.78E+00	13.0
20.9156	.68E+00	.79E+00	16.2
22.4146	.68E+00	.78E+00	14.7
24.0311	.68E+00	.76E+00	11.8
25.7541	.68E+00	.75E+00	10.3
27.6093	.68E+00	.74E+00	8.8
29.5935	.67E+00	.73E+00	9.0
31.7203	.67E+00	.73E+00	9.0
34.0000	.67E+00	.72E+00	7.5

NORTH-SOUTH $\xi = 7\%$

PERIOD(SEC)	DESIGN SPECTRUM	ENVELOPE SPECT.	DIFF(PER CENT)
.2000	.15E+00	.19E+00	26.7
.2144	.15E+00	.20E+00	25.0
.2295	.15E+00	.21E+00	31.3
.2453	.17E+00	.21E+00	23.5
.2540	.18E+00	.22E+00	22.2
.2630	.19E+00	.23E+00	21.1
.3033	.20E+00	.24E+00	20.0
.3251	.21E+00	.25E+00	23.8
.3485	.22E+00	.27E+00	22.7
.3735	.23E+00	.28E+00	21.7
.4004	.25E+00	.25E+00	12.0
.4291	.25E+00	.23E+00	7.7
.4600	.27E+00	.31E+00	14.8
.4930	.29E+00	.36E+00	24.1
.5285	.30E+00	.35E+00	16.7
.5664	.32E+00	.35E+00	9.4
.6071	.33E+00	.36E+00	9.1
.6508	.35E+00	.42E+00	20.0
.6975	.37E+00	.35E+00	-2.7
.7477	.39E+00	.44E+00	12.8
.8014	.41E+00	.54E+00	31.7
.8590	.44E+00	.52E+00	18.2
.9207	.47E+00	.58E+00	23.4
.9869	.49E+00	.65E+00	34.7
1.0578	.53E+00	.72E+00	35.8
1.1334	.57E+00	.74E+00	29.8
1.2193	.61E+00	.98E+00	64.3
1.3027	.65E+00	.85E+00	33.3
1.3963	.69E+00	.83E+00	20.3
1.4967	.72E+00	.83E+00	15.3
1.6042	.75E+00	.85E+00	14.7
1.7195	.75E+00	.83E+00	11.5
1.8431	.81E+00	.99E+00	23.8
1.9756	.86E+00	.11E+01	34.7
2.1175	.85E+00	.11E+01	31.8
2.2697	.87E+00	.10E+01	19.5
2.4328	.93E+00	.91E+00	3.4
2.6077	.98E+00	.10E+01	15.5
2.7951	.97E+00	.97E+00	6.6
2.9959	.92E+00	.11E+01	15.2
3.2113	.98E+00	.11E+01	20.4
3.4421	.98E+00	.11E+01	17.2
3.6894	.93E+00	.11E+01	16.1
3.9545	.99E+00	.13E+01	26.3
4.2388	.10E+01	.12E+01	21.0
4.5434	.98E+00	.12E+01	21.4
4.8700	.95E+00	.12E+01	29.2
5.2205	.99E+00	.12E+01	24.7
5.5961	.97E+00	.11E+01	13.2
5.9972	.97E+00	.94E+00	5.6
6.4262	.97E+00	.94E+00	-3.4
6.8852	.93E+00	.89E+00	-4.7
7.3764	.93E+00	.89E+00	-4.8
7.9021	.91E+00	.90E+00	-1.2
8.4651	.93E+00	.86E+00	7.5
9.0679	.94E+00	.82E+00	3.8
9.7435	.95E+00	.85E+00	9.0
10.4441	.95E+00	.89E+00	17.1
11.2030	.95E+00	.88E+00	15.8
12.0232	.95E+00	.94E+00	2.6
12.8877	.95E+00	.95E+00	1.3
13.7425	.95E+00	.94E+00	-1.3
14.7387	.88E+00	.82E+00	20.6
15.9462	.88E+00	.82E+00	20.6
15.9351	.83E+00	.90E+00	17.5
15.2057	.83E+00	.79E+00	16.2
19.5141	.83E+00	.75E+00	14.7
20.9156	.87E+00	.74E+00	16.4
22.4198	.87E+00	.77E+00	14.9
24.0311	.87E+00	.79E+00	13.4
25.7551	.87E+00	.74E+00	10.4
27.6093	.87E+00	.74E+00	10.4
29.5785	.87E+00	.73E+00	9.0
31.7203	.87E+00	.73E+00	9.0
34.0000	.87E+00	.72E+00	7.5

NORTH - SOUTH $\xi = 20\%$

FREQ(HZ)	DIFF(PER CENT)
.2030	61.60
.2144	56.57
.2296	51.03
.2453	38.98
.2540	44.61
.2830	51.15
.3033	55.31
.3251	56.03
.3435	58.23
.3735	56.05
.4034	51.31
.4291	45.85
.4630	38.72
.4930	32.95
.5285	25.24
.5554	18.35
.6071	17.39
.6538	16.49
.6975	15.20
.7477	26.74
.8014	40.77
.8590	47.57
.9207	50.93
.9859	53.07
1.0576	54.12
1.1339	54.37
1.2153	52.91
1.3027	46.51
1.3963	34.78
1.4967	23.05
1.6042	19.52
1.7195	18.80
1.8431	22.97
1.9756	25.90
2.1175	27.51
2.2697	23.79
2.4328	20.15
2.6077	15.03
2.7951	10.25
2.9950	13.20

3.2113	20.85
3.4421	27.37
[illegible]	31.25
[illegible]	23.87
4.2338	22.95
4.5434	25.10
4.8730	27.16
5.2230	26.50
5.5451	22.10
5.9372	14.93
6.4232	7.25
6.8732	2.47
7.3354	1.53
7.9151	2.74
8.4351	4.15
9.0949	5.01
9.7435	6.78
10.4491	7.13
11.2033	4.99
[illegible]	1.05
12.0577	-1.21
13.7425	-.33
14.7337	11.54
15.8452	12.77
16.9851	13.67
18.2057	13.33
19.5141	12.59
20.9156	11.46
22.4198	11.01
24.0311	10.48
25.7531	9.70
27.6043	8.83
29.5935	7.87
31.7203	6.85
34.0000	5.81

IMPELL CORPORATION

REACTOR BUILDING

PURPOSE

- TO GENERATE FLOOR RESPONSE SPECTRA IN THE REACTOR BUILDING

IMPELL CORPORATION

METHODOLOGY

1. BUILDING MODELS

- USE SAME REACTOR BUILDING MODEL PREVIOUSLY CREATED BY BPC, USING BSAP PROGRAM
- FROM R.B. FIXED BASE MODEL, GET MODE SHAPES, FREQUENCIES, COMPOSITE STRUCTURE MODAL DAMPING VALUES AND MASS MATRIX
- DEVELOP ENCLOSURE BUILDING FIXED BASE MODEL, USING EDSGAP PROGRAM. MODEL IS SIMPLIFIED STICK
- FROM E.B. FIXED BASE MODEL, GET MODE SHAPES, FREQUENCIES, COMPOSITE STRUCTURE MODAL DAMPING VALUES AND MASS MATRIX

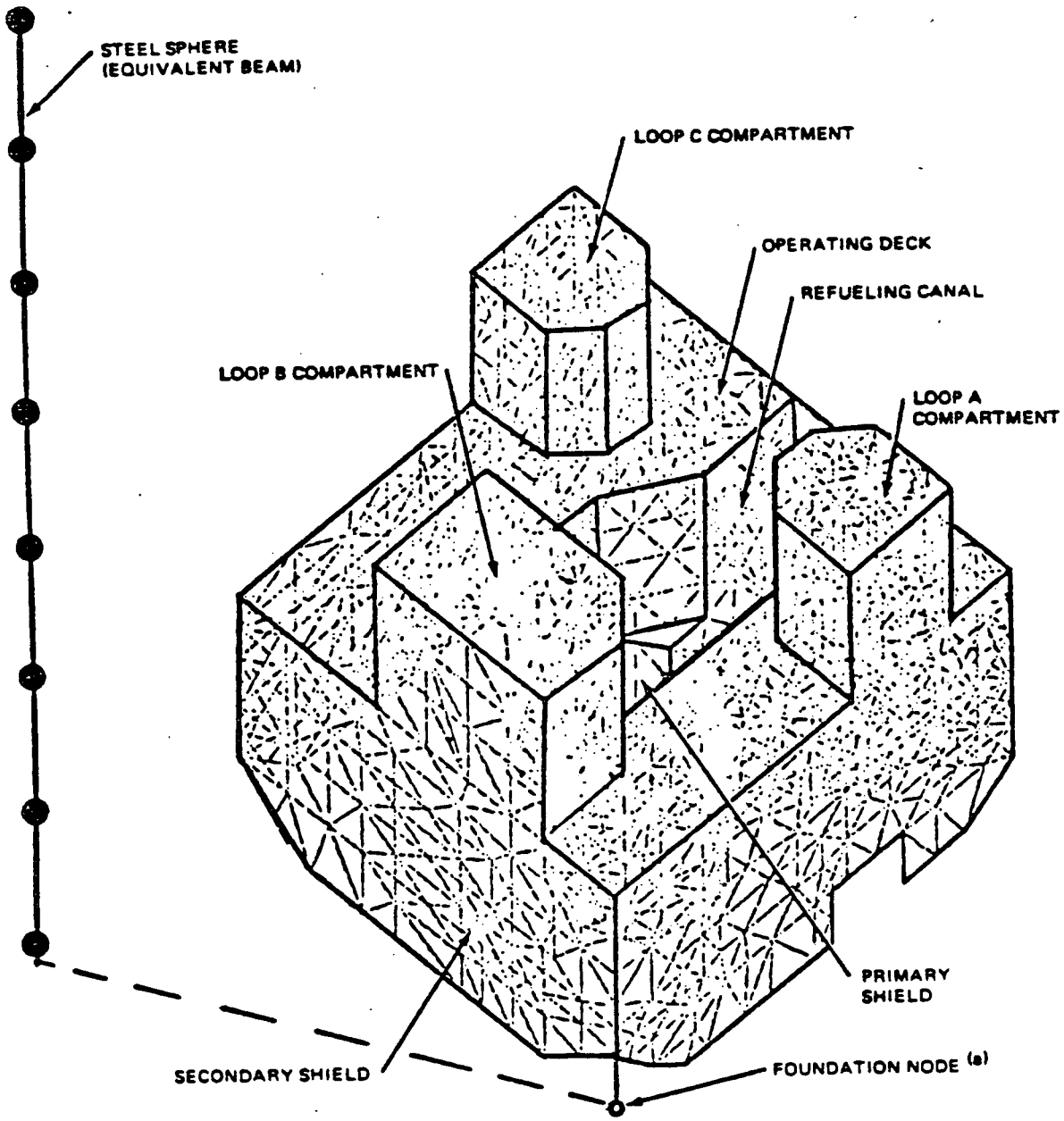

a. RIGIDLY LINKED TO THE BASE OF THE PRIMARY AND SECONDARY SHIELD WALLS

FINITE ELEMENT MODEL OF REACTOR CONTAINMENT BUILDING AND CONTAINMENT SPHERE

Ref. Figure 3.7.2-3 (SONGS-1 NRC DOCKET 50-206 Seismic Reevaluation and Modification, April 29, 1977

IMPELL CORPORATION

REACTOR BUILDING SOIL PROPERTIES

- SOIL PROPERTIES DEVELOPED BY WOODWARD CLYDE
- SOIL PROPERTIES HAVE PREVIOUSLY BEEN PRESENTED TO NRC (BETHESDA, JUNE 10 & 11, 1985)
- UNIFORM HALFSPACE SOIL MODULUS G = 1390 KSF
- EFFECTIVE DBE SEISMIC STRAIN = 0.2 PERCENT
- SOIL MATERIAL DAMPING AT 0.2 PERCENT STRAIN IS OVER 11 PERCENT. FOR CONSERVATISM, ONLY 8 PERCENT IS USED IN SSI ANALYSIS.

IMPELL CORPORATION

2.0 FOUNDATION-SOIL MODEL

- DEVELOP A THREE-DIMENSIONAL FINITE ELEMENT MODEL OF THE REACTOR BUILDING AND ENCLOSURE BUILDING FOUNDATIONS AND SOIL USING SASSI PROGRAM.

- BASEMAT RIGIDITY CONFIRMED BY SEPARATE AXISYMMETRIC REACTOR BUILDING FOUNDATION MODEL.

- CALCULATE FOUNDATION-SOIL IMPEDANCES OF COMBINED REACTOR BUILDING, ENCLOSURE BUILDING AND SOIL SITE USING SASSI PROGRAM.

- COMPONENTS OF IMPEDANCES GENERATED: HORIZONTAL; VERTICAL; ROCKING; TORSION: COUPLING BETWEEN HORIZONTAL AND ROCKING.

- RESULTS OF FOUNDATION-SOIL MODEL: A TWELVE-BY-TWELVE FREQUENCY DEPENDENT MATRIX DEVELOPED FOR THE REACTOR BUILDING, THE ENCLOSURE BUILDING, AND THE R.B. - E.B. INTERACTIONS, FROM Ø.5 TO 2Ø HZ.

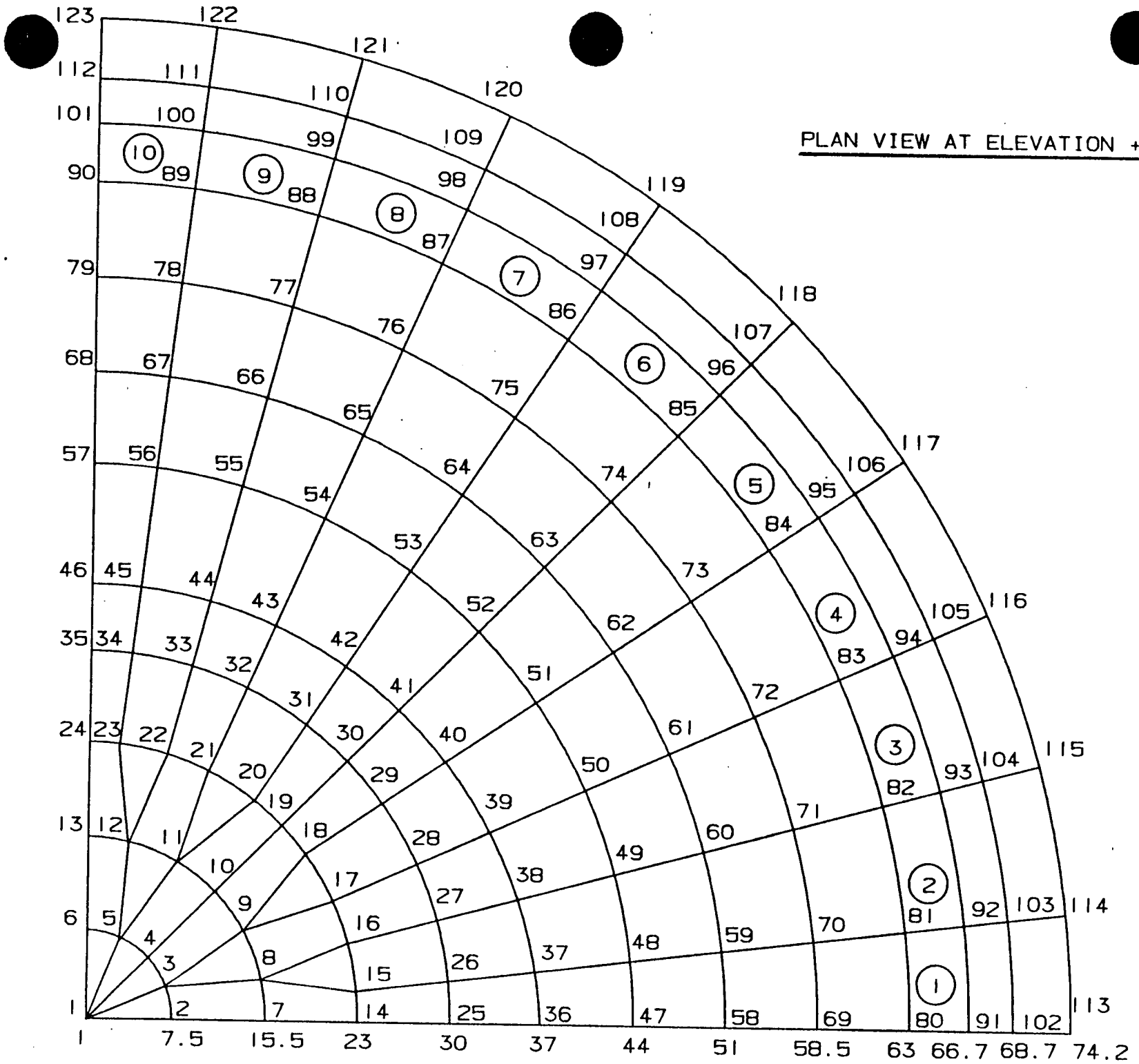
PLAN VIEW AT ELEVATION +20.0'
1
2
3
4
5
6
7
8
9
10
1
7.5
15.5
23
30
37
44
51
58.5
63
66.7
68.7
74.2

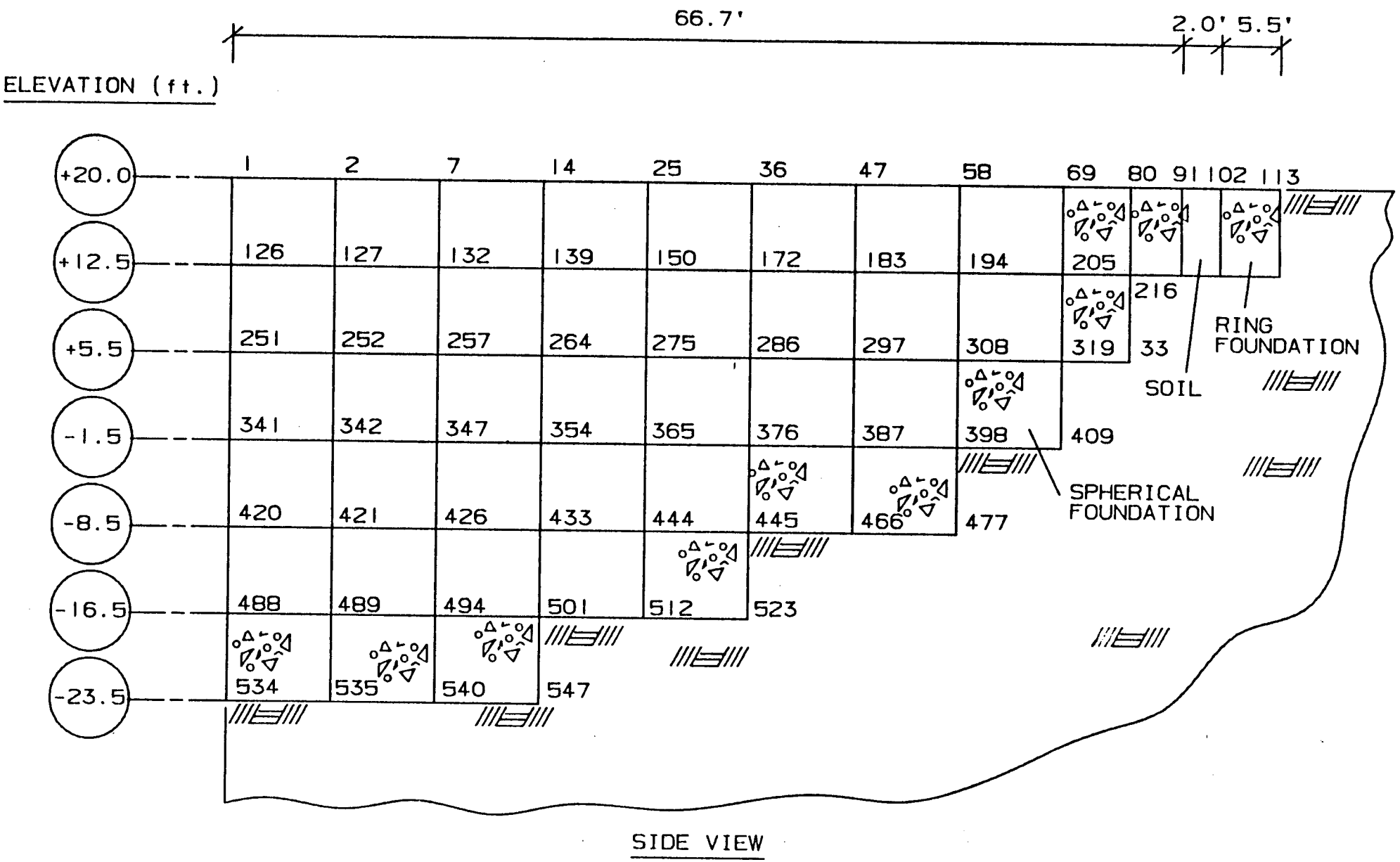
66.7'
2.0'
5.5'
ELEVATION (ft.)
+20.0
+12.5
+5.5
-1.5
-8.5
-16.5
-23.5
1
2
7
14
25
36
47
58
69
80
91
102
113
126
127
132
139
150
172
183
194
205
216
251
252
257
264
275
286
297
308
319
33
341
342
347
354
365
376
387
398
409
420
421
426
433
444
445
466
477
488
489
494
501
512
523
534
535
540
547
RING FOUNDATION
SOIL
SPHERICAL FOUNDATION

SIDE VIEW

IMPELL CORPORATION

3. COUPLED ANALYSIS

- THE CLASSI PROGRAM IS USED TO PERFORM THE TIME HISTORY ANALYSIS.

- INPUT TO CLASSI IS:
  - FIXED BASE RESULTS FROM BSAP REACTOR BUILDING MODEL
  - FIXED BASE RESULTS FROM EDSGAP ENCLOSURE BUILDING MODEL
  - TWELVE-BY-TWELVE FREQUENCY DEPENDENT IMPEDANCE MATRIX OF FOUNDATION - SITE SYSTEM, FROM SASSI MODEL
  - THREE SIMULTANEOUS COMPONENTS OF EARTHQUAKE

- OUTPUT FROM CLASSI IS:
  - TIME HISTORIES OF ACCELERATIONS AT ALL NODES WHERE FLOOR SPECTRA ARE DESIRED

IMPELL CORPORATION

REACTOR BUILDING

NODES	LOCATION
1	OPERATING DECK, ELEV. 40.5 FEET
82	OPERATING DECK, ELEV. 40.5 FEET
102	OPERATING DECK, ELEV. 40.5 FEET
202	OPERATING DECK, ELEV. 40.5 FEET
345	OPERATING DECK + SECONDARY SHIELD WALL, ELEV. 42.0 FEET
648	OPERATING DECK, ELEV. 42.0 FEET
532	NORTH REFUELING CANAL, ELEV. 30.0 FEET
536	EAST REFUELING CANAL, ELEV. 30.0 FEET
714	STEAM GENERATOR COMPARTMENT 1B, ELEV. 66.5 FEET
773	STEAM GENERATOR COMPARTMENT 1A, ELEV. 64.5 FEET
778	STEAM GENERATOR COMPARTMENT 1C, ELEV. 64.5 FEET
1001	TOP OF STEEL SPHERE
1006	EQUIPMENT HATCH, ELEV. 47.0 FEET
1048	CENTER OF GRAVITY OF FOUNDATION, ELEV. -0.25 FEET
	STRUCTURE FOUNDATION, ELEV. -10.0 FEET

ENCLOSURE BUILDING

1	TOP OF ENCLOSURE BUILDING, ELEV. 135.75 FEET
4	MIDDLE OF ENCLOSURE BUILDING, ELEV. 75.0 FEET
	FOUNDATION, ELEV. 20.0 FEET

IMPELL CORPORATION

4. GENERATION OF FLOOR SPECTRA

- RAW FLOOR RESPONSE SPECTRA ARE CALCULATED AT FIVE DAMPING VALUES (2%, 3%, 5%, 7%, 15%) FROM THE CLASSI OUTPUT TIME HISTORIES

- RAW FLOOR RESPONSE SPECTRA ARE ENVELOPED FOR SEVERAL NODES, TO PRODUCE A SINGLE FLOOR SPECTRA. EXAMPLE: FOUR NODES ON THE OPERATING DECK

- ALL SPECTRA ARE BROADENED, ± 15 PERCENT TO ACCOUNT FOR UNCERTAINTIES IN THE ANALYSIS

- FOR PIPING ANALYSIS PURPOSES USING PVRC FREQUENCY-DEPENDENT DAMPING, A SET OF PVRC SPECTRA ARE PRODUCED. (FROM 0 TO 10 HZ, DAMPING IS 5 PERCENT; FROM 10 TO 20 HZ, DAMPING RANGES FROM 5 TO 2 PERCENT; OVER 20 HZ, DAMPING IS 2 PERCENT)

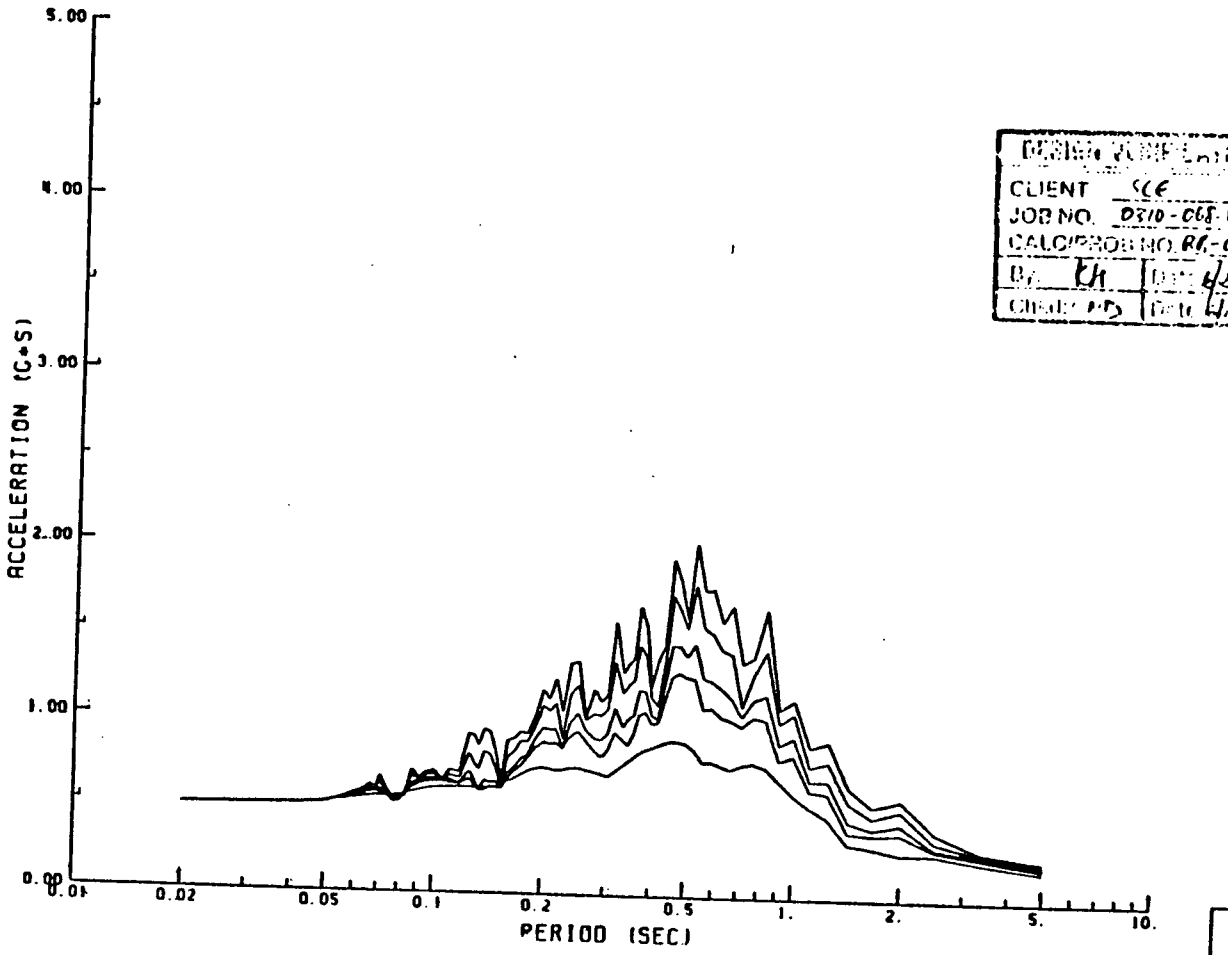

CLIENT SCE
JOB NO. 0310-068-KAT
CALC/PROB NO. RR-01
BY EH DATE 4/20/95
CHKD BY [illegible] DATE [illegible]

SPEC. SONGS-1 REAC. BLDG. X-DIR RESP. OPERATING DECK EL. 40.5FT NODE 1
DAMPING 2%, 3%, 5%, 7%, 15%

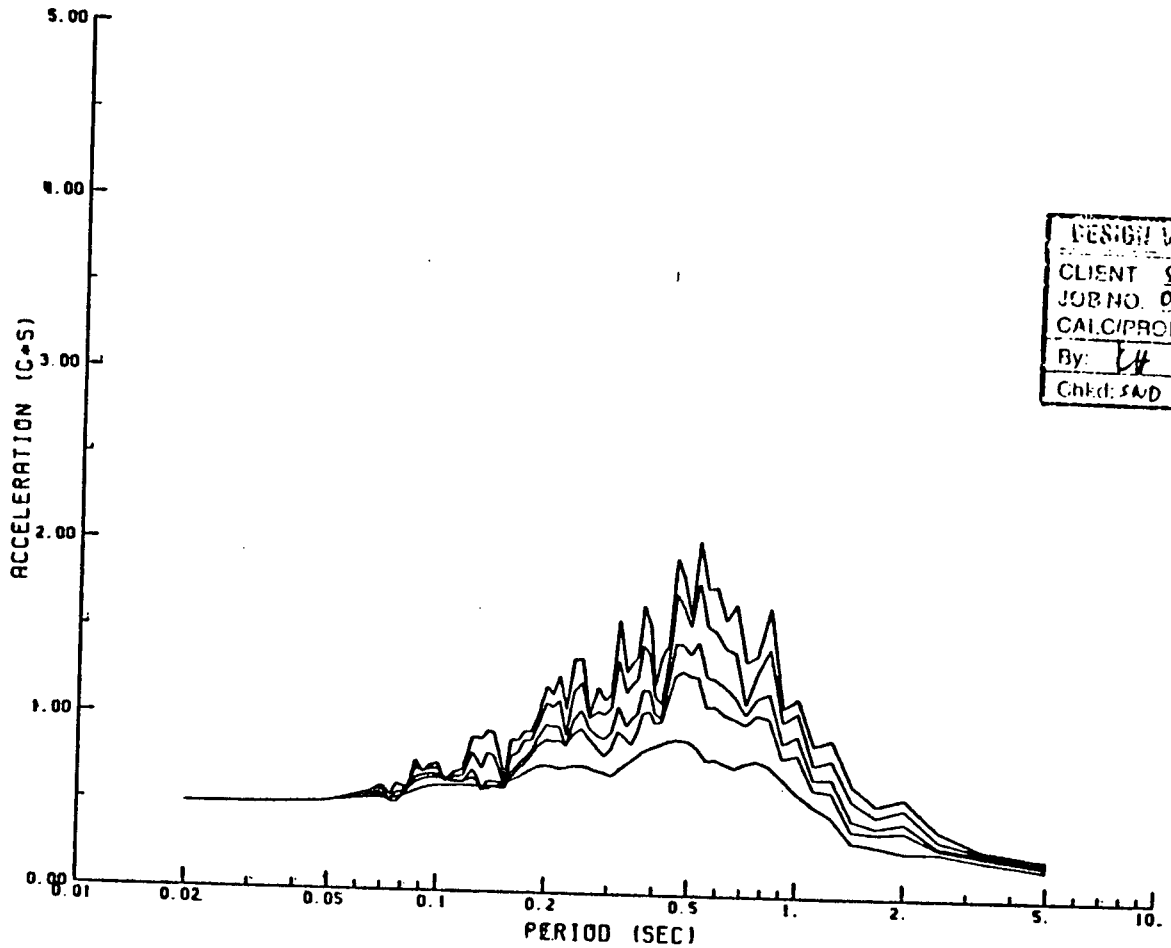

DESIGN VERIFICATION
CLIENT SCE
JOB NO. 0310-065-135
CALC/PROB NO. RB-07
By: [illegible] Date 4/20/95
Chkd: SMD Date 6/2/95

SPEC. SONGS-1 REAC. BLDG. X-DIR RES. OPERATING DECK EL. 40.5FT NODE 82
DAMPING 2%, 3%, 5%, 7%, 15%

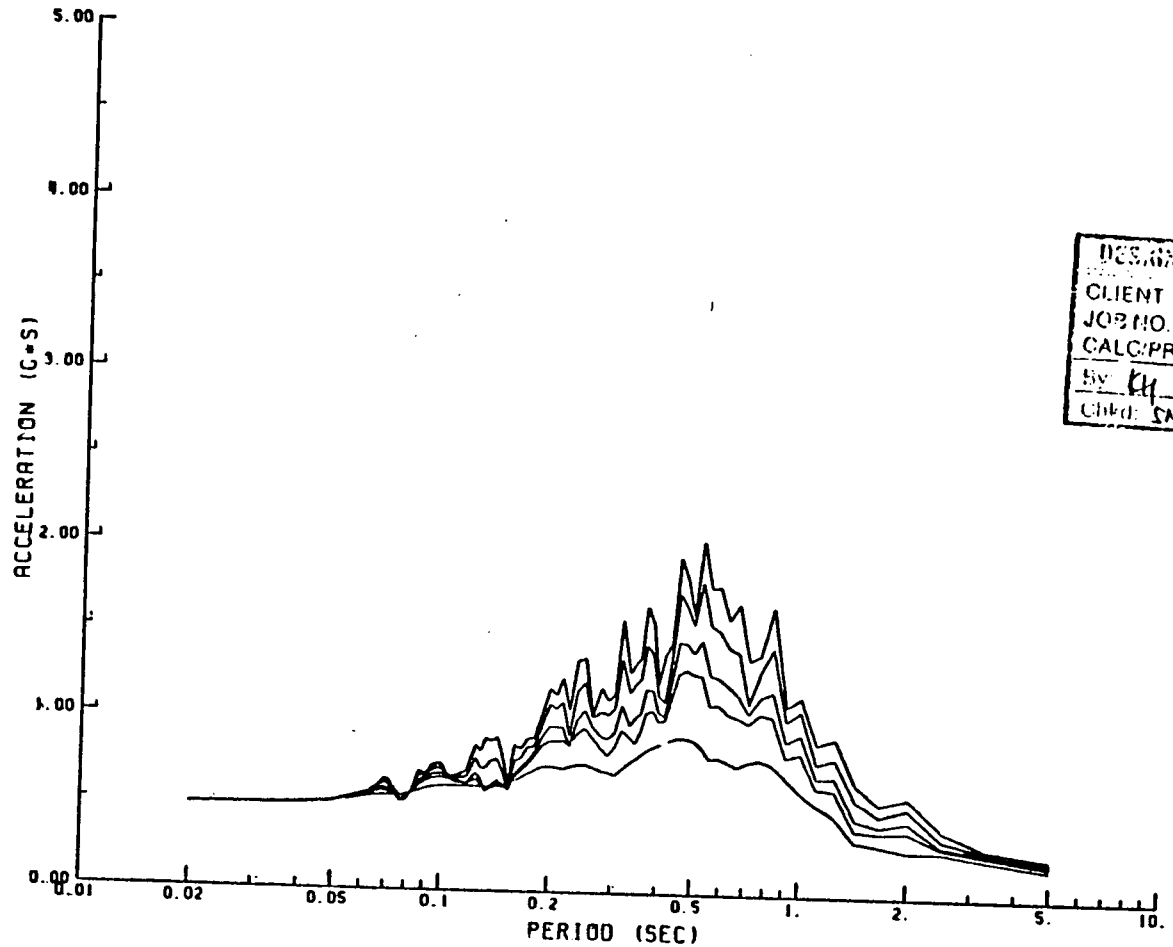

DESIGN VERIFICATION
CLIENT SCE
JOB NO. 0210-049-1355
CALC/PROB NO. RB-07
By: KH Date 4/10/95
Chkd: SMD Date 6/20/95

SPEC. SONGS-1 REAC. BLDG. X-DIR RES. OPER. DECK EL. 40.5FT NODE 102
DAMPING 2%, 3%, 5%, 7%, 15%

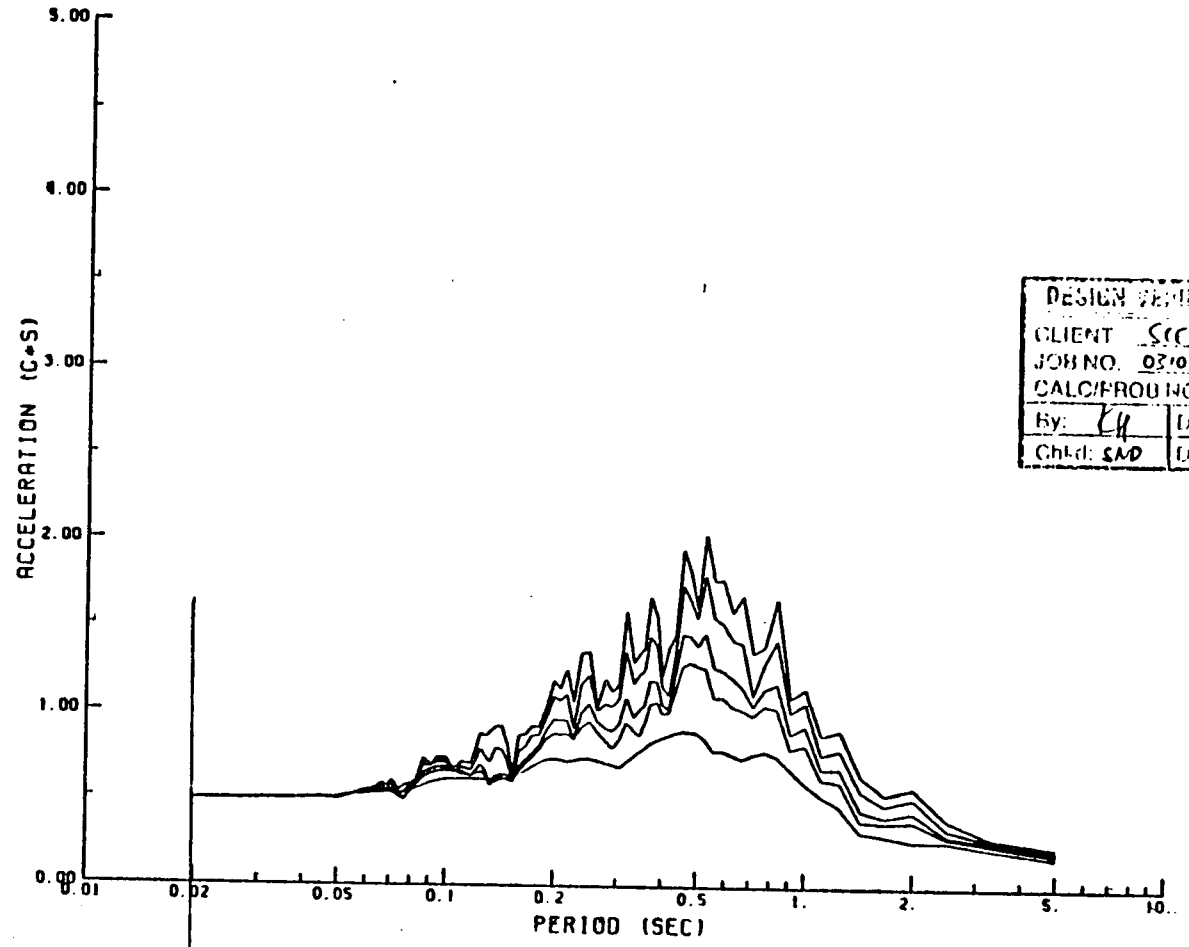

DESIGN VERIFICATION
CLIENT SCE
JOB NO. 0210-068-13TT
CALC/PROG NO. AB.07
By: KH Date: 6/20/85
Chkd: SMD Date: 6/20/85

SPEC. SONGS-1 REAC. BLDG. X-DIR RES. OPER. DECK EL. 40.5FT NODE 202
DAMPING 2%, 3%, 5%, 7%, 15%

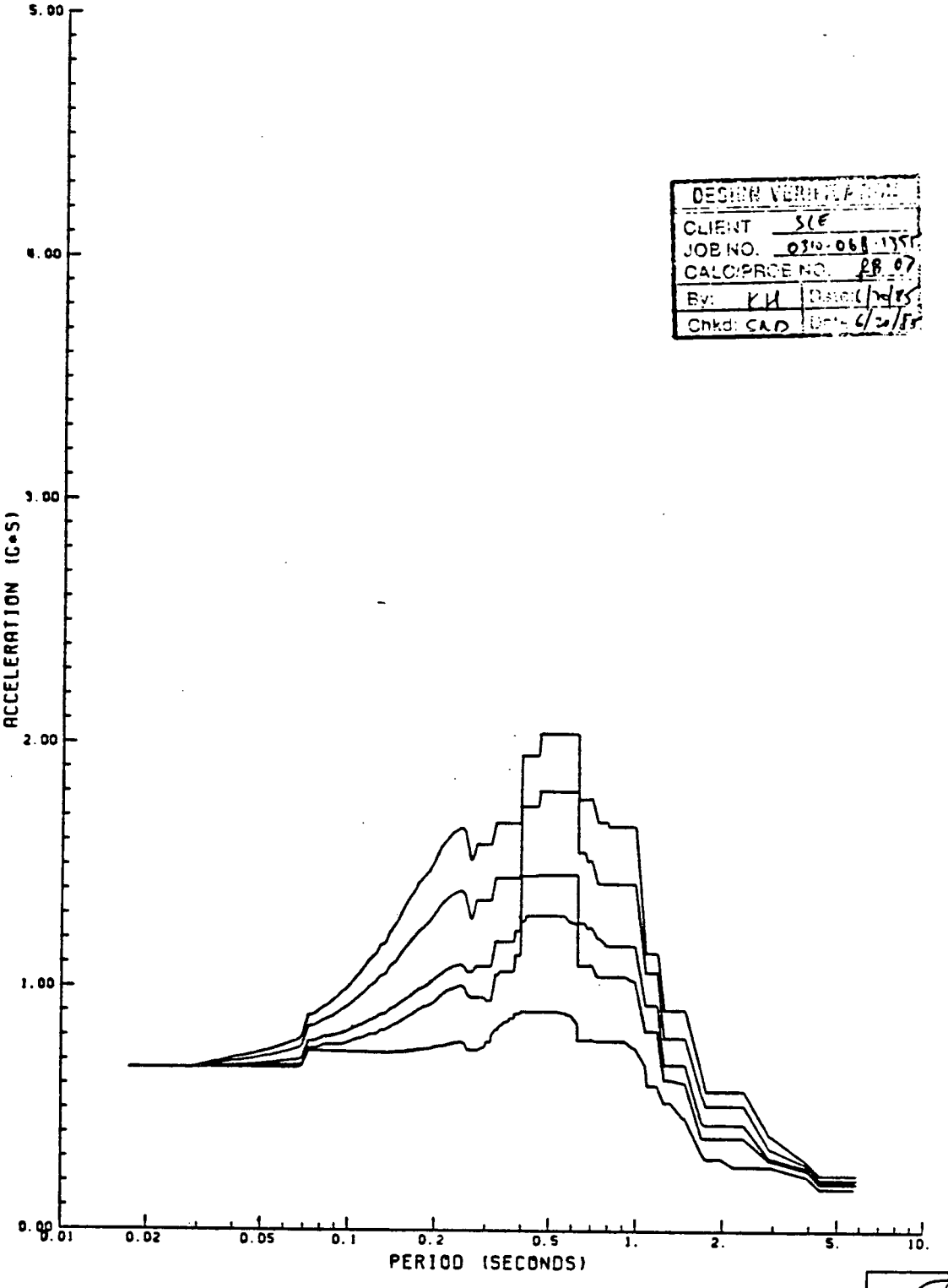

DESIGN VERIFICATION
CLIENT SCE
JOB NO. 0310-068-135
CALC/PRICE NO. 88.07
By: KH Date: 6/20/85
Chkd: CAD Date: 6/20/85

SPECTRA SONGS-1 REACTOR BLDG. N-S DIR. ENVELOPED WITH HOUSNER RESPONSE
OPERATING DECK EL. 40.5 FT NODES 1,82,102,202,345,648
DAMPING 2%, 3%, 5%, 7%, 15%

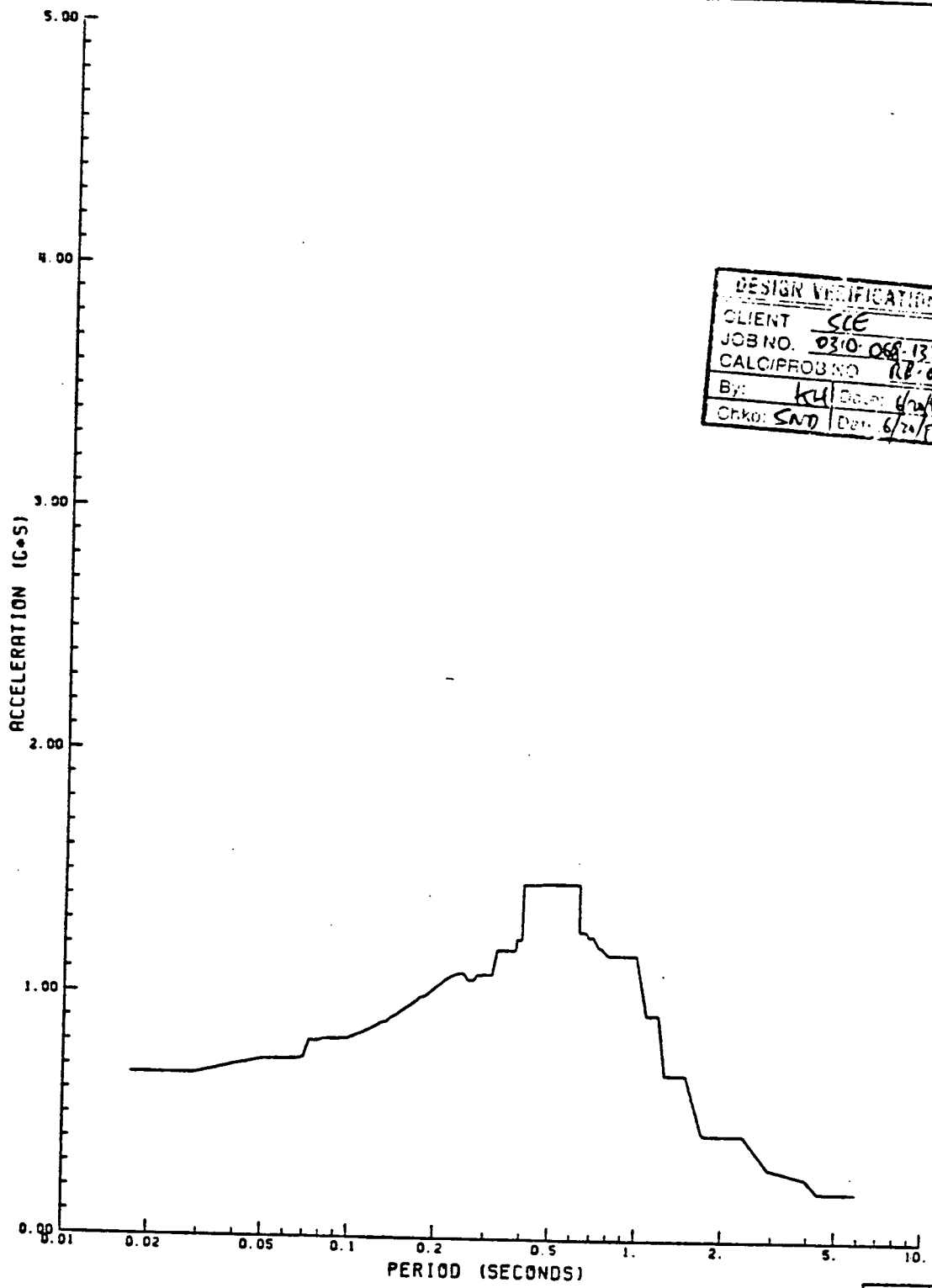

DESIGN VERIFICATION
CLIENT SCE
JOB NO. 0310-068-1351
CALC/PROB NO RB-04
By: KH Date: 6/24/91
Chkd: SND Date: 6/24/91

SPECTRA SONGS-1 REACTOR BLDG. N-S DIR. ENVELOPED WITH HOUSNER RESPONSE
OPERATING DECK EL. 40.5 FT NODES 1,82,102,202,345,648
DAMPING PVRC DAMPING CASE 2

IMPELL CORPORATION

REACTOR BUILDING

DISCUSSION OF RESULTS

IMPELL

REACTOR BUILDING

MARGINS REMAINING IN FLOOR RESPONSE SPECTRA

- NO DECONVOLUTION TAKEN (40 TO 60 PERCENT REDUCTION)
- FREE FIELD TIME HISTORIES HAVE EXCESS ENERGY (10 TO 20 PERCENT REDUCTION)

CONCLUSION

- FLOOR SPECTRA HAVE AMPLE MARGIN

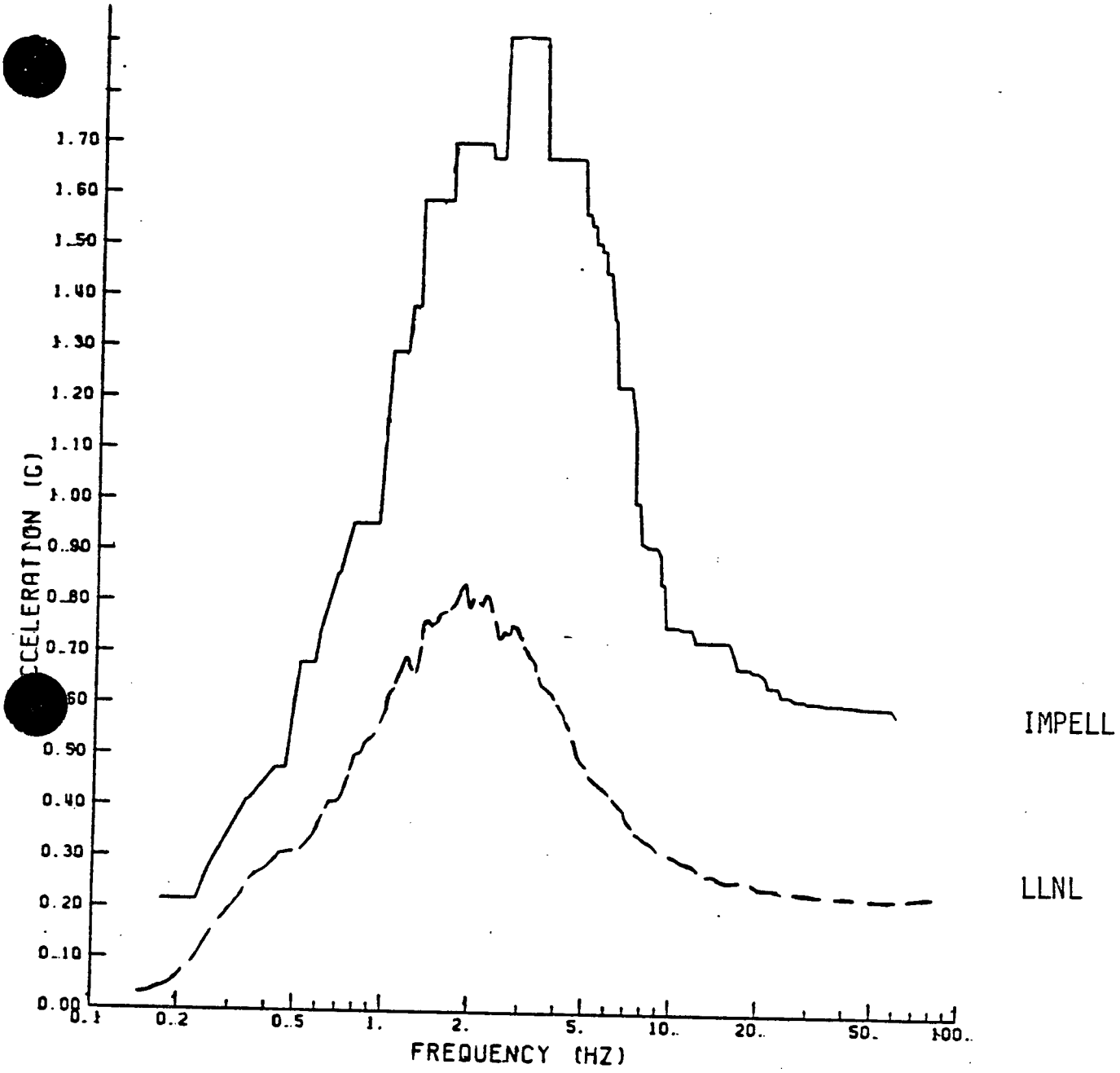

SPECTRA SONGS-1 REACTOR BLDG. E-W DIR. RESPONSE
NODE 1048 ELEV. 0 FT.
DAMPING 2%

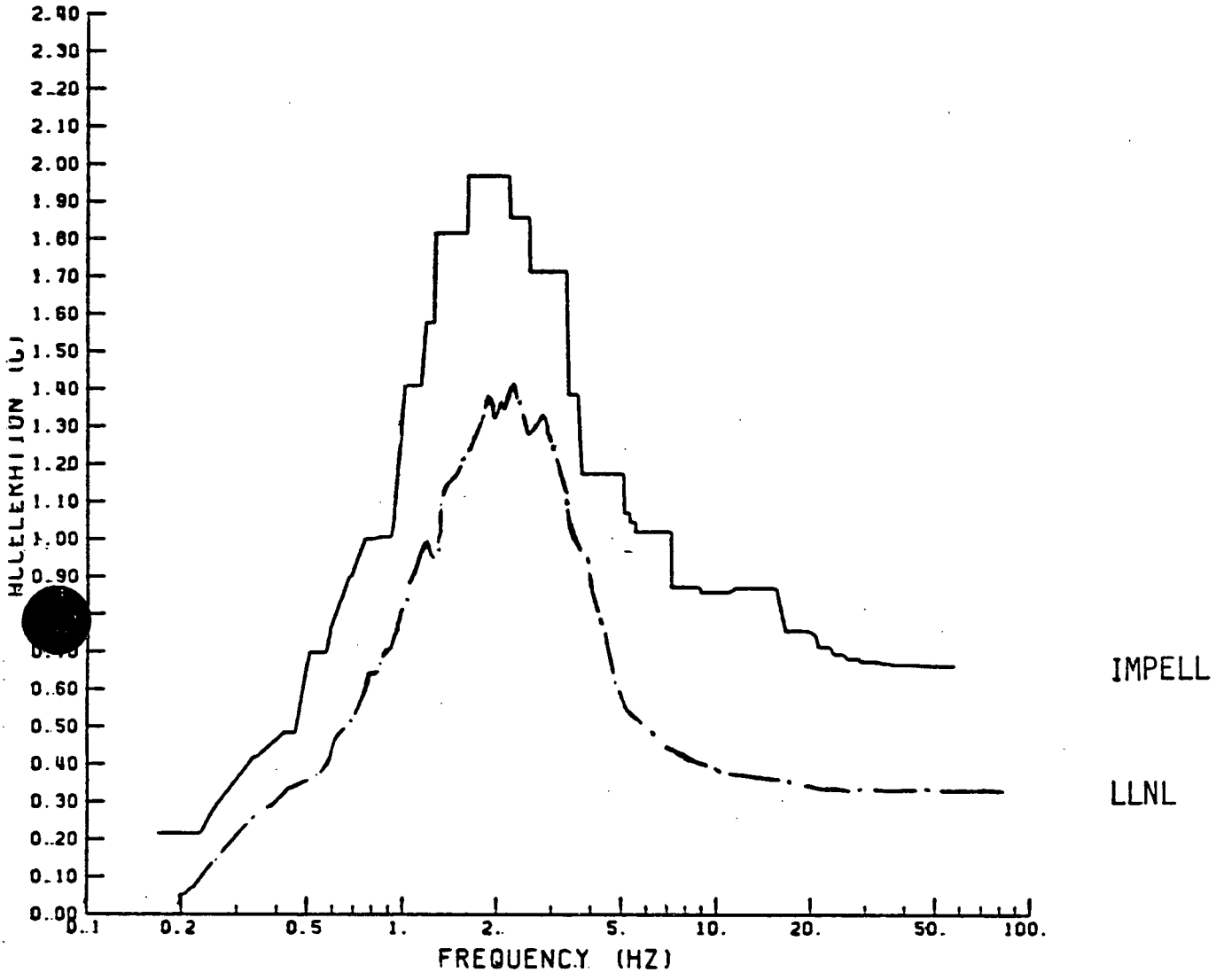

SPECTRA SONGS-1 REACTOR BLDG. E-W DIR. RESPONSE
ERATING DECK EL. 40.5 FT NODES 1,82,102,202,345,648
DAMPING 2%

IMPELL CORPORATION

TURBINE BUILDING

PURPOSE

- TO GENERATE FLOOR RESPONSE SPECTRA IN THE TURBINE BUILDING

IMPELL CORPORATION

METHODOLOGY

1. BUILDING MODEL

- USE SAME TURBINE BUILDING MODEL PREVIOUSLY CREATED BY BPC USING BSAP PROGRAM.
- CONSIDER CASE OF IN-SITU SOIL.

2. SOIL PROPERTIES

- SOIL SPRINGS DEVELOPED BY WOODWARD CLYDE FOR EACH FOUNDATION, CONSIDERING IN-SITU SOIL PROPERTIES.
- COMPOSITE SOIL-STRUCTURE MODAL DAMPING LIMITED TO 20 PERCENT.
- SSI CONSIDERED BY LUMPED PARAMETER FREQUENCY INDEPENDENT METHOD.

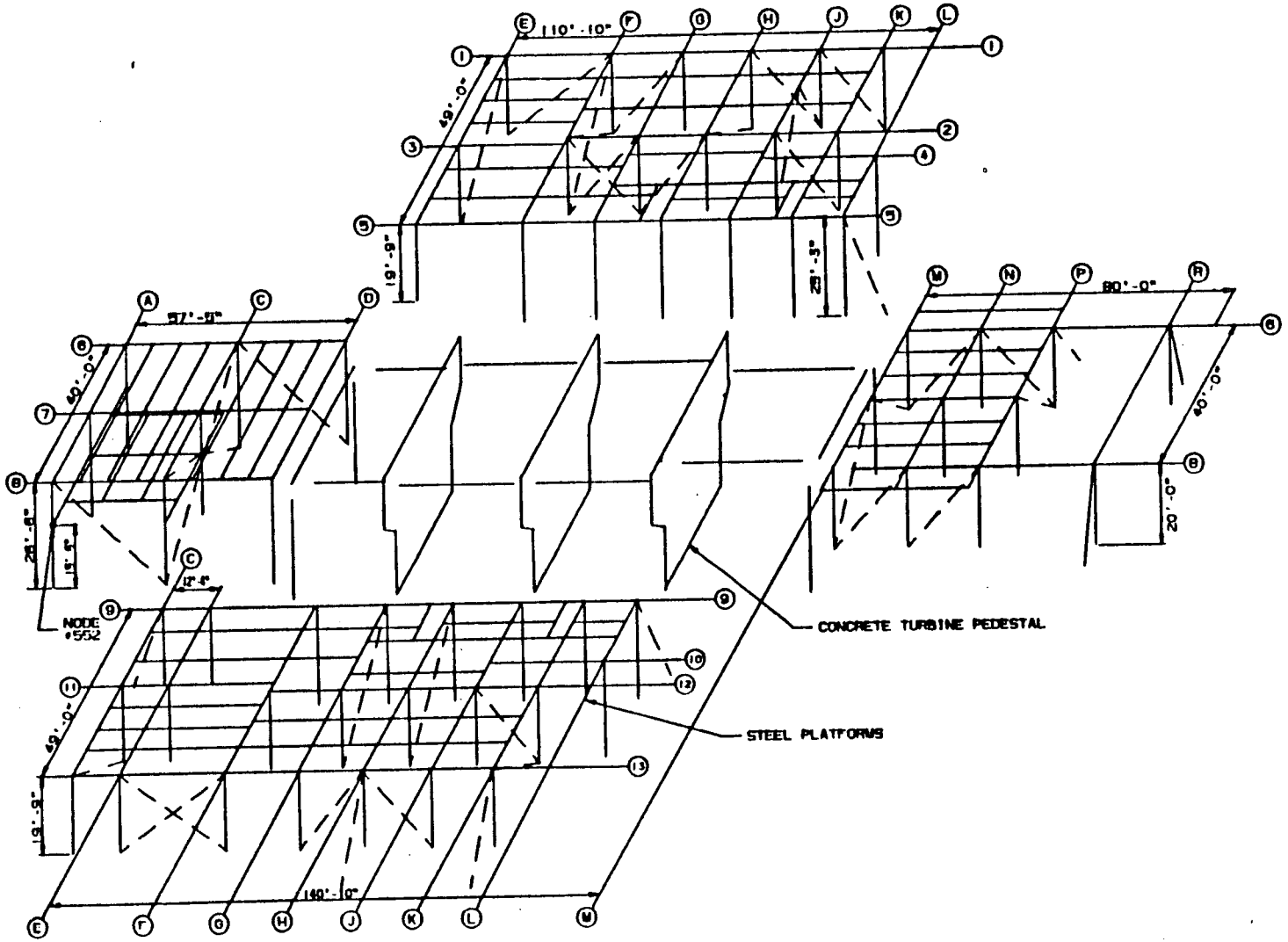

TURBINE BUILDING MODEL

IMPELL CORPORATION

METHODOLOGY (CONTINUED)

3. SOIL STRUCTURE INTERACTION ANALYSIS

- THE EDSGAP PROGRAM IS USED TO PERFORM THE TIME HISTORY SSI ANALYSIS.
- INPUT TO EDSGAP IS:
  - TURBINE BUILDING BSAP MODEL (ON SOIL SPRINGS), INCLUDING: MODE SHAPES, FREQUENCIES, MASS PARTICIPATION FACTORS, MASS MATRIX.
  - THREE SIMULTANEOUS COMPONENTS OF EARTHQUAKE.
- OUTPUT FROM EDSGAP IS:
  - TIME HISTORIES OF ACCELERATION AT ALL NODES WHERE FLOOR SPECTRA ARE DESIRED.

IMPELL CORPORATION

TURBINE BUILDING

NODES ENVELOPED	LOCATION
29, 71, 86	AREA 6 DECK (WEST HEATER PLATFORM) ELEV. 35.5 FEET
329, 371, 386	AREA 5 DECK (EAST HEATER PLATFORM) ELEV. 35.5 FEET
580, 586, 610	AREA 2 DECK (NORTH EXTENSION) ELEV. 42.0 FEET
620	AREA 2 MEZZANINE COLUMNS (NORTH EXT.) ELEV. 30.0 FEET
706, 732, 751	AREA 7 DECK (SOUTH EXTENSION) ELEV. 42.0 FEET
951	AREA 4 DECK (TURBINE PEDESTAL) ELEV. 42.0 FEET
1037, 1098	AREA 4 (TURBINE PEDESTAL) ELEV. 24.0 FEET

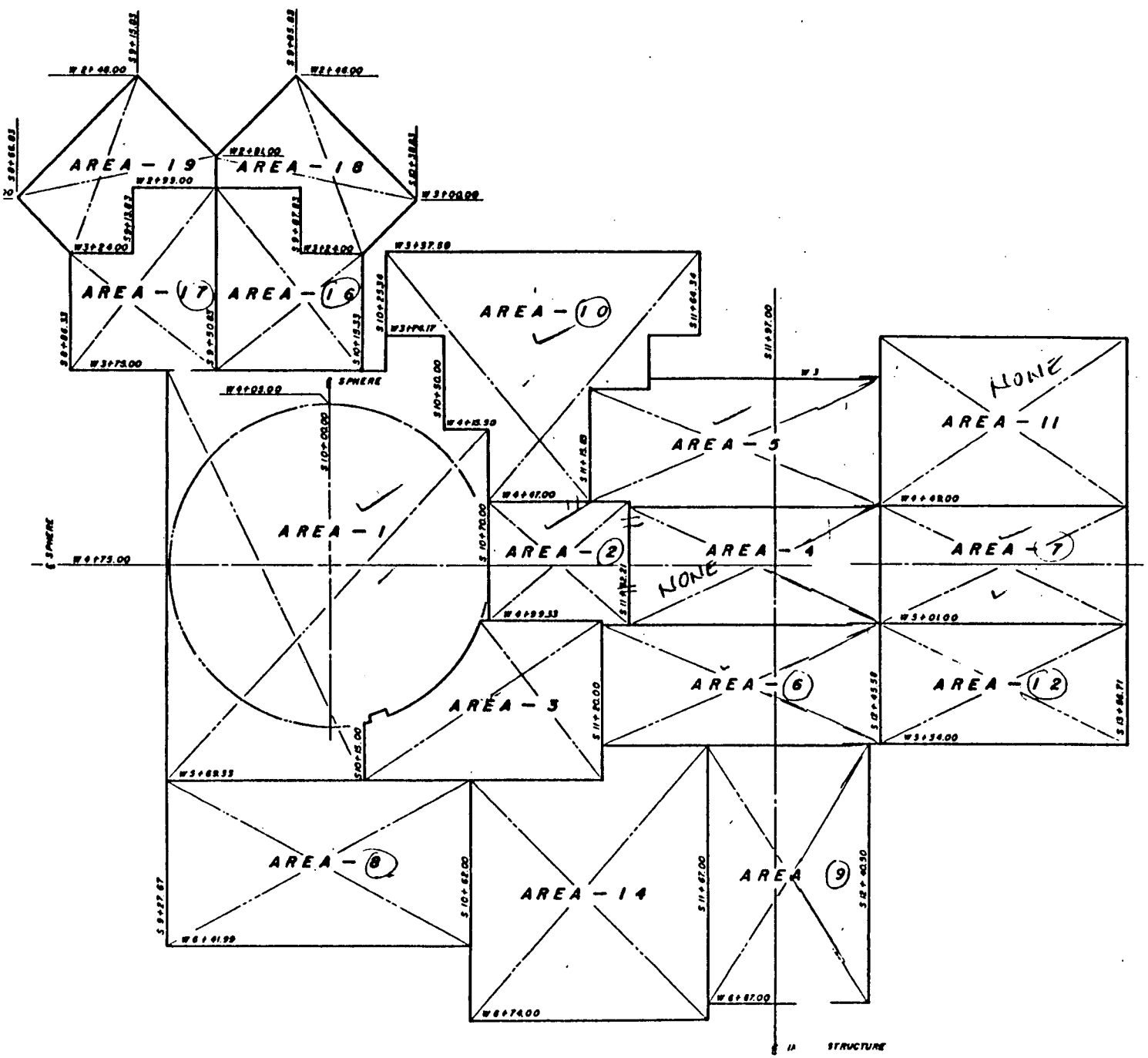
AREA – 19
AREA – 18
AREA – 17
AREA – 16
AREA – 10
AREA – 1
AREA – 2
AREA – 3
AREA – 4
AREA – 5
NONE
AREA – 11
AREA – 7
AREA – 6
AREA – 12
AREA – 8
AREA – 14
AREA 9
℄ SPHERE
℄ STRUCTURE

IMPELL CORPORATION

METHODOLOGY (CONTINUED)

4. GENERATION OF FLOOR RESPONSE SPECTRA

- RAW FLOOR RESPONSE SPECTRA ARE CALCULATED AT FIVE DAMPING VALUES (2%, 3%, 5%, 7%, 15%) FROM THE EDSGAP OUTPUT TIME HISTORIES.

- RAW FLOOR RESPONSE SPECTRA ARE CORRECTED TO ACCOUNT FOR DIFFERENCES BETWEEN THE FREE FIELD INPUT SPECTRA OF THE ARTIFICIAL TIME HISTORY MOTIONS AND THE MODIFIED HOUSNER DESIGN SPECTRA.

- RAW CORRECTED FLOOR RESPONSE SPECTRA ARE ENVELOPED FOR SEVERAL NODES TO PRODUCE A SINGLE FLOOR SPECTRA. EXAMPLE: THREE NODES ON THE WEST HEATER PLATFORM.

- ALL SPECTRA ARE BROADENED, ±15%, TO ACCOUNT FOR UNCERTAINTIES IN THE ANALYSIS.

- FOR PIPING ANALYSIS PURPOSES USING PVRC FREQUENCY-DEPENDENT DAMPING, A SET OF PVRC SPECTRA ARE PRODUCED. (FROM 0 TO 10 HZ, DAMPING IS 5 PERCENT; FROM 10 TO 20 HZ, DAMPING RANGES FROM 5 TO 2 PERCENT; OVER 20 HZ, DAMPING IS 2 PERCENT.)

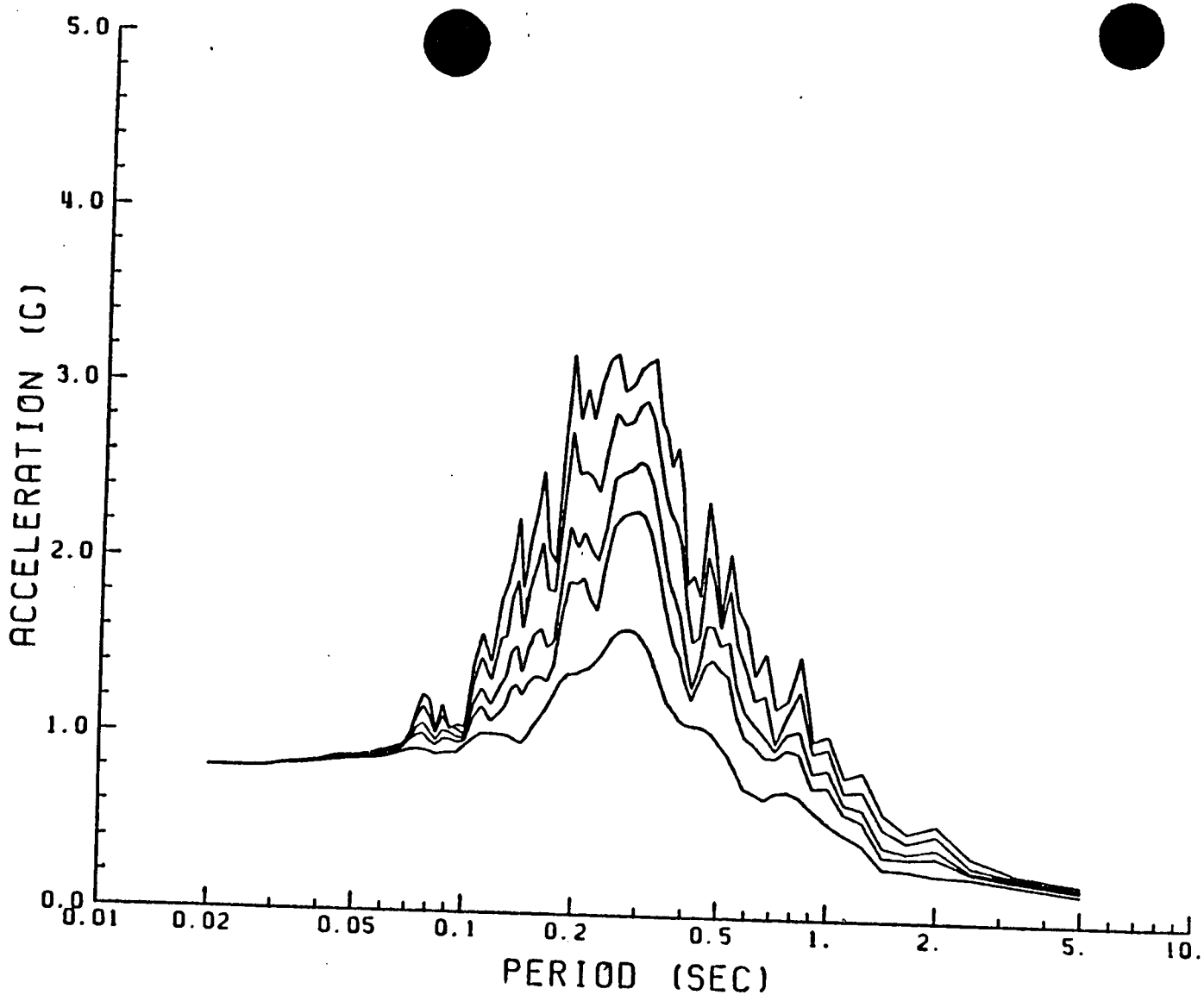

SCE-SONGS1
TURBINE BUILDING SPECTRA / INSITU SOIL / CRANE SOUTH
NODE 29 X-DIR (AREA 6 ELEVATION 35.5 FT)

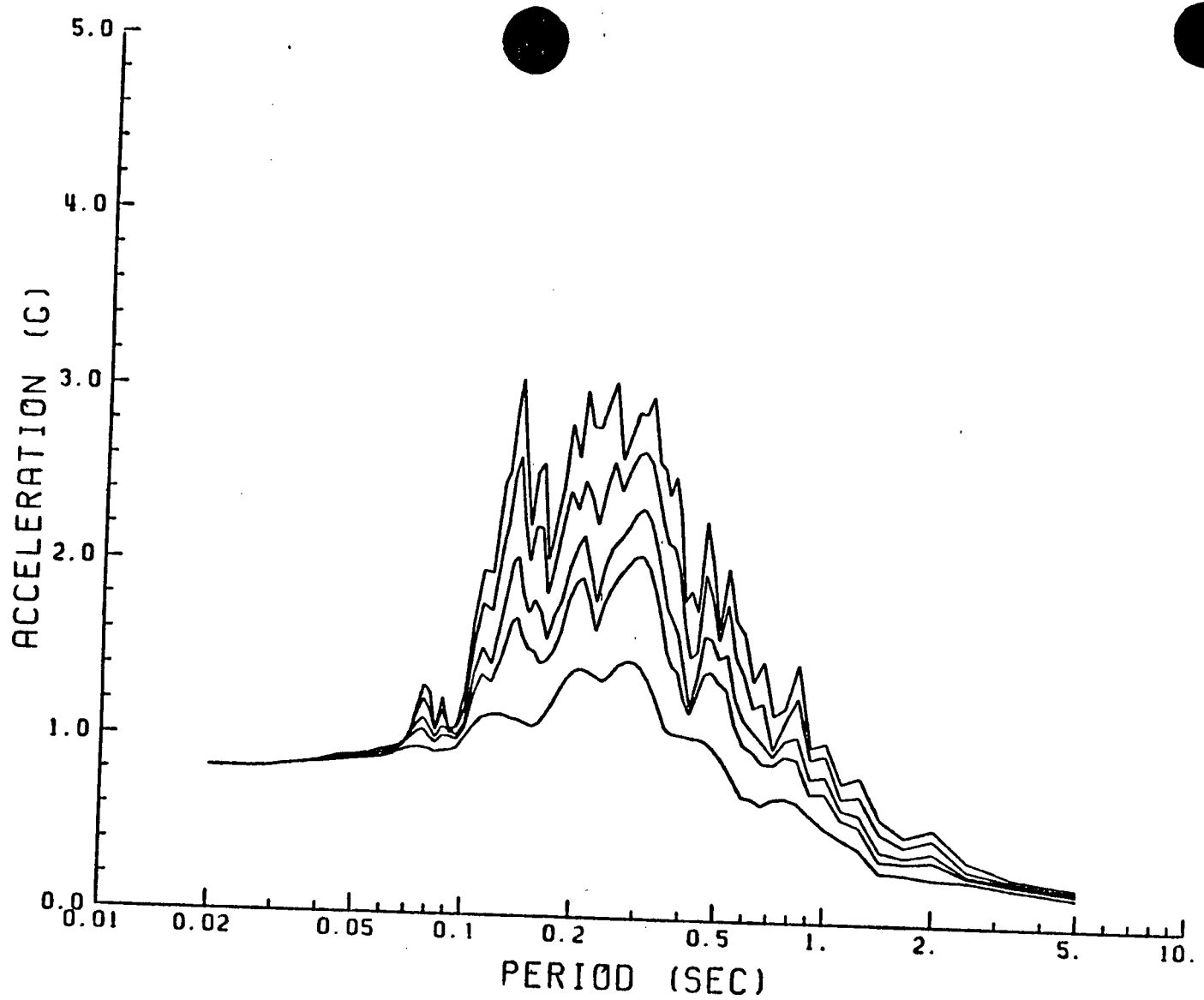

SCE-SONGS1
TURBINE BUILDING SPECTRA / INSITU SOIL / CRANE SOUTH
NODE 71 X-DIR (AREA 6 ELEVATION 35.5 FT)

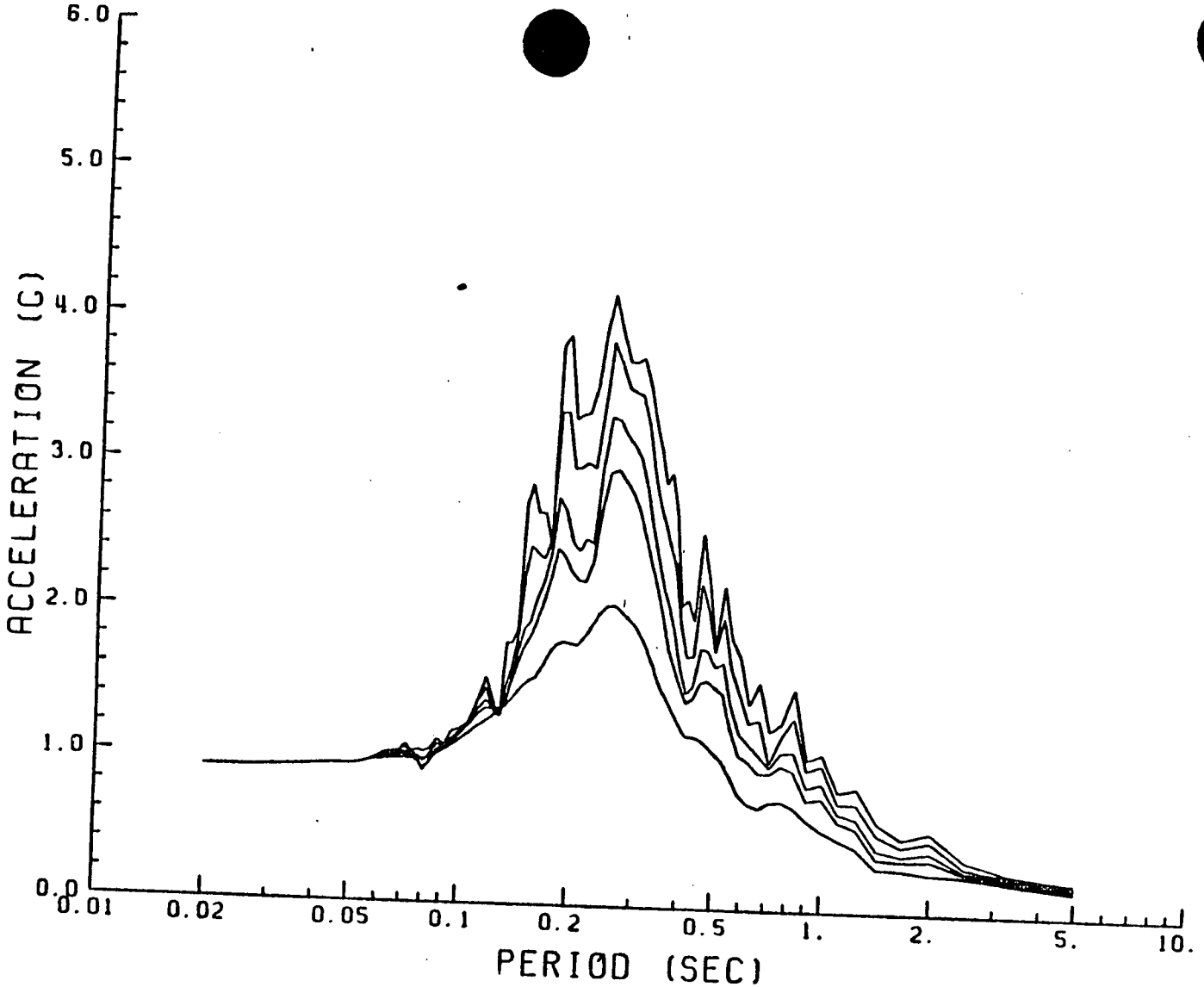

INFORMATION ONLY

SCE-SONGS1
TURBINE BUILDING SPECTRA / INSITU SOIL / CRANE SOUTH
NODE 86 X-DIR (AREA 6 ELEVATION 35.5 FT)

IMPELL CORPORATION

METHODOLOGY (CONTINUED)

5. CORRECTION FACTORS

- AS PREVIOUSLY DISCUSSED, THE FREE FIELD ARTIFICIAL TIME HISTORIES PRODUCE ENVELOP RESPONSE SPECTRA WHICH ARE NOT PERFECT MATCHES WITH THE MODIFIED HOUSNER DESIGN RESPONSE SPECTRA.

- ON AVERAGE, FROM 0.2 HZ TO 33 HZ, THE ENVELOP RESPONSE SPECTRA EXCEED THE DESIGN SPECTRA BY:

DAMPING LEVEL	CONSERVATISM (= (ENVELOP-DESIGN)/(DESIGN))
2%	6% - 10%
4%	16% - 20%
7%	14% - 17%
20%	23% - 26%

- A SIMPLE CORRECTION FACTOR BASED SOLELY ON THE ABOVE CONSERVATISMS OVER SIMPLIFIES THE EFFECTS, AS THE CONSERVATISM IS NOT CONSTANT OVER THE 0.2 HZ TO 33 HZ RANGE.

IMPELL CORPORATION

METHODOLOGY (CONTINUED)

5. CORRECTION FACTORS (CONTINUED)

- AN ACCURATE CORRECTION FACTOR IS CALCULATED FOR EACH NODE IN THE TURBINE BUILDING WHERE FLOOR SPECTRA ARE CALCULATED. THE CORRECTION FACTOR VARIES FOR EACH FLOOR SPECTRA DAMPING VALUE (2%, 3%, 5%, 7%, 15%), AND FOR EACH OF EIGHTY CALCULATION FREQUENCIES FOR THE SPECTRA.

- THE DIRECT GENERATION METHODOLOGY IS USED TO CALCULATE THESE CORRECTION FACTORS.

DIRECT GENERATION METHODOLOGY FOR CORRECTION FACTORS

- METHOD USED IS BASED ON FLORA.

- SUMMARY OF METHOD:

  - USE DIRECT GENERATION METHOD TO CALCULATE FLOOR RESPONSE SPECTRA AT ALL DESIRED NODES, AT ALL DESIRED DAMPING VALUES.

  - CALCULATE THESE SPECTRA TWICE.
    CASE 1: INPUT SPECTRA = ENVELOP (FROM ARTIFICIAL TIME HISTORIES)
    CASE 2: INPUT SPECTRA = DESIGN (MODIFIED HOUSNER)

METHODOLOGY (CONTINUED)

5. CORRECTION FACTORS (CONTINUED)

- CORRECTION FACTOR = $R_n\ (\omega,\xi) = \dfrac{S_d\ (\omega,\xi)}{S_e\ (\omega,\xi)}$

  R_n = CORRECTION FACTOR AT NODE n, FREQUENCY ω, DAMING ξ

  S_d = DIRECT GENERATION FLOOR SPECTRA ORDINATE, USING DESIGN INPUT SPECTRA, AT NODE n, FREQUENCY ω, DAMPING ξ

  S_e = DIRECT GENERATION FLOOR SPECTRA ORDINATE, USING ENVELOP INPUT SPECTA, AT NODE n, FREQUENCY ω, DAMPING ξ

- FINAL SPECTRA = $S_f\ (\omega,\xi) = R_n\ (\omega,\xi) * S_{th}\ (\omega,\xi)$

  S_f = FINAL SPECTRA

  S_{th} = TIME HISTORY FLOOR SPECTRA ORDINATE, USING ARTIFICIAL TIME HISTORY MOTIONS, AT NODE n, FREQUENCY ω, DAMPING ξ

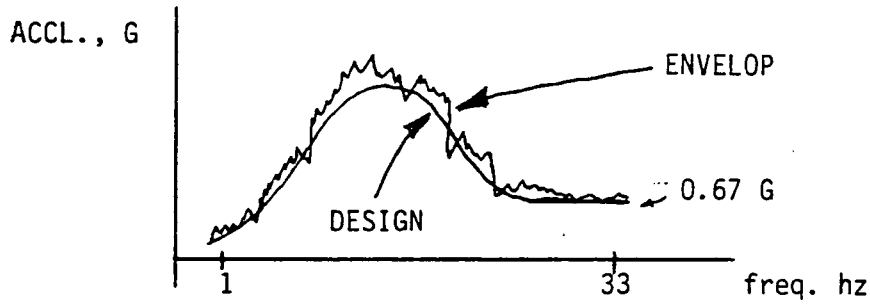

1. RUN TIME HISTORY ANALYSIS OF TURBINE BUILDING WITH EDSGAP: USE ARTIFICIAL TIME HISTORIES
2. DEVELOP FLOOR SPECTRA FROM TIME HISTORIES
3. RUN DIRECT GENERATION ANALYSIS OF TURBINE BUILDING WITH FLORA METHODOLOGY: RUN THIS TWICE, USING ENVELOP AND DESIGN INPUT SPECTRA
4. RESULTS:

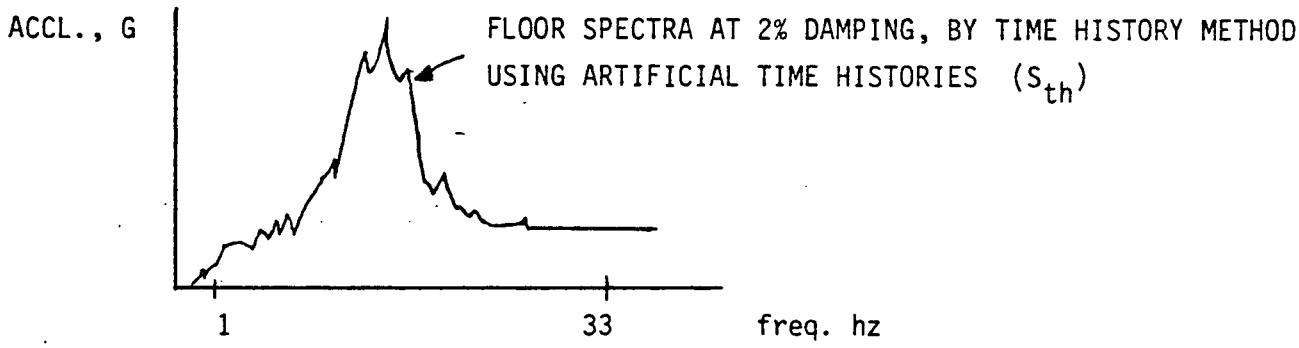

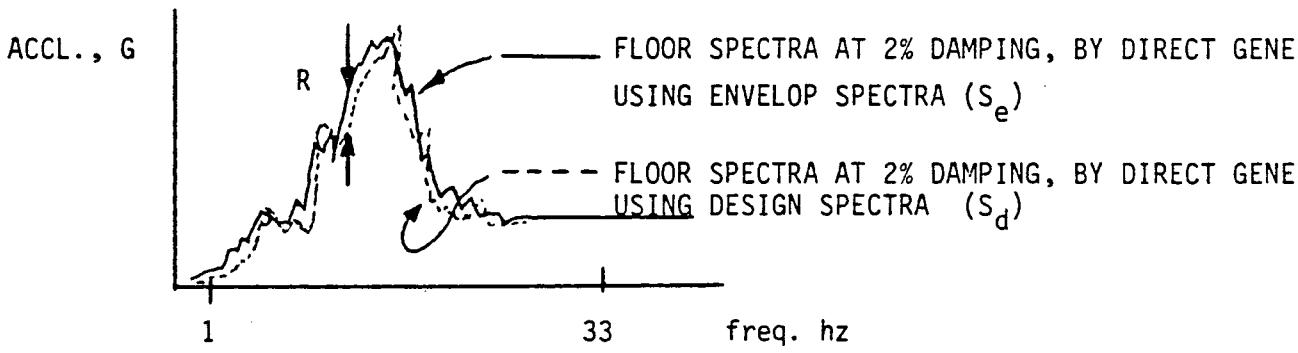

R = CORRECTION FACTOR = RATIO BETWEEN TWO DIRECT GENERATION SPECTRA

5. FINAL SPECTRA = S_f = R * S_{th}

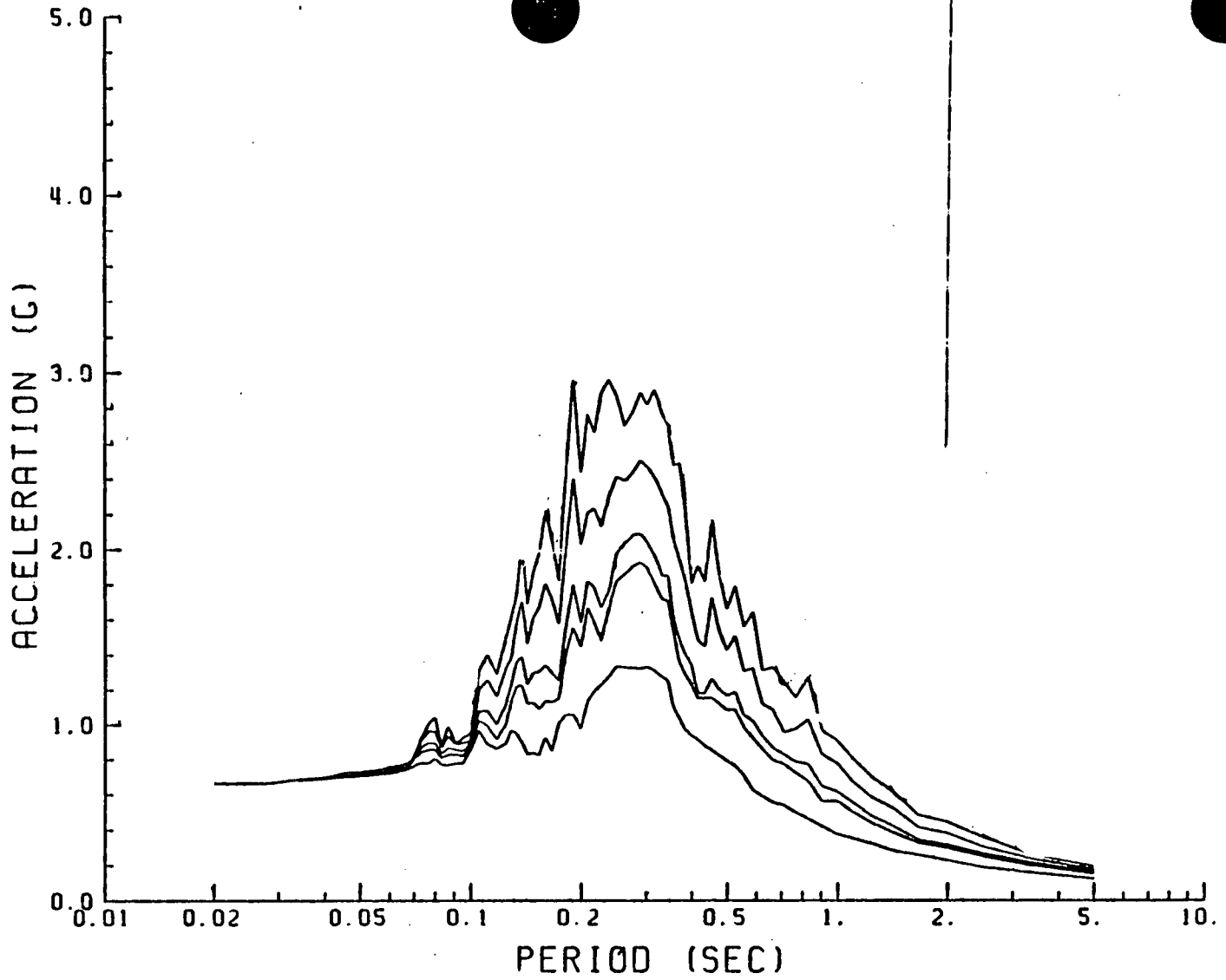

INFORMATION ONLY

SCE-SONGS1
TURBINE BUILDING / INSITU SOIL / CRANE SOUTH
2, 3, 5, 7, 15% DAMPING CORRECTED RESPONSE SPECTRA
NODE 22 X DIR (ORED 6 ELEVATION 35.5 FT)

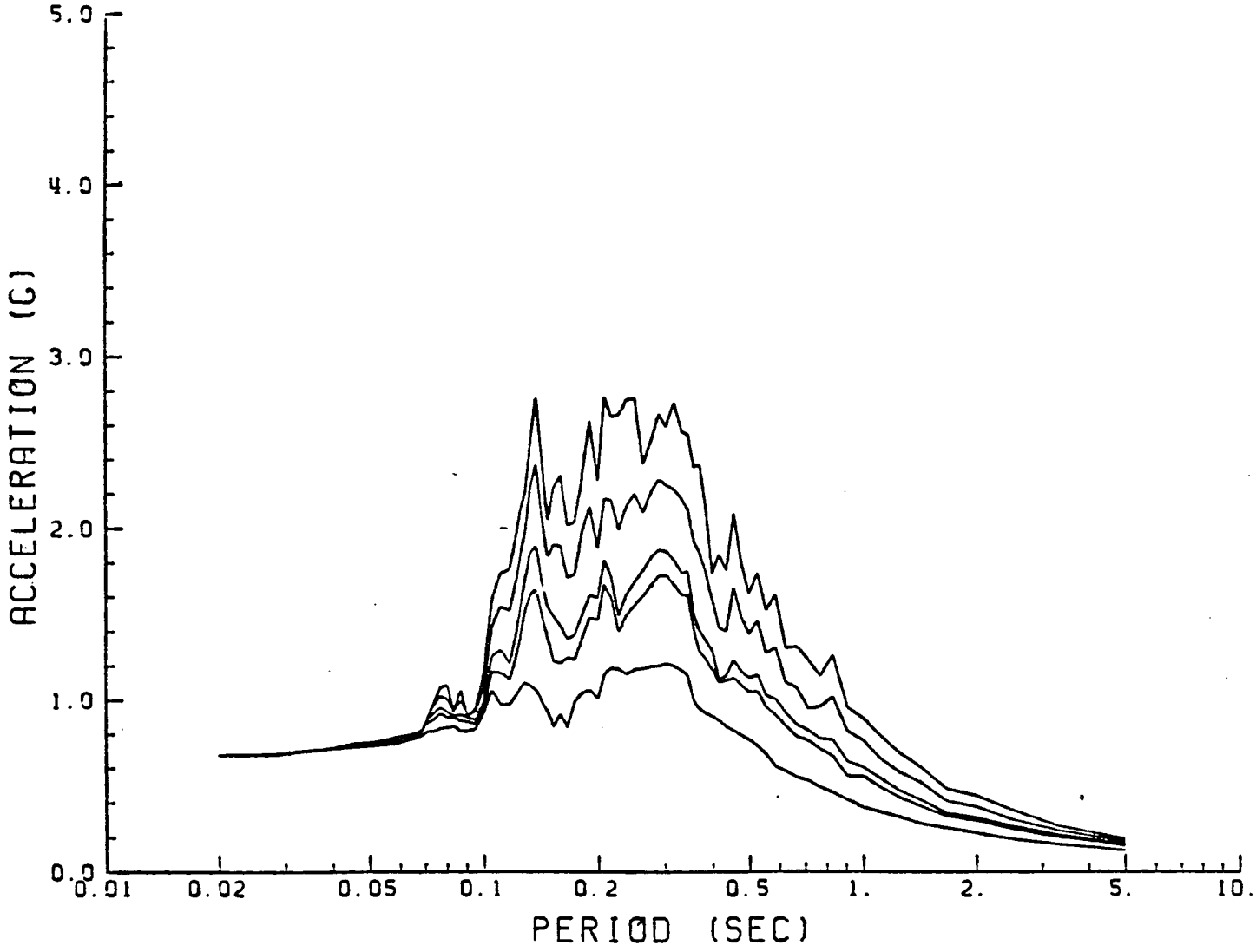

SCE-SONGS1
TURBINE BUILDING / INSITU SOIL / CRANE SOUTH
3, 5, 7, 15% DAMPING [illegible] RESPONSE SPECTRA
NODE 71 X-DIR (AREA 6 ELEVATION 35.5 FT)

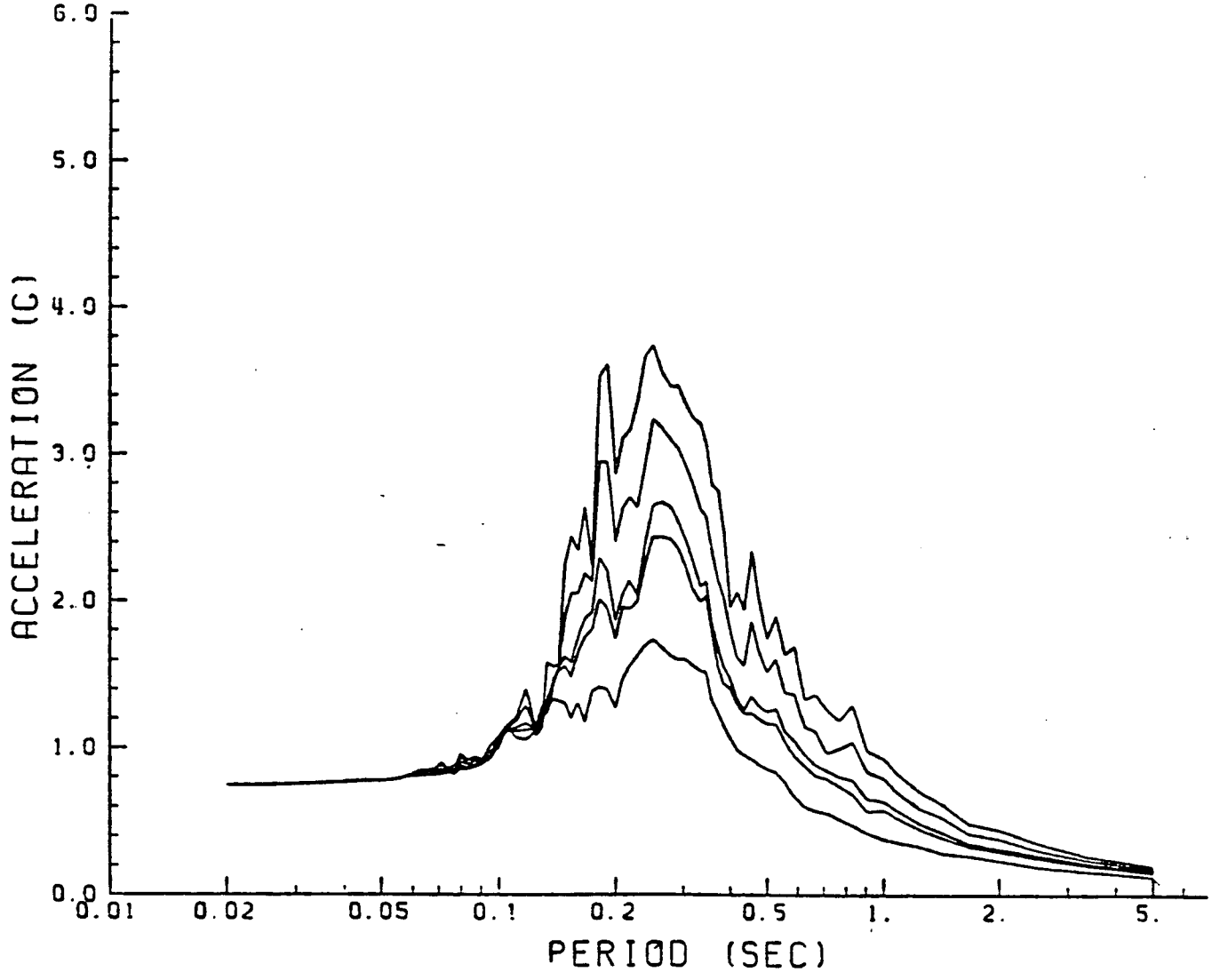

SCE-SONGS1
TURBINE BUILDING / INSITU SOIL / CRANE SOUTH
2, 3, 5, 7, 15% DAMPING CORRECTED RESPONSE SPECTRA
NODE 86 X-DIR (AREA 6 ELEVATION 35.5 FT)

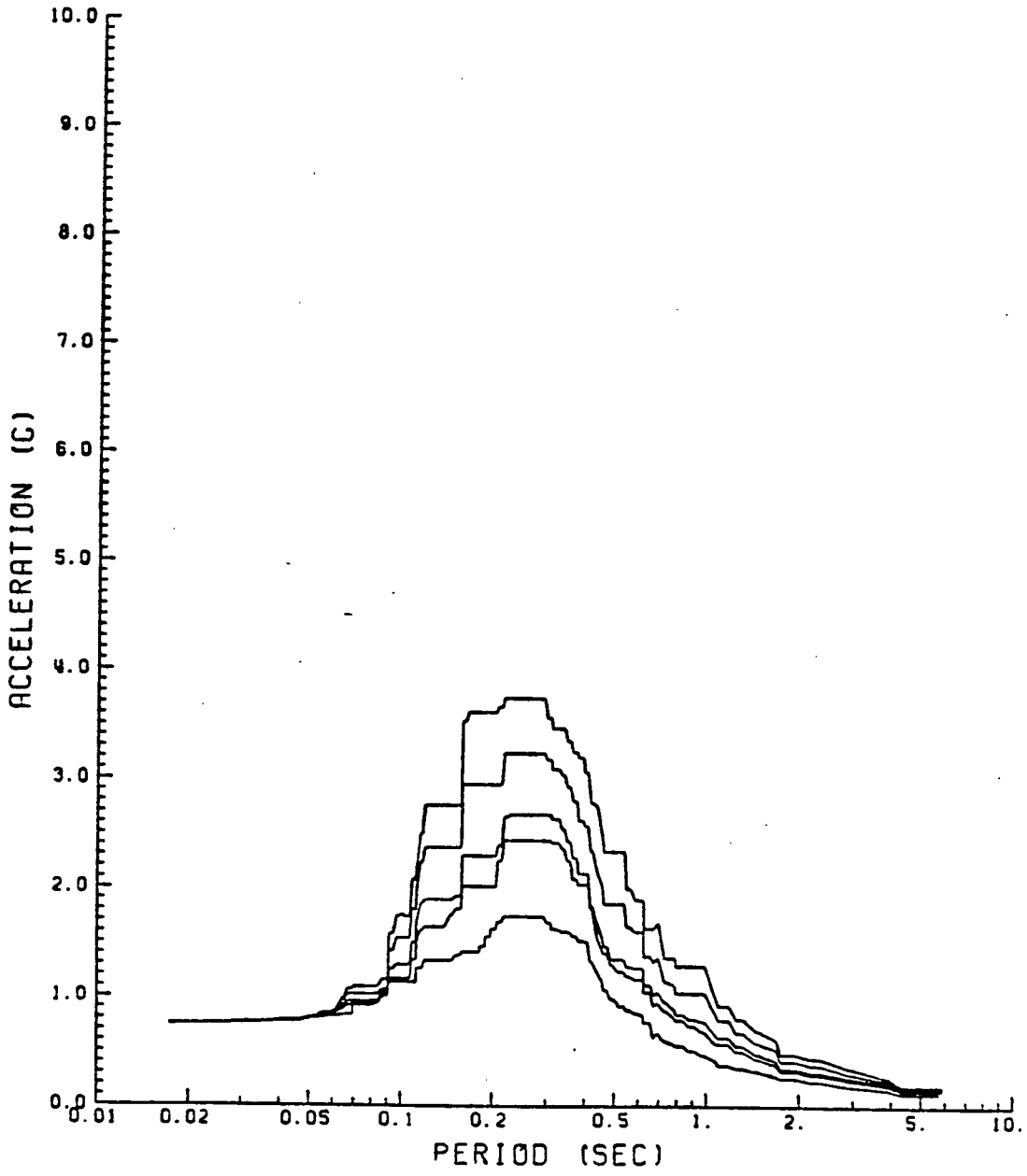

SCE-SONGS1
TURBINE BUILDING / INSITU SOIL / CRANE SOUTH,
2, 3, 5, 7, AND 15% DAMPING RESPONSE SPECTRA CORRECTED
MODIFIED HOUSNER EARTHQUAKE NORTH-SOUTH DIR.
AT EL. (+) 35 FT. 6 IN. AREA 6 DECK (A-59)

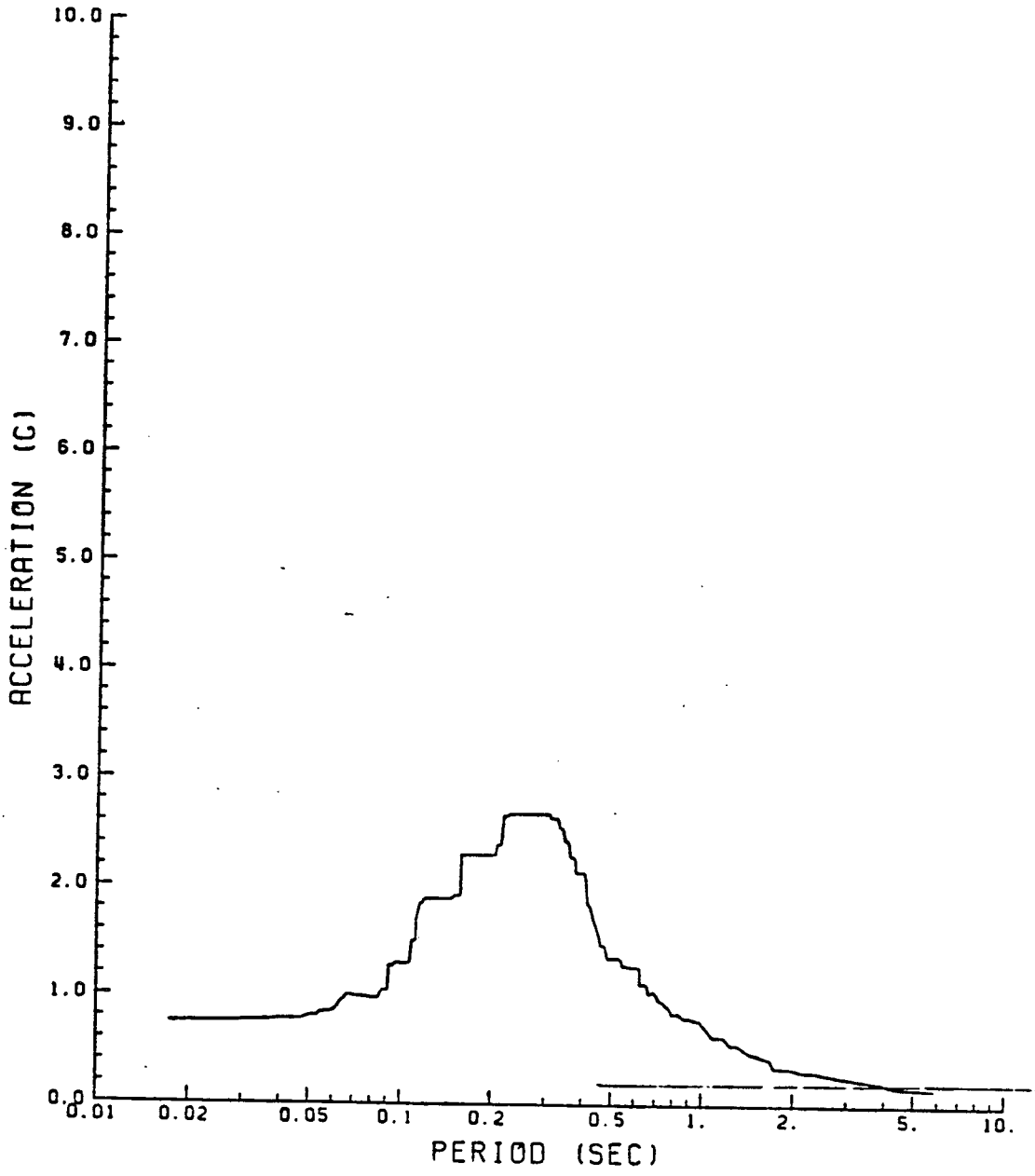

SCE-SONCS1
TURBINE BUILDING / INSITU SOIL / CRANE SOUTH
PVRC DAMP. RESPONSE SPECTRA CORRECTED
MODIFIED HOUSNER EARTHQUAKE NORTH-SOUTH DIR.
AT EL. (+) 35 FT. 6 IN. AREA 6 DECK (A-59)

INFORMATION ONLY

IMPELL CORPORATION

TURBINE BUILDING

DISCUSSION OF RESULTS

IMPELL CORPORATION

TURBINE BUILDING

- DEVELOPMENT OF FLOOR SPECTRA, THROUGH TIME HISTORIES: THIS IS TRADITIONAL SEISMIC ANALYSIS OF AN ESSENTIALLY SINGLE FLOOR BUILDING, ON SOIL SPRINGS. THE ONLY DIFFERENCE WITH PREVIOUS BPC ANALYSIS IS THAT THREE EARTHQUAKE MOTIONS ARE APPLIED SIMULTANEOUSLY.

- DEVELOPMENT OF CORRECTION FACTORS: DIRECT GENERATION METHODOLOGY WAS APPROVED BY NRC FOR THIS PROJECT. IMPELL HAS APPLIED IT TWICE, AND THEN TOOK THE RATIOS OF THE SPECTRA. THE RATIOS THEN ARE MULTIPLIED BY THE SPECTRA DEVELOPED BY TRADITIONAL TIME HISTORY METHOD TO PRODUCE THE FINAL SPECTRA.

  THEREFORE, THE RATIOING OF THE DIRECT GENERATION RESULTS ELIMINATES ANY UNCERTAINTY INTRODUCED BY THE DIRECT GENERATION METHOD.

  THEREFORE, THE FINAL FLOOR SPECTRA ARE ACCURATE.

IMPELL CORPORATION

TURBINE BUILDING

MARGINS REMAINING IN FLOOR RESPONSE SPECTRA

- SOIL DAMPING (MATERIAL PLUS RADIATION) LIMITED TO 20 PERCENT (10 TO 20 PERCENT REDUCTION).
- NODES ENVELOPED TO PRODUCE DESIGN SPECTRA (5 TO 30 PERCENT REDUCTION IN SOME FREQUENCY RANGES).

CONCLUSION

- FLOOR SPECTRA HAVE AMPLE MARGIN.

SAN ONOFRE NUCLEAR GENERATING STATION UNIT 1

LONG TERM SEISMIC REEVALUATION PROGRAM

CALCULATION OF PIPING STRAINS FROM LINEAR, ELASTICALLY - CALCULATED STRESSES

CONTENTS

- STRAIN LIMITS
- PIPING ANALYSIS PROCEDURE
- DEVELOPMENT OF STRAIN CALCULATION METHODOLOGY
- SUMMARY

STRAIN LIMITS

- CARBON STEEL

$$\varepsilon \leq 0.01 \quad (1\%)$$

- STAINLESS STEEL

$$\varepsilon \leq 0.02 \quad (2\%)$$

- CONSIDERATIONS FOR EXCEEDING STAINLESS STEEL 1% STRAIN LIMITS

  - FATIGUE EVALUATION
  - COMPRESSIVE STRAIN LIMITS (NUREG 1061 VOL. 2)

    $\varepsilon \leq 0.2 \ (T/R)$

PIPING ANALYSIS PROCEDURE

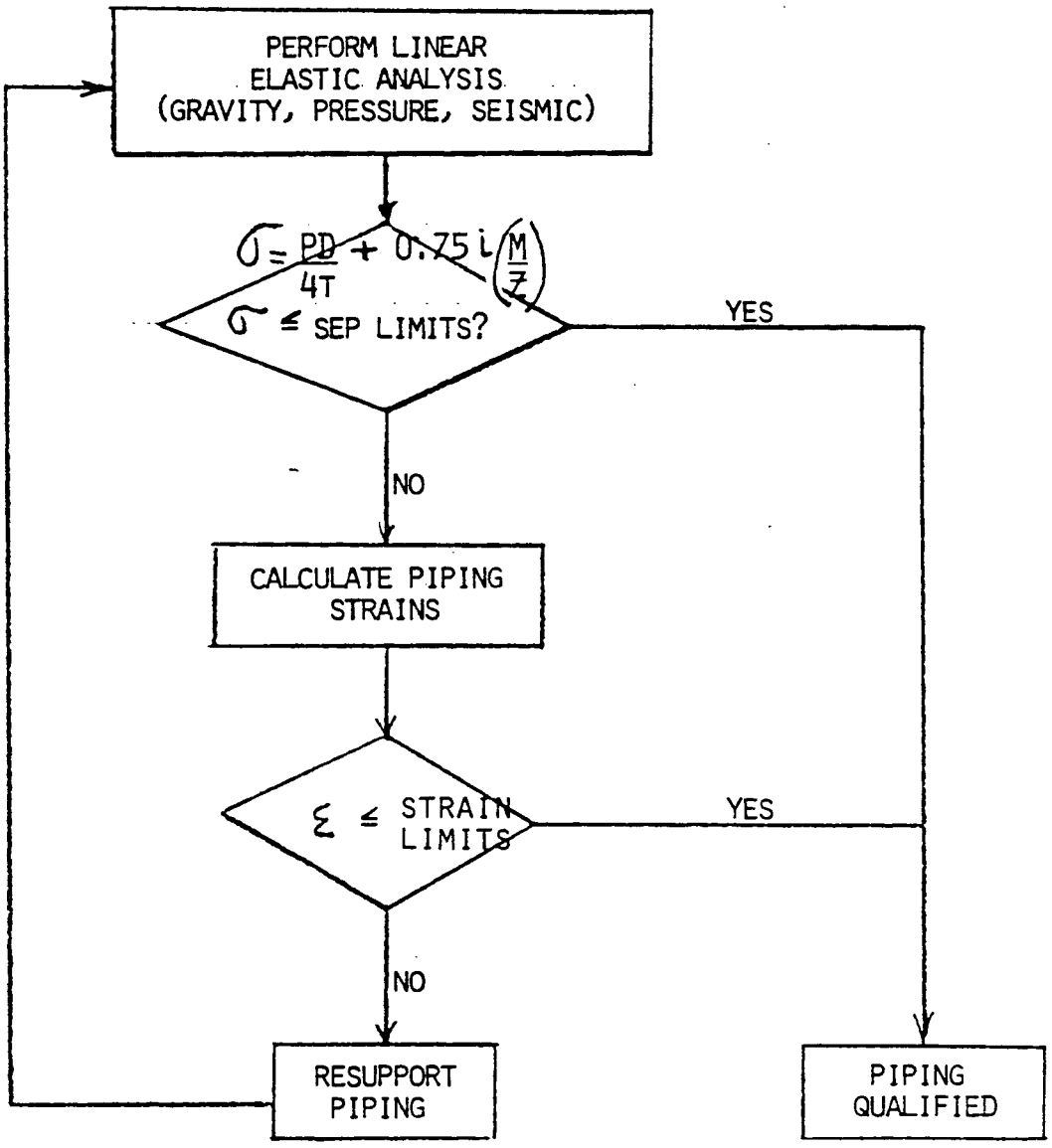

DEVELOPMENT OF STRAIN CALCULATION METHODOLOGY

- PURPOSE

  DEVELOP A PROCEDURE TO CALCULATE PIPING STRAINS FROM LINEAR ELASTICALLY - CALCULATED PIPING STRESSES

ELASTIC STRAIN VS. ACTUAL STRAIN

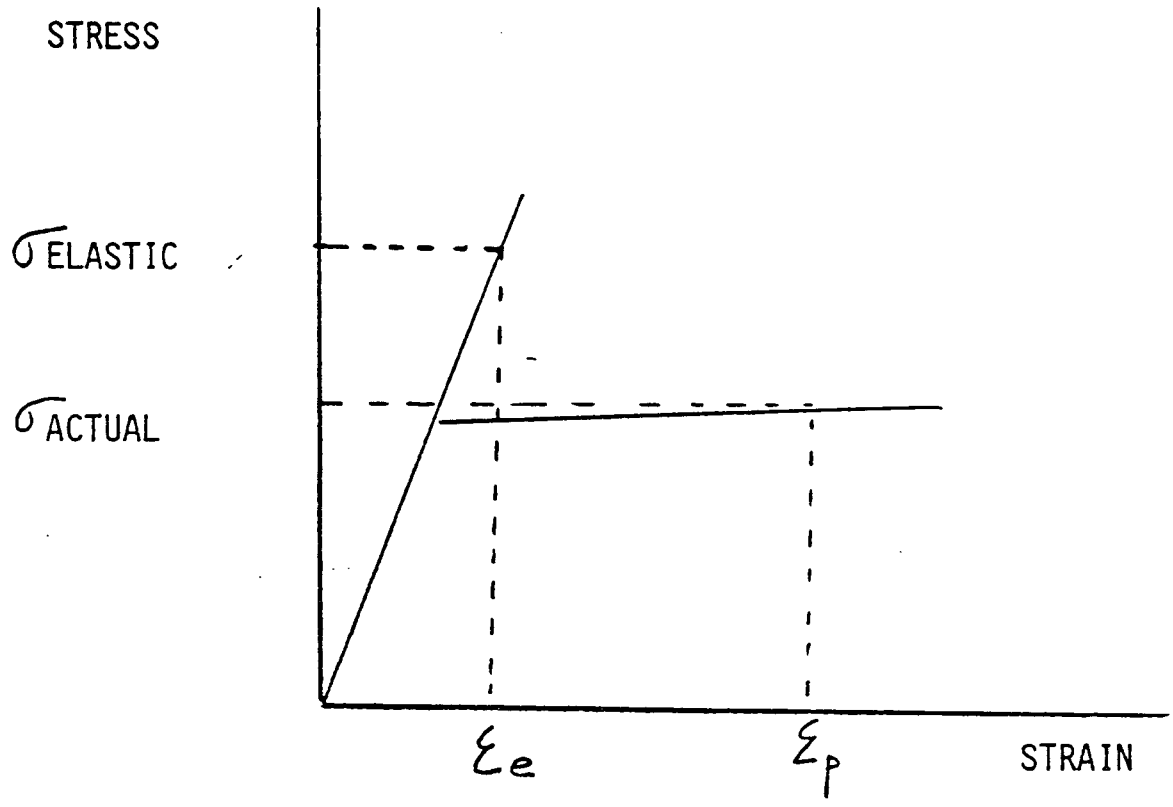

STRAIN CONCENTRATION EFFECTS

- TESTS ON NOTCHED SPECIMENS

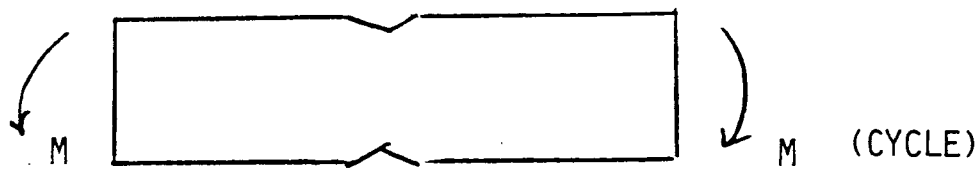

- ACTUAL STRAINS MEASURED AT NOTCH REGION

- ELASTIC STRAINS CALCULATED BASED ON STRESS ANALYSIS USING THEORETICAL STRESS CONCENTRATION FACTORS

STRAIN CONCENTRATION EFFECT (ACTUAL)

ACTUAL STRAIN

ELEASTICALLY-CALCULATED STRAIN

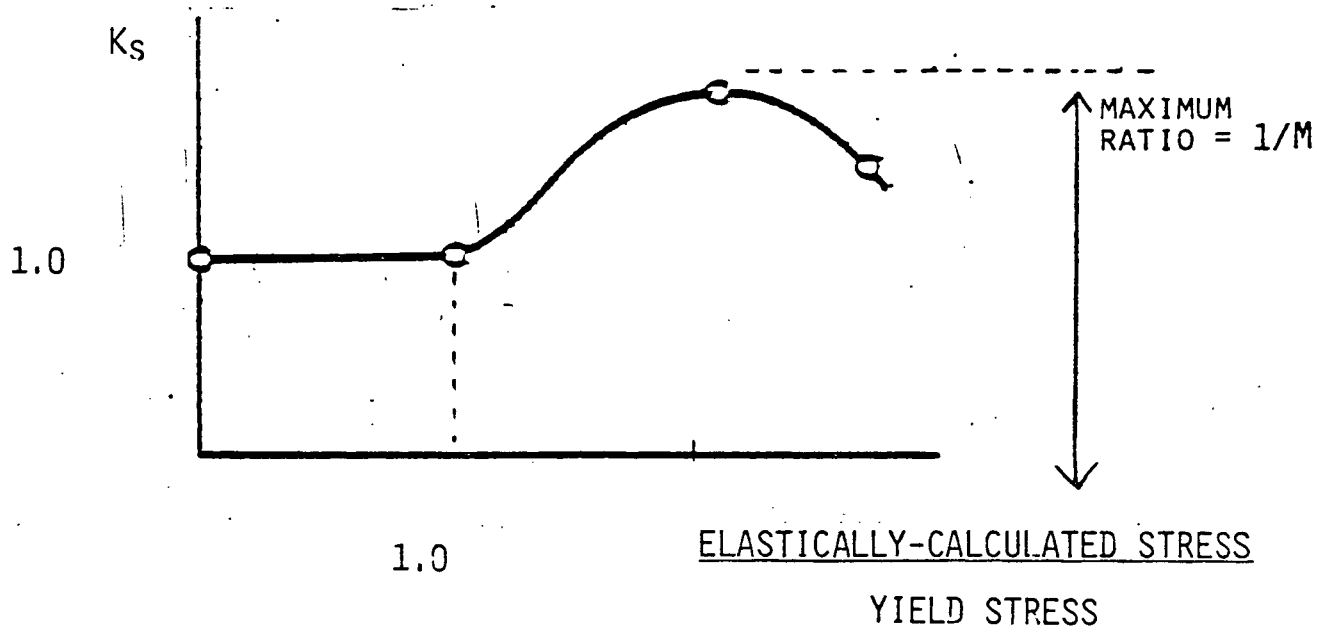

- BASED ON TESTS OF NOTCHED MEMBERS
- DEVELOPED FOR USE WHEN STRESSES EXCEED ELASTIC LIMIT
- MAXIMUM RATIO IS 1/M WHERE M IS STRAIN HARDENING EXPONENT OF MATERIAL.

STRAIN CONCENTRATION EFFECT (ANALYTICAL)

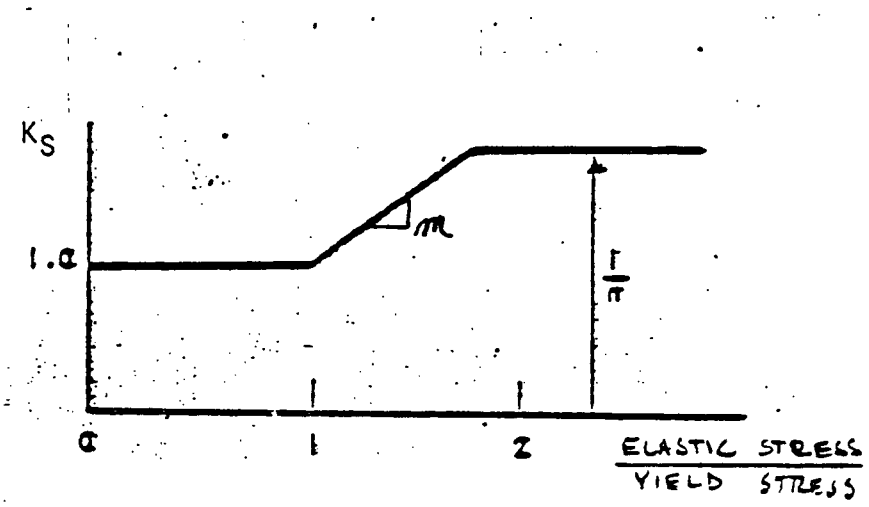

WHERE: n = STRAIN HARDENING EXPONENT

m = SLOPE OF CURVE BETWEEN K_S (ELASTIC) AND K_S (MAXIMUM)

K_S = RATIO OF ACTUAL STRAIN TO ELASTIC STRAIN

STRAIN CONCENTRATION EFFECTS (EXPERIMENTAL)

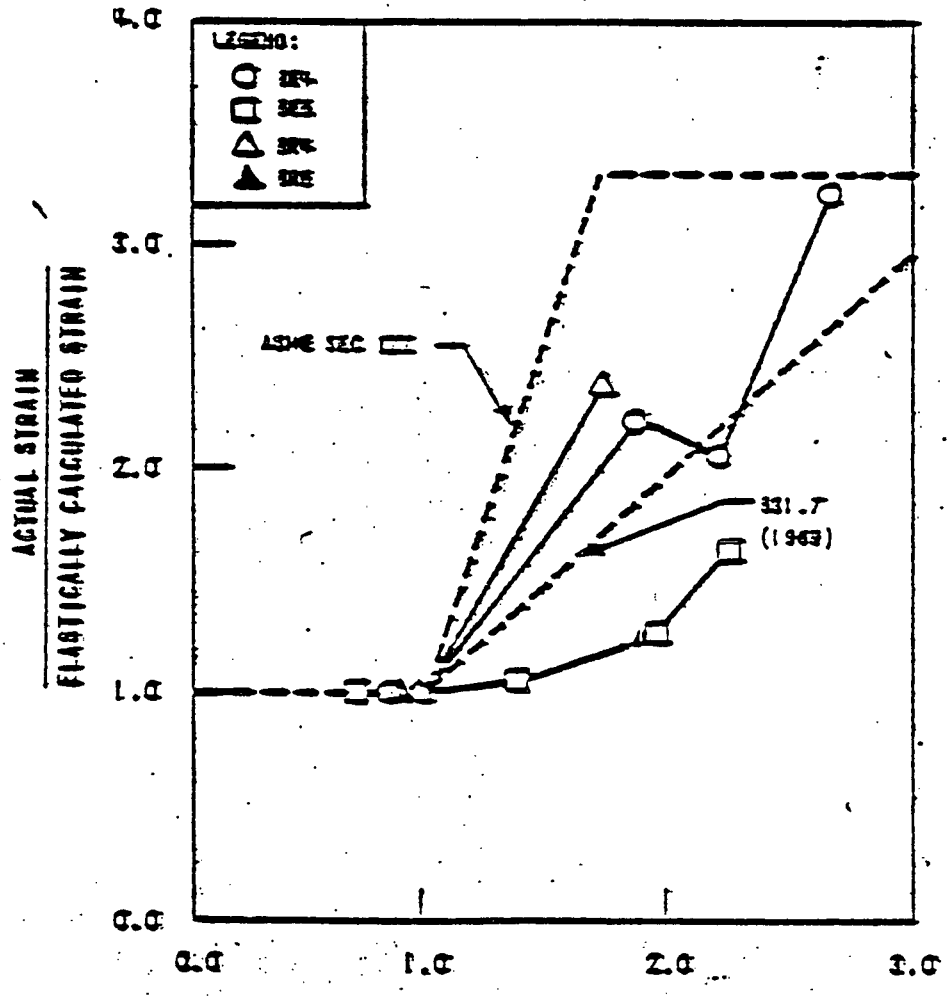

ELASTICALLY CALCULATED STRESS /YIELD STRESS

STRAIN CONCENTRATION FACTOR

$K_S = 1.0$ WHEN $\sigma_E \leq S_Y$

$$K_S = 1.0 + \frac{(1-n)}{n(m-1)}\left\{\frac{\sigma_E}{S_Y} - 1\right\} \quad \text{WHEN} \quad S_Y \leq \sigma_E \leq mS_Y$$

$K_S = 1/m$ WHEN $mS_Y \leq \sigma_E$

WHERE σ_E = ELASTICALLY-CALCULATED STRESS

K_S = RATIO OF ACTUAL STRAIN TO ELASTIC STRAIN

MATERIAL PROPERTIES

MATERIAL	n	m
CARBON STEEL	0.2	3.0
STAINLESS STEEL	0.3	1.7

STRAIN CALCULATION

- ELASTIC STRAIN

$$\varepsilon_e = \sigma_E / E$$

- PRIMARY STRAIN

$$\varepsilon_t = K_S \, \varepsilon_e$$

SUMMARY

- STRAIN LIMITS

  $\varepsilon \leq 1\%$ FOR CARBON STEEL

  $\varepsilon \leq 2\%$ FOR STAINLESS STEEL

- STRAIN CALCULATION

  $\varepsilon_{TOTAL} = K_S \sigma_e / E$

  WHERE

  K_S = STRAIN CONCENTRATION FACTOR

  $\sigma_E = PD/4t + 0.75i(M/Z)$

  E = YOUNG'S MODULUS

Plastic Fatigue Analysis of Pressure Components

S. W. TAGART, JR.

INTRODUCTION

Plastic fatigue analysis prediction has been the subject of intensive study since the fundamental materials work (1,2)[1] began in the early 1950's. Upon publication of the "Tentative Structural Design Basis (TSDB) for Reactor Pressure Vessels and Directly Associated Components" in 1958, this early materials work resulted in a widespread application in the nuclear industry. The TSDB publication made use of a small, polished and unnotched, reversed loading, low cycle fatigue specimen to establish acceptable levels of cyclic loading far into the plastic material behavior region. The methods of elastic stress analysis were required to relate the fatigue behavior of actual pressure components with that of the small polished specimens. Although the ASA B31.1—1955 power piping code also contained rules for cyclic design well into the plastic material region, this piping code was based upon direct fatigue tests (3) of power piping components under simulated service loading rather than on a laboratory type materials fatigue specimen. Although the approach used in the ASA B31.1 code generally involves relatively simple design rules, it lacks the desired versatility to handle other forms of fatigue loading not actually tested on the simulated components such as pressure pulsations or local thermal strains in combination with the piping expansion effects. The TSDB in using the low cycle fatigue small specimen as a basis required the extensive use of theoretical and experimental elastic stress analysis in order to compare the effective strains in the pressure component with the strains causing fatigue in the small specimen. The strains from the elastic analysis were expected to be reasonable approximations to the actual strains even though the elastic calculated stresses were fictitious. The 1963 ASME Section III Code for nuclear pressure vessels was a refinement and extension of the TSDB document in which it was clearly recognized that the methods of theoretical and experimental elastic stress analysis had limitations in the accurate prediction of strains which are to be compared with the low cycle fatigue specimen.

[1] Underlined numbers in parentheses designate References at the end of the paper.

The recognition of these limitations brought about a seemingly new requirement in ASME III which had not appeared in TSDB. The new requirement was the so-called primary plus secondary stress range or $3S_m$ requirement. The basis for this requirement was the concept that at a stress range of 2 times the yield point ($3S_m \leq 2\sigma_{y.p.}$) together with limitations on primary stresses which insure elastic action under the primary stresses alone, a favorable distribution of residual stresses will develop after a few cycles of loading so that the total primary plus secondary strain ranges and amplitudes of cyclic loading can be accurately predicted from methods of elastic analysis. This concept is rigorously correct provided that the basic material behaves elastically through a stress range of two times the yield point. The proof of this concept is demonstrated through the fundamental shakedown theorem of plasticity which in essence states that if the structure can shake down, then it will shake down after a few cycles of loading. It is assumed that the effective stress range of the actual component is compared to the effective stress range of the uniaxial specimen.

In practice, the application of this shakedown principle used in ASME III and USAS B31.7 runs into a complication. Whenever a stress concentration occurs so that a nonlinear (other than simple uniform or linear) stress distribution through the thickness of the pressure retaining component occurs; ASME III and B31.7 have made the inference that the so-labeled peak strains will also be properly predicted from purely elastic calculated values even when the range of peak stress is greater than $3S_m$. This inference is an oversimplification which is not strictly accurate. The fatigue life (to vessel or piping leakage) using the code design fatigue curves may be conservatively predicted using elastically evaluated strains, but the elastic evaluated strains are not necessarily as large as the actual plastic peak strains. As plastic action begins in the peak regions the strain concentration goes above the elastic value even though the nominal stresses are within the shakedown limit. Several analyses and experiments have proven this quite conclusively (4,5,6). USAS B31.7 (as well as ASME III) does

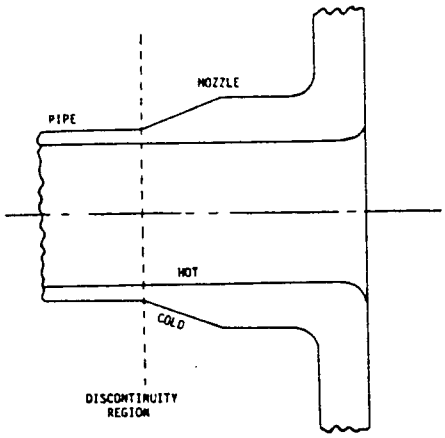

Fig.1 Typical discontinuity

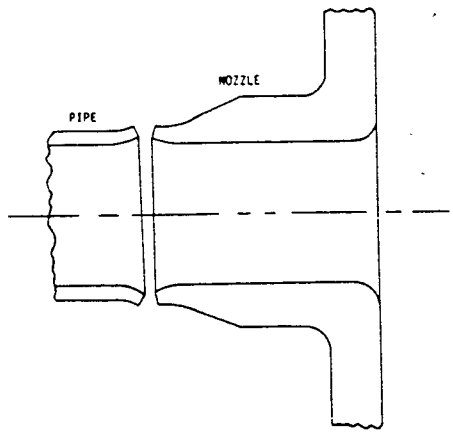

Fig.2 Free thermal distortions

not require the evaluation of this possible peak plastic strain concentration when the $3S_m$ limit is met because it is believed that the crack growth stage of the fatigue life offsets the plastic strain concentration effect. However, it is important to recognize that when exceeding $3S_m$ the plastic strain concentration may get very high and should be accounted for.

Although the fatigue design rules in ASME III and USAS B31.7 are quite similar in most respects there is one area where they apparently [illegible] concerning the treatment of thermal gradients through the thickness of the pressure retaining member. In ASME III N-412 (m) (2) and Table N-413 it is shown that thermal gradients through plate or shell thickness are not to be considered in the $3S_m$ stress comparison. In B31.7 the linear component of thermal gradient through a plate or shell thickness is required to be considered in the $3S_m$ stress comparison. This was done in B31.7 because the linear temperature gradient or sometimes called "moment generating" gradient can produce structural distortion at a pressure shell discontinuity.

For example (Fig.1) the usual case of a pipe to nozzle discontinuity where radial thermal gradients exist produces such a case. If the nozzle in Fig.1 is cut along the discontinuity the exaggerated distortions would occur as shown in Fig.2 which illustrates the free thermal distortions. Such free thermal distortions generally produce shear forces and moments acting across the discontinuity. In the special case, where the nozzle was of the same thickness as the pipe and of the same material, the shear would be zero and the moments would produce exactly opposing deformations in the two parts and there would be no deformation [illegible]d by the radial thermal gradients, but in [illegible] than this case (involving no discontinuity) there may be deformations associated with the linear radial thermal gradients which should be considered in the $3S_m$ stress category. Because of this different treatment of radial temperature gradients and because of general piping expansion stresses which must be accounted for in piping, the practical problems of designing a piping system to everywhere meet a $3S_m$ limit is more difficult and restrictive than it is for pressure vessel components. ASME III does acknowledge that $3S_m$ is not a mandatory limit in N-417.5 (b) (2) and USAS B31.7 has included a simplified (and what is believed to be a very conservative) method to demonstrate the effect on the fatigue life due to exceeding the $3S_m$ limit.

In summary, it should be recognized that elastically calculated strains become progressively more inaccurate for both gross and local type discontinuities as the $3S_m$ (or $2\sigma_{y.p.}$) limit becomes exceeded. The next portion of this paper describes the rules and reasoning behind the simplified elastic-plastic analysis of USAS B31.7.

SIMPLIFIED ELASTIC-PLASTIC ANALYSIS OF B31.7

When considering the effects associated with exceeding the $3S_m$ limit, the following factors are important: (1) the effect on the peak plastic strain calculations, (2) the effect of the plastic redistribution of nominal strains (3) the possible effects of ratcheting and (4) the effects on crack growth following crack initiation. The first three factors generally have the effect of reducing the actual fatigue life below what would be obtained in simply ignoring $3S_m$ and calculating the fatigue life on a purely elastic basis following the usual TSDB procedure. This means that as one goes higher and higher above $3S_m$ the elastic evaluated fatigue life becomes progressively less reliable and that appropriate corrections should be made. The fourth factor is not specif-

ically dealt with in ASME III or B31.7 other than in the rules given for the maximum overall fatigue strength reduction factor of 5 in its relation to crack growth and component leakage. It is not clear precisely what the fourth factor by itself will do; for example, should the 5 factor be raised as one goes beyond the $3S_m$ limit when using the basic low cycle fatigue curve of B31.7 or ASME III? Since the ASME III fatigue curve is not a good measure of the crack growth process, this question is postponed until a later discussion of possible improved methods of low cycle fatigue analysis. For the present discussion, the subject of crack growth will be completely ignored because the B31.7 simplified elastic-plastic method disregards the beneficial effect of the crack growth stage with mild notches (theoretical stress concentrations < 3). The reason that the crack growth stage has been ignored is because a complete and reliable procedure to account for it has not been available. Therefore, if assurance can be obtained that all important factors have been properly evaluated, it seems logical that future code revisions should exploit this area of apparent conservatism.

EFFECTS OF PLASTIC STRAIN CONCENTRATION

Several approximate methods (5,7,8,9) have been proposed (Stowell, Hardrath and Ohman, Crews, Zwicky, Haydl) to analytically calculate the effect of plastic strain concentration by use of actual or ideal stress-strain curves. There is no question that such methods may be extremely useful after sufficient evaluation and experimental verification, however, the emphasis for the present analysis is on the fatigue strain concentration effect under possible fully plastic sections where little analysis attention has been focused to date. Therefore, advantage was taken of direct evaluation of such effects measured by Krempl (6,10) as they relate to what might be termed "engineering crack initiation" on three specific types of nuclear piping materials. This approach has the advantage of avoiding the necessity of making numerous questionable assumptions such as choosing proper stress-strain curves which should be applied to any cyclic plastic analysis. The basic experiments are described in reference (10) where both notched and unnotched fatigue testing has been conducted and where careful observation has identified the point of crack initiation. Crack initiation has been defined here as a surface crack of approximately 0.010-in. length. It has not been possible to measure the depth of these cracks to date, however; it may be estimated that they are approximately 0.003-in. deep at crack initiation. In the unnotched specimens, the point of

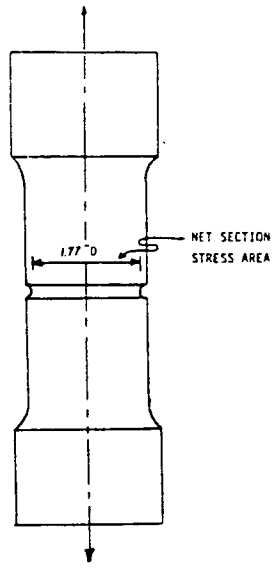

Fig.3 Krempl tension compression notched cylinder specimen

crack initiation occurs toward the end of total fatigue life or about 80 to 90 percent of the cycles to completely fail the specimen. In the notched tests crack initiation may occur very early in the total fatigue life and in one case of the carbon steel at the very high strain range it occurred in less than 10 percent of the total fatigue life. Most of the data for crack initiation in Krempl's notched tests occurred in the region of 20 to 40 percent of the total fatigue life. Krempl's use of such a very small crack as the point of crack initiation makes his data difficult to directly compare with other data where a different definition of crack initiation was used. It seems highly desirable to establish some standard for crack initiation so that all investigators' work could be properly compared. It would appear that a crack size somewhat larger than the one used by Krempl would be desirable for such standardized testing.

Krempl made experimental studies of the effects of temperature on his crack initiation results. Of the three types of materials tested, only the 304 stainless steel showed a significant reduction in notched fatigue life at elevated temperatures such as 500 F to 600 F. This suggests that some caution should be exercised in interpreting notched room temperature low cycle fatigue tests of 304 stainless steel. Krempl's notched tests which were used for the B31.7 fatigue rules consist of a fully reversed loading notched cylinder with a cyclic nominal uniform average stress across the minimum section. The specimen is shown in Fig.3.

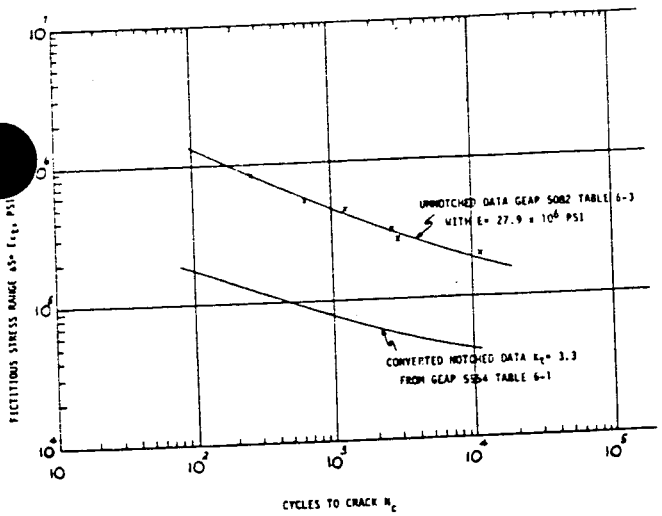

Fig.4 Carbon steel crack initiation data

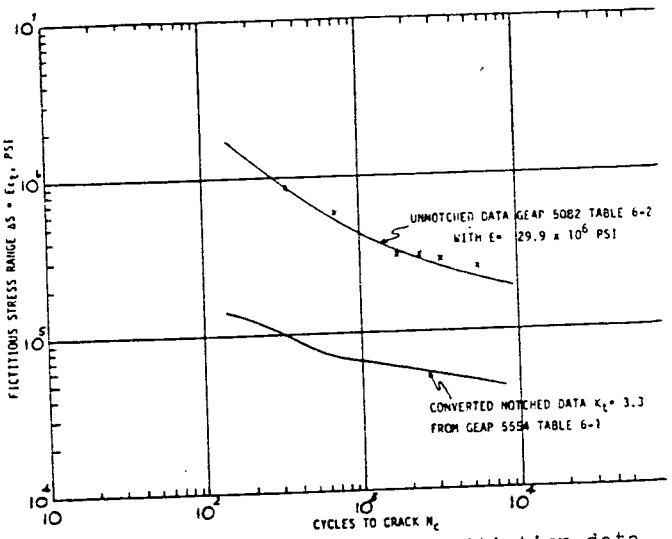

Fig.5 $2^1/_4$Cr-1Mo steel crack initiation data

Although the B31.7 rules are intended to be used on nominal bending stress fields, the bending notched fatigue test in the very low cycle region is less simple to interpret than the tension-compression test. Some work has been done in such notched bending tests where one side of the specimen is strain gaged and the opposite side has a small notch. (Usually, however, these tests have not used the same definition of crack initiation so their results are not directly comparable to Krempl's.) It has been believed in the past that if a notch is placed in a high gradient nominal bending stress field, the fatigue life will be improved over what it would be in a uniform stress field if the maximum nominal stresses are the same in both tests. This belief is obviously correct if failure is defined by specimen failure, and if as the crack progresses, the nominal stresses across the section reduce due to changes in specimen compliance. In fact, very different results will be obtained depending upon whether the applied moment is deflection controlled or load controlled where specimen failure is the definition of fatigue failure. However, if crack initiation is delineated as failure, then the same reasoning concerning the effect of nominal stress gradient may not be true. In fact, some have suggested that crack initiation depends only on the plastic peak strains in the notch region regardless of the type of nominal stress field. This suggests that sharply notched specimens may have little or no crack initiation stage which seems to be borne out in careful fractographic examinations of fillet weld fatigue failures. The variety of interpretations of notched low cycle fatigue tests that has caused confusion in the past can in part be attributed to the failure to distinguish between crack initiation and crack growth. Many variables can change the cycles required to grow a small crack to specimen failure, however, at present, crack initiation is believed to be mostly dependent on the effective peak strain range in the notch. At any rate, if results from notched fatigue testing on uniform stress fields is used as the basis for present code rules, and, then if later is found an effect on crack initiation due to nominal stress gradient, the present B31.7 code rules would be expected to be conservative relative to this effect. Krempl's notched tests require only one dependant variable to be measured, the nominal cyclic load range, corresponding to a given number of cycles to produce crack initiation. The basis for the B31.7 rules utilizes only the fully reversed loading tests with zero mean stress. Fatigue tests were performed on notched and unnotched specimens with the same surface finish. The force range during the displacement controlled notched and unnotched tests was recorded at several intervals throughout the test in order to establish the "asymptotic" or "shakedown" value of force range which persisted during most of the cycles to crack. Generally, the force range varied no more than ± 5 percent during 90 percent of the cycles to crack. A smooth curve was fitted to the unnotched fatigue data in which the abscissa is log of cycles to failure and the ordinate is log of strain range for each specimen (Figs.4,5,6). An average smooth curve was drawn through the data illustrating the asymptotic stress range (load range divided by minimum section area) of the notched tests and are shown in Figs.7,8,9. In order to convert the measured nominal stress ranges of the notched tests to an equivalent nominal strain range which could be properly compared

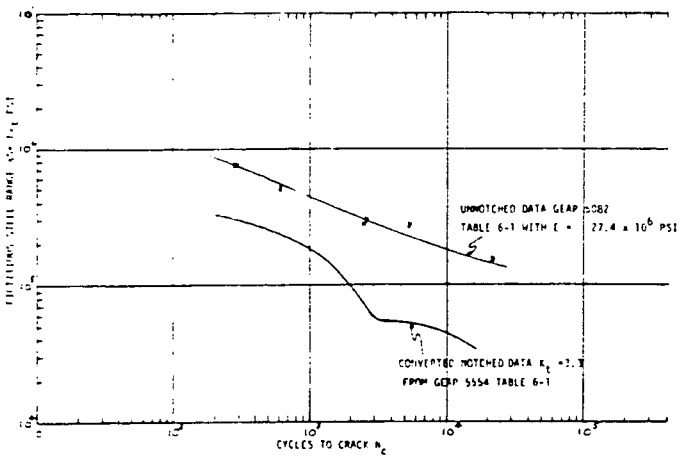

Fig.6 304 stainless steel crack initiation data

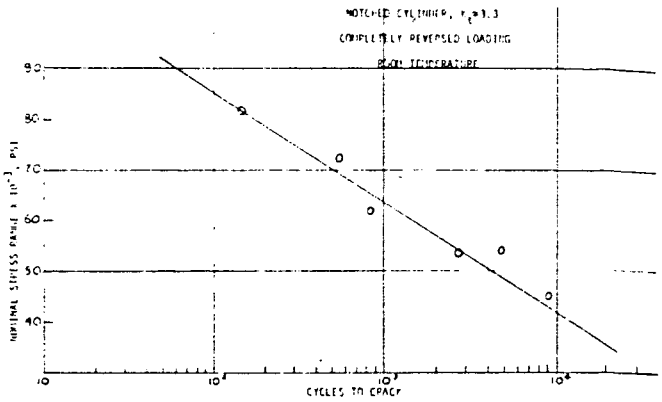

Fig.8 $2^1/_4$Cr-1Mo alloy steel

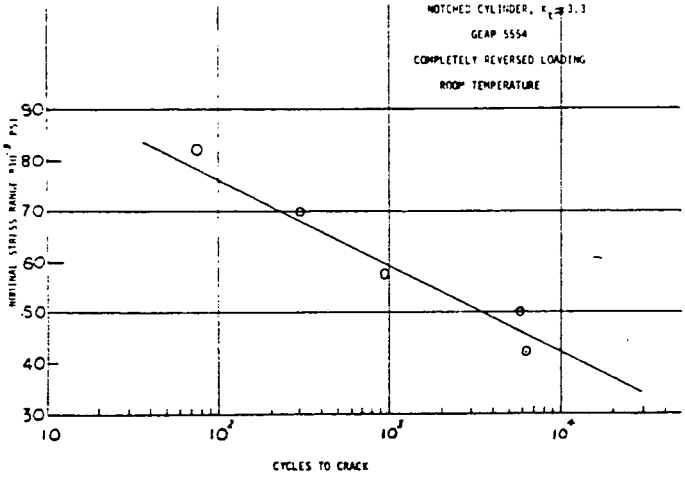

Fig.7 Carbon steel

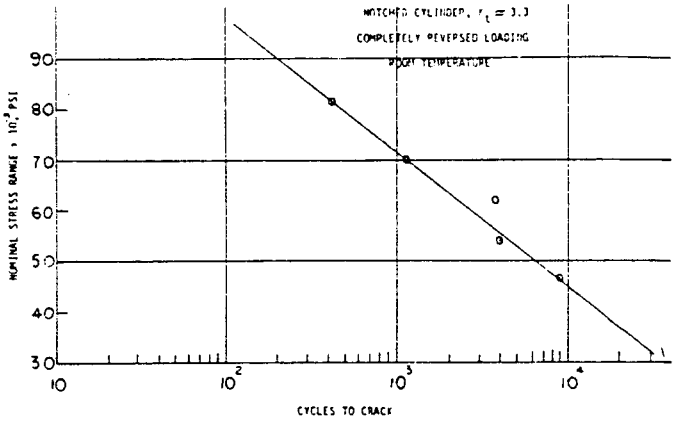

Fig.9 Type 304 stainless steel

with the strain range of the unnotched tests, use was made of the so-called cyclic-stress strain curve obtained from the unnotched tests. The data for these curves is shown in Figs.10,11 and 12, together with the type of fit suggested by Manson (11) which is used to smooth the data. Instead of using the endurance limit range as suggested by Manson, the value of $3S_m$ for each material was used as the deviation from purely elastic behavior because this coincides with the procedures assumed in ASME III and B31.7. The nominal stress of the notched tests was entered on the ordinate of Figs. 10,11, and 12 and the corresponding strain was read on the abscissa. These nominal converted strains of the notched tests could then be plotted with the same coordinates as those for the unnotched tests of Figs.4,5, and 6. Note that the ordinate is plotted as fictitious stress range which is simply Young's modulus times the appropriate strain quantity. This was done simply to show the direct comparison with ASME III type fatigue curves which are also plotted this way. The fatigue strength reduction factor K_f for each of these notched tests can be read from Figs.4,5, and 6 as the ratio of the unnotched and notched curves at each specific value of cycles to failure. This corresponds to the following definition for the fatigue strength reduction factor

$$K_f = \frac{\Delta\epsilon_u}{\Delta\epsilon_n} \qquad (1)$$

where $\Delta\epsilon_u$ is the strain range causing a crack in N_c cycles of the unnotched test. $\Delta\epsilon_n$ is the converted equivalent nominal strain range (at the minimum section) causing a crack in N_c cycles of the notched test.

In order to relate this specific data taken for only one value of the theoretical stress concentration in these notched tests, to that for other notches, the following linear relationship was proposed

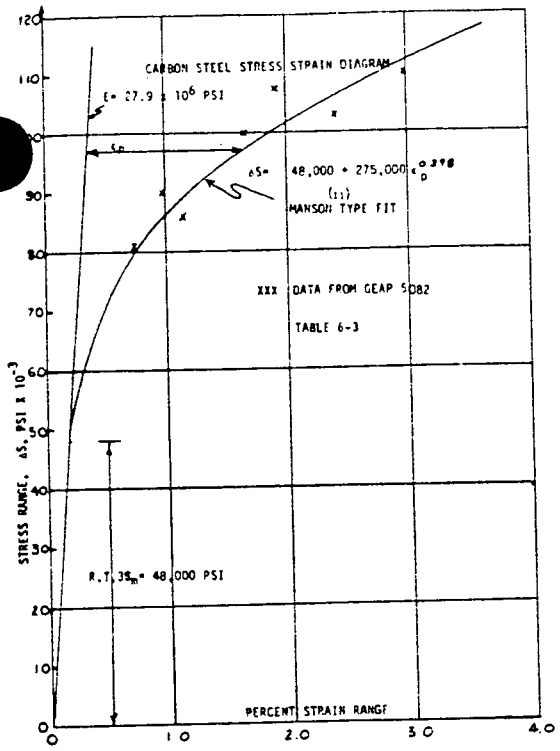

Fig.10 Carbon steel stress strain diagram

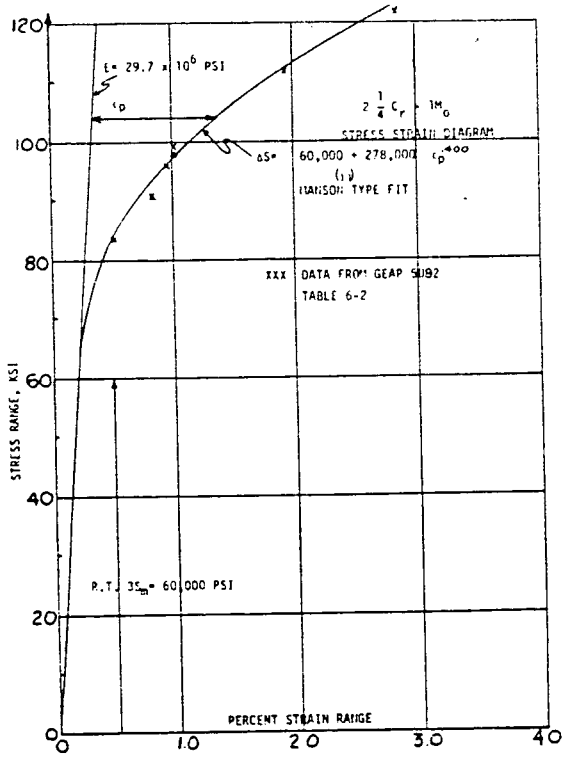

Fig.11 $2^1/4$Cr-1Mo stress strain diagram

$$K_f = K_t + A\,(K_t - 1) \qquad (2)$$

where A is a function of the nominal applied stress or strain at the minimum section and K_t is the theoretical stress concentration for the notch. There is a strong similarity of the "A" factor to the usual notch sensitivity factor q used in high cycle fatigue defined by

$$K_f = 1 + q\,(K_t - 1) \qquad (3)$$

and actually the exact form of defining the A factor is quite arbitrary because as long as the K_f is assumed to be a linear function of K_t the interpolation of tests results to different K_t values will produce identical results. The accuracy of relating the results from fairly sharp notches K_t = 3.3 to more mild notches K_t = 1.5 in such a manner can be determined by further testing at the different notch values of interest. The possible inaccuracy in this assumption used in the B31.7 code rules can be improved if necessary. The usual K_t values in piping are in the region of 1.5 to 2.0 so that the proposed relationship does not require an extrapolation but only an interpolation.

With the proposed relationship it can be that the A factor will be determined from

$$A = \frac{\frac{\Delta\epsilon_u}{\Delta\epsilon_n} - K_t}{K_t - 1} \qquad (4)$$

Since we are concerned with proper A values to be applied to a notched pressure component, the A values from equation (4) can be plotted as a function of the fictitious elastic calculated nominal stress range by using N_c as a parameter. Thus, for a given N_c there is a value of $E\Delta\epsilon_n$ (nominal fictitious stress range) and a value of A which is used in the B31.7 code. These values for the A factor have been plotted for the three materials tested and are shown on Figs.13,14 and 15. It can be seen that the fatigue strength reduction factors defined in this way for the carbon steel and $2^1/4$ Cr-1 Mo steel increases with increasing nominal stress range beyond the $3S_m$ value. Also it is seen that even below $3S_m$ the K_f value is larger than the usual stress concentration factor as would be expected, because we are defining crack initiation here as the failure point. Notice the different behavior of the 304 stainless steel material which has a different type stress strain curve than the carbon steels. Since the 304 material deviates from purely elastic behavior at a lower stress value relative to code allowable stress values than the other materials, we see

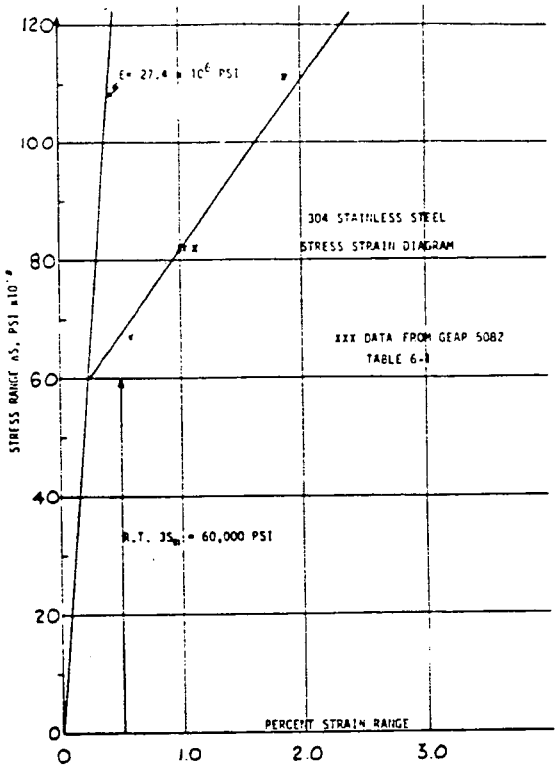

Fig.12 304 stainless steel stress strain diagram

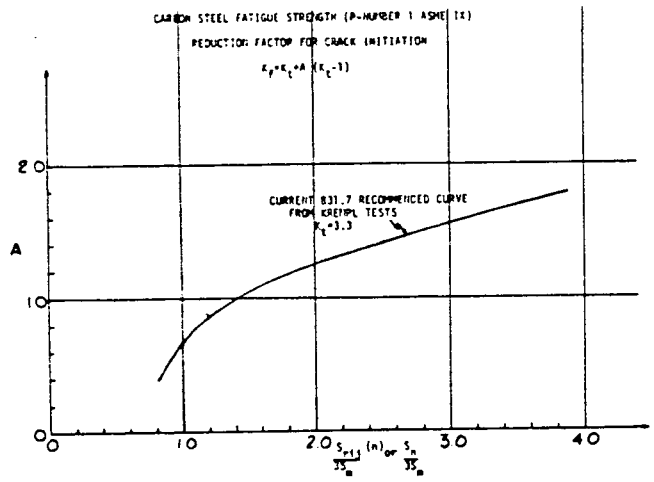

Fig.13 Carbon steel fatigue strength reduction factor for crack initiation

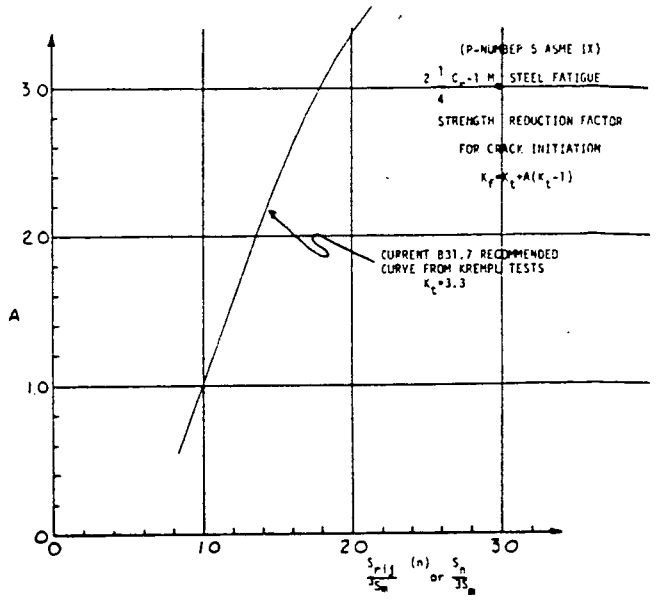

Fig.14 $2^{1}/_{4}$Cr-1Mo steel fatigue strength reduction factor for crack initiation

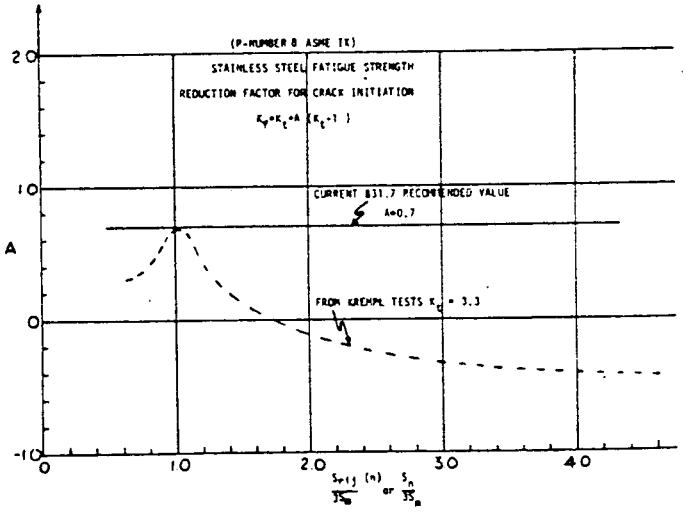

Fig.15 Stainless steel fatigue strength reduction factor for crack initiation

that the plastic effects of the notch are emphasized at a lower value of nominal stress. However, because of the cyclic strain hardening characteristics of the 304 material, the maximum value of the A curve does not reach as high a value, and in fact, it actually reaches a point where it begins to diminish. This is a graphic illustration of the beneficial effect in 304 of the large strain hardening characteristics and tends to reinforce the use of a different basis (from ferritic steels) for selecting the code allowable stresses as is done in ASME III and USAS B31.7. One would expect the same type of maximum value for the other two materials but evidently higher nominal stresses are required to reach this maximum. Because the exact shape of the A value curves is fairly sensitive to the smoothing which was done of all data to arrive at the resultant A values, one should not be surprised to find somewhat different results if further data are taken. The curves presented here are intended to be used quantitatively in the USAS B31.7 code until this technology can

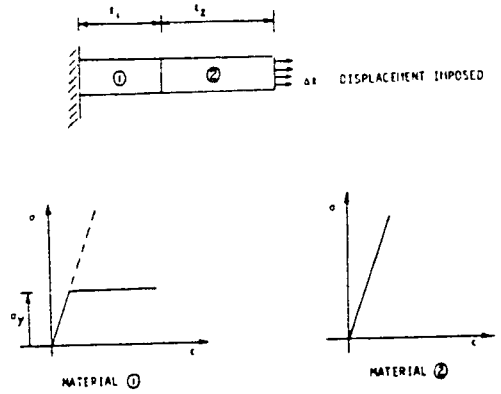

Fig.16 One dimensional elastic-plastic example

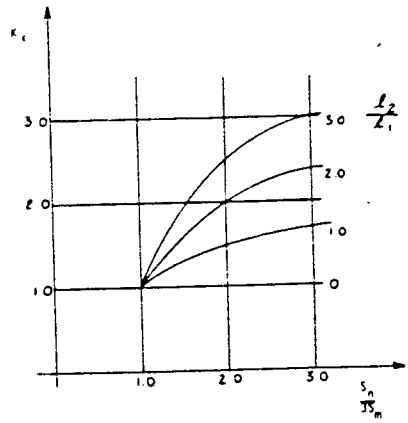

Fig.17 Elastic-plastic correction factor for example in Fig.16

be further refined. However, it should be recognized that these test results are not extensive enough to more than demonstrate crudely the types of corrections on K_f which are needed when one has nominal plastic stress ranges beyond $3S_m$. In the case of 304 stainless steel, since the material is not very notch sensitive and since the exact curve is probably the least accurate due to the sharp peak in the curve as well as unaccounted for temperature effects previously mentioned a horizontal line was drawn for the A factor over the peak value obtained from this data. This arbitrary conservatism is included in the current A values the first draft publication of the USAS B31.7

PLASTIC REDISTRIBUTION OF NOMINAL STRAIN

It is desirable to permit the use of elastic methods of analysis in pressure component design even when gross plasticity is present because one can superimpose linearly stresses from all types of loading and because methods of elastic analysis have become fairly highly developed. In addition, general methods of plastic or elastic plastic analysis applied to even simple shells must be considered only in a very infant stage of application. Manson et al have shown that strain results from detailed elastic plastic analysis is often reasonably approximated from elastic strain analysis especially if the major source of the strains is through thermal or other secondary loading. The B31.7 code has adopted this use of the strains obtained from an elastic analysis as an elementary step in the simplified elastic-plastic analysis. This plastic procedure is often called the method of "elastic strain invariance." It is recognized that this could often involve nonconservative type errors. Manson (11) has shown that the error gets gressively larger as loading extends further o the plastic domain. With this in mind, it was desirable to develop a simple correction factor, say K_ϵ, greater than unity that can be applied to a purely elastic analysis to account for an unfavorable redistribution of nominal plastic strains. That such a correction is needed is illustrated by reference to Fig.2. If one calculates on a purely elastic basis the forces required to fit the distorted pieces together, and if the thin weaker section on the left begins to get into the plastic region, one will calculate an artificially high force resultant in the weak member. This in turn will produce more deflection in the right stronger member of the discontinuity than it would actually have to carry. Thus, instead of the two members across the discontinuity sharing the thermal distortions as they would elastically, the weaker yielding member will be forced to carry a larger fraction of the discontinuity displacements than would be found on the elastic basis. Thus, the plastic strain will have a tendency to concentrate in the right member, this tendency increasing as the thermal loading increases. This situation clearly depends upon the relative flexibility of the right and left halves of the discontinuity. If the weak right member is very much more flexible than the left member elastically, then the strain concentration would not be so great because the weaker member would be carrying most of the total discontinuity displacements both elastically and plastically.

A simple example will illustrate the nature of the K_ϵ factor which should generally be imposed. Suppose we consider a bar composed of two parts upon which we will impose a displacement as shown in Fig.16. Assume further that part 1 is composed of a material which is elastic-perfectly plastic while part 2 is a stronger material which remains elastic in this discussion. The displacement at which the combination remains elastic is

$$\Delta \ell_e = \frac{\sigma_{y.p.}}{E}(\ell_1 + \ell_2) \qquad (5)$$

If we impose a displacement greater than this, ($\Delta \ell > \Delta \ell_e$) the fictitious elastic calculated strain in the weaker member will be

$$\epsilon_{1e} = \frac{\Delta \ell}{\ell_1 + \ell_2} \qquad (6)$$

while the true strain in the weaker member will be

$$\epsilon_{1P} = \frac{\sigma_{y.p.}}{E} + \frac{\Delta \ell - \Delta \ell_e}{\ell_1} \qquad (7)$$

For this problem, the K_ϵ factor which must be applied to the elastic solution to produce correct plastic strains in the weaker member is the ratio $\epsilon_{1P}/\epsilon_{1e}$ or

$$K_\epsilon = \left(\frac{\ell_2}{\ell_1} + 1\right) - \left(\frac{\ell_2}{\ell_1}\,\frac{\Delta \ell_e}{\Delta \ell}\right) \qquad (8)$$

If we equate $\Delta \epsilon_e / \Delta \epsilon$ to $3S_m/S_n$ where $3S_m$ is the limit of elastic behavior and S_n is the nominal elastic calculated stress range, we can then plot the K_ϵ factor relevant to this particular problem as shown in Fig.17.

Here we see that when $\epsilon_2 < \epsilon_1$ (where the weaker member is more flexible than the strong member) the plastic correction factor K_ϵ is quite small, but as $\epsilon_2 > \epsilon_1$ the plastic correction can become very large. One can also plot a similar diagram to Fig.17 for a two-piece bar with a bending moment and applied rotations as the input. It is clear that corresponding K_ϵ factors would be lower than those of Fig.17 because the yielding part of the bar would be capable of assuming higher moment values beyond the initial yielding and thus, more of the imposed rotation would shift into the strong member. In more complex problems of pressure component discontinuity analysis where there are further complications, it is not clear how a diagram such as Fig.17 can be directly applied. For example, if combination of forces and displacements cause biaxial stresses, the force induced loading would be expected to produce higher K_ϵ effects than illustrated in Fig.17.

It can be seen from this discussion that the selection of an accurate K_ϵ factor for a particular problem would involve solving in some depth the actual elastic-plastic problem. Since it is not possible to be general and specific with regard to geometries at the same time, the approach used was to solve a simple problem which contains the major ingredients of the more difficult situations, and generalize the results. Two ideal cases are used which are quite similar to the cases used in arriving at the rules for primary stress limits of B31.7 and ASME III. To review the cases in their original context for primary stress limits, Fig.18 was reproduced from reference (12).

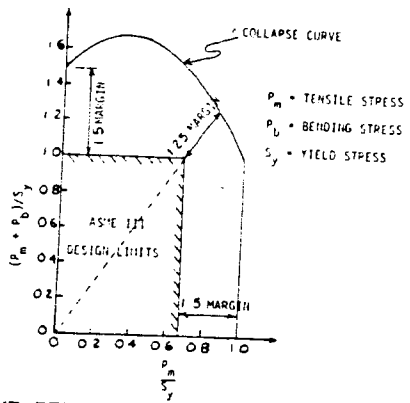

Fig.18 ASME III and B31.7 primary stress limits

The collapse curve was obtained by plotting the collapse load of a rectangular section under combined bending and tensile primary load stress. The design limits were arbitrarily selected to provide what was judged to be an adequate safety margin, although a closer examination of Fig.18 can lead to questions. For example, the minimum margin against collapse of Fig.18 is 1.23 off the upper right corner of the ASME III design limits. If one applies the rules of ASME III to the austenitic stainless steels where $0.9S_y$ is used for the tabulated S_m stress allowables instead of $2/3\ S_y$, the design limit box appears to exceed the collapse curve

$$\frac{0.9}{2/3} = 1.34 > 1.23$$

This apparent anomaly is partially cleared up if one recognizes that the austenitic stainless steels have a high strain hardening capability so that $0.9S_y$ for that material is actually equivalent to $2/3\ S_y$ of the ferritic materials. However, it can be seen that in specific cases the design rules for primary stresses in ASME III and USAS B31.7 have some area where caution should be exercised. To this extent, the B31.7 method for computing K_ϵ suffers the same type of shortcomings, that is, because it is simple it cannot account for all possible effects. (Guide lines will be discussed later as to where caution should be exercised.)

The K_ϵ curves which appear in the first

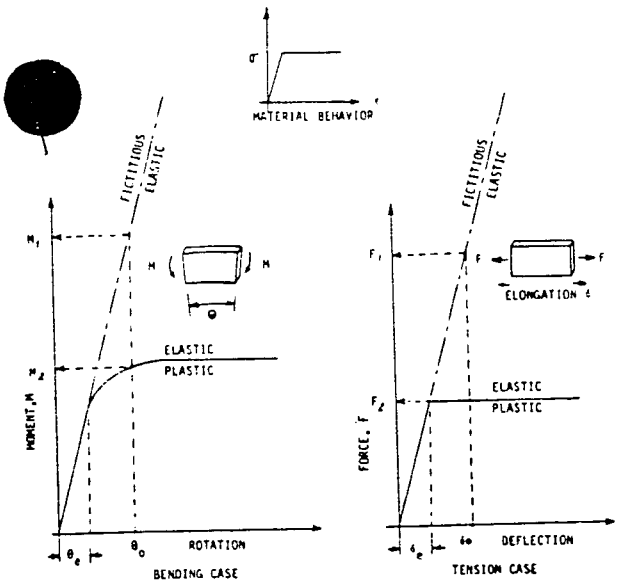

Fig.19 Development of B31.7 K_ϵ factors

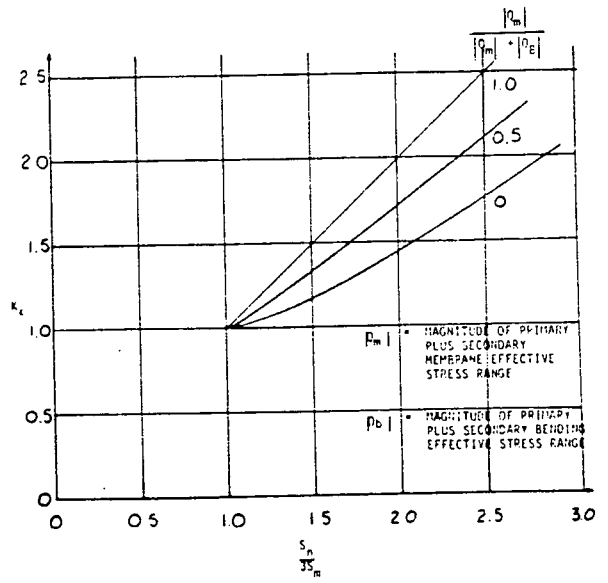

Fig.20 USAS B31.7 elastic-plastic correction factor, K_ϵ

draft of USAS B31.7 were developed from the following considerations. Taking the same two loading cases that are used for primary stress limits, i.e., the rectangular bar with tension as one case and bending loading as the other case, and instead of applying loading to produce the stress apply displacements to produce the stress. The results are shown in Fig.19. The reason for using displacements instead of loading here is that we are dealing principally with secondary or displacement induced loading in comparing stress ranges to the $3S_m$ requirement.

We now recognize that for each specific displacement θ_o or δ_o (the loading mechanism) two values of the corresponding force resultant can readily be calculated. These values are the fictitious elastic resultants M_1 and F_1 and the plastic resultants M_2 and F_2. The artificially high force resultants M_1 and F_1 are the principal cause for the elastic strain invariance method producing nonconservative strain results in the weaker members, because these fictitious resultants drive too much of the discontinuity displacements into the stronger member. It is assumed that for a given margin above the $3S_m$ stress range, the maximum error in strains in the yielding member is proportional to the ratio of the elastic to plastic force resultant in that member or

$$\text{for bending} \quad K_\epsilon \propto \frac{M_1}{M_2}$$

$$\text{for membrane} \quad K_\epsilon \propto \frac{F_1}{F_2}$$

It is clear that this is not exactly correct because it takes no account of the relative flexibilities of weak and strong members as was done in the discussion of Fig.17. However, we can gain some insight as to the applicability of the results of Fig.19 by comparison with those of Fig.17. If we equate θ_o/θ_e and δ_o/δ_e to $S_n/3S_m$ we can plot K_ϵ curves for the two cases as shown in Fig.20. Fig.20 shows the curves which appear in the USAS B31.7 code. Combinations of bending and membrane stresses are covered by linear interpolation between these curves using as a parameter the ratio of membrane stress to membrane plus bending stress. See Fig.21 for graphic explanation of the interpolation.

Since Fig.17 involved only membrane stresses, it is of interest to compare the membrane curve of Fig.20 with those of Fig.17. They are shown together on Fig.22. Since an analytic expression is available for the curves of Fig.22, they can readily be differentiated

$$\frac{d\,K_\epsilon}{d\left(\frac{S_n}{3S_m}\right)} = \frac{\mathcal{I}_2}{\mathcal{I}_1}\left(\frac{3S_m}{S_n}\right)^2 \qquad \text{(For Fig.17 curves)} \qquad (11)$$

$$\frac{d\,K_\epsilon}{d\left(\frac{S_n}{3S_m}\right)} = 1.0 \qquad \text{(For Fig.20 membrane curve)} \qquad (12)$$

It can be seen that because the Fig.17 curves are concave downward that if $dK_\epsilon/d(S_n/3S_m)$ is evalu-

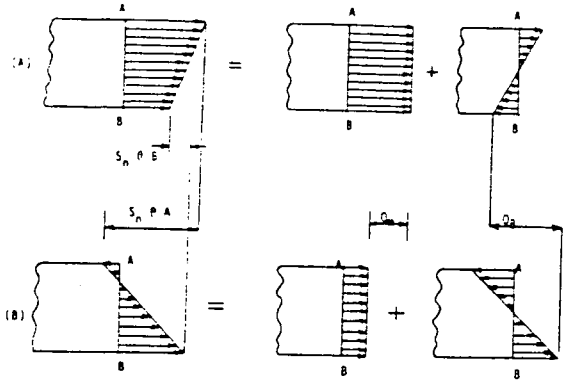

(A) EFFECTIVE STRESS STATE AT ONE EXTREME OF STRESS CYCLE

(B) EFFECTIVE STRESS STATE AT SECOND EXTREME OF STRESS CYCLE

Fig.21 Explanation of K_ϵ factors for USAS B31.7 code

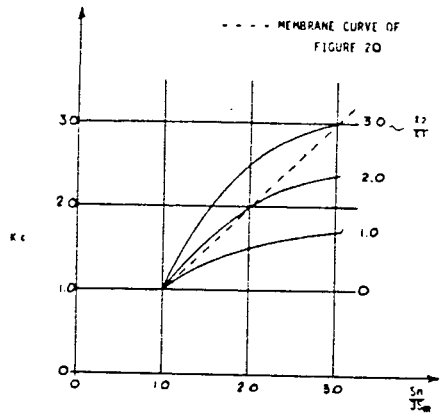

Fig.22 Comparison of B31.7 K_ϵ factor with exact simple membrane elastic-plastic correction

ated at $S_n/3S_m = 1.0$, a maximum value for ℓ_2/ℓ_1 can be found which makes the curve of Fig.17 always less than the membrane curve of Fig.20. This maximum value of ℓ_2/ℓ_1, is found to be 1.0. The significance of this can be generally interpreted as follows; if the relative flexibilities of the elastic members involved in the plastic discontinuity is such that the weaker yielding member is at least as flexible as the stronger member $\ell_2/\ell_1 \leq 1.0$, then the application of the K_ϵ curves of Fig.20 would be expected to produce conservative K_ϵ factors. In most cases which arise in practice, this requirement will be fulfilled. It is important, however, to recognize where this requirement is not fulfilled, and this can be illustrated with two examples shown in Fig.23.

In Fig.23(a) we see that the weak yielding member or region is surrounded on both sides by a large volume of strong material so that the relative flexibility of the weak member may be less than that of the adjacent strong material. Here the K_ϵ curves of B31.7 should not be applied. In Fig.23(b) it is obvious that the shell flexibility of the weak member is greater than that of the adjacent strong member, and, therefore, the K_ϵ curves of B31.7 can be applied. With this rule of thumb in mind, the K_ϵ curves of USAS B31.7 can be generally applied without concern provided one does not attempt to use them where severe strain concentrations can pile up such as in the example of Fig.23(a). A specific example in pressure component design is next shown to further illustrate the K_ϵ concept in greater detail. We consider a typical discontinuity which often occurs, and apply a more rigorous elastic-plastic analysis (13) to determine specifically the K_ϵ factor.

In this problem the following type of loading was used, Fig.24. Pressure loading was assumed

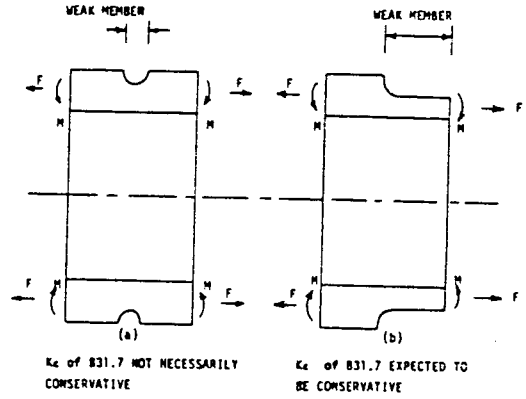

Fig.23 Limitations to B31.7 elastic-plastic K_ϵ factor

to the limits of B31.7 allowable stresses. In addition, thermal discontinuity loading in the form of temperature gradients through the thickness were superimposed to put region 1 beyond the $3S_m$ limit. Fig.25 shows the detailed K_ϵ value found from the computer (14) solution together with the appropriate curve of the B31.7 code.

It is seen that the elastic plastic computer solution produces a K_ϵ factor which is everywhere lower than the B31.7 curve. It would be expected that where the application warrants such detailed computer calculations, the more accurate value of K_ϵ would be used in conjunction with the B31.7 code. It may be anticipated that as digital computer programs are applied to these types of plastic problems, specific plots such as Fig.25 could be published and compiled into a reference document for designers so that fairly accurate K_ϵ values could be applied to the specific problems. In this way, the K_ϵ concept could be generally applied to plastic problems in much the same way as the usual stress concentration concept is ap-

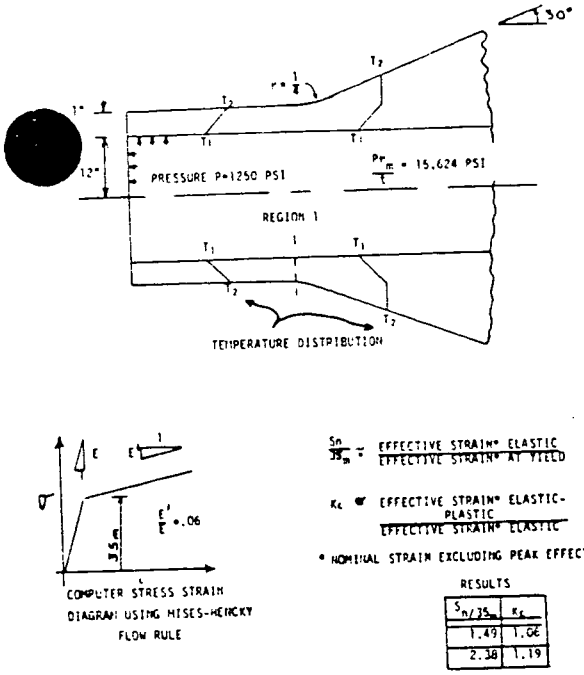

$S_n/3S_m$	K_ϵ
1.49	1.06
2.38	1.19

Fig.24 Elastic-plastic computer analysis

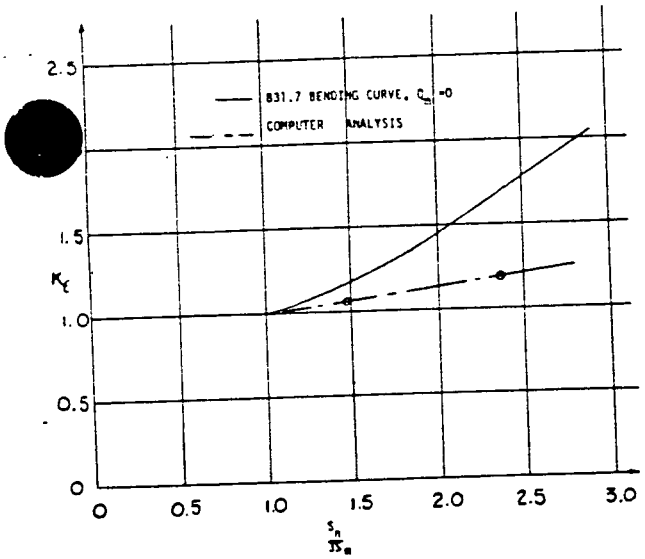

Fig.25 Comparison of B31.7 K_ϵ factor with computer elastic plastic analysis

plied to purely elastic problems. The advantage in design calculations of retaining a basic elastic solution and using a K_ϵ factor where needed is tremendous compared to the task of computing elastic-plastic solutions for each specific problem.

CHETING AND THE B31.7 RULES

The third factor discussed earlier in conjunction with the USAS B31.7 simplified elastic plastic analysis is the treatment of ratcheting. The present B31.7 code controls this important subject with only one requirement. The requirement is that the total cyclic events which exceed the $3S_m$ requirement and use the simplified elastic plastic method are limited to 250 cycles. That is, no specific account of ratcheting is required if the total cyclic events are less than or equal to 250 cycles. The B31.7 fatigue rules are here illustrated and compared with the ASME III fatigue rules.

ASME III

$$S_n \leq 3S_m \qquad S_{alt} = \frac{1}{2} K_t S_n$$

$$S_n \geq 3S_m \qquad \text{(suggests plastic analysis, but no specific guidance)} \tag{13}$$

USAS B31.7

$$S_n \leq 3S_m, \qquad S_{alt} = \frac{1}{2} K_t S_n$$

$$S_n > 3S_m; \text{ total cycles} \leq 250, \quad S_{alt} = \frac{1}{2} K_f K_\epsilon S_n \tag{14}$$

where

S_m is the code tabulated stress allowable at the appropriate temperature

S_n is the nominal stress range excluding stress concentrations or local thermal effects

K_t is defined here as the ratio of the peak surface elastic calculated stress range including effects of stress concentrations and local thermal effects, to the S_n nominal stress range

S_{alt} the alternating fictitious stress amplitude which is entered into the ASME III or B31.7 fatigue curves to determine fatigue usage following the Miner hypothesis

$K_f = K_t + A\,(K_t - 1)$ is an overall fatigue strength reduction factor to account for geometric stress concentrations and local thermal effects

A a measured material dependent factor which is a function of the nominal fictitious elastic applied stress range, S_n, in which the localized plastic effect resides (Figs.13,14,15)

Notice that the B31.7 rules are identical to the ASME III rules when $3S_m$ is not exceeded (except as explained earlier in that B31.7 requires that

linear thickness temperature gradient effects be included in the $3S_m$ evaluation).

With respect to ratcheting, ASME III suggests that a shakedown state must be achieved where $3S_m$ is exceeded while B31.7 suggests that when $3S_m$ is exceeded either shakedown can be demonstrated (cyclic elastic-plastic analysis would be generally required to accomplish this) or that if the total accumulated ratcheting strain prior to shakedown is accounted for in the fatigue analysis that shakedown is not required. The distinction between the codes in this area is important but it is believed that the B31.7 approach is equally as sound as the ASME III approach and yet permits more flexibility in application to this difficult area. To further emphasize the problem with the ASME III requirement of shakedown, it is pointed out that it is an extremely difficult problem to clearly demonstrate shakedown except in very simple cases. The reason why it is difficult is that one must generally apply an incremental plasticity theory capable of tracking the entire loading and stress-strain history through perhaps several complete hysteresis loops. Attempts to solve this problem were undertaken by Miller (15) which resulted in the rules which now appear in ASME III concerning ratcheting in two very simple cases completely away from geometric discontinuities. It is difficult to generalize or extend this to the important cases of interest at geometric discontinuities. Therefore, in effect, ASME III has suggested that exceeding $3S_m$ is permissible but acceptable methods of performing the required plastic analysis is not generally available. The B31.7 code has attempted to fill this gap. In addition, the B31.7 code does not presently permit the use of the simplified elastic plastic analysis to allow the gross pipe expansion effects to exceed $3S_m$ so that possible gross ratcheting distortions of piping need not be considered in the simplified elastic-plastic analysis of B31.7. It is usually agreed in pressure component design that some limited amount of localized ratcheting is permissible (except at non-integral connections or joints where leakage or disengagement of mating points is of concern). The problem is to decide upon a basis to evaluate the effect of ratcheting, and to determine how much ratcheting will be present in any specific application.

For both problems a paper by Benham and Ford (16) has proven to be useful in which uniaxial tests on a carbon steel and an aluminum alloy were conducted where ratcheting was quantitatively evaluated. Benham and Ford performed uniaxial load controlled tests on unnotched bars under two conditions in which ratcheting was observed. The two conditions were zero to tension loading where

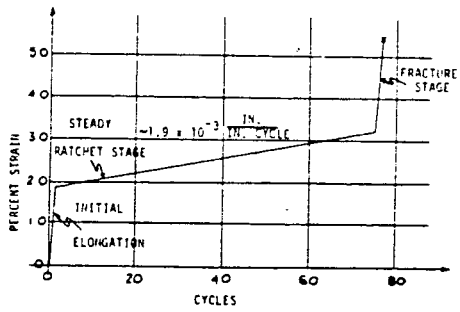

Fig.26 Carbon steel ratchet behavior

mean stress is 1/2 the stress range and fully reversed loading where the mean stress was zero. In the zero-tension tests very severe ratcheting takes place as the maximum stress gets near the nominal ultimate strength. The maximum rate of steady ratcheting for carbon steel short or necking the specimen on the first few loading cycles was about 1.9×10^{-3} in./in. per cycle in which the specimen failed in 74 cycles. The typical strain versus cycles plot for these zero tension tests is shown in Fig.26. It is seen that three distinct stages are present, (1) an initial elongation, (2) a steady ratchet or apparent creep stage and (3) a final fracture stage. In this plot the cyclic tensile loading was about 98 percent of the conventional ultimate strength or about 160 percent of the yield strength. Each of the plots at higher cycles to failure had these same three distinct stages and the steady ratchet stage occupied about a 10 to 20 percent total ratcheting elongation almost independent of the steady ratchet state or cycles to failure. Under the fully reversed loading conditions, no effect of ratcheting was detected at the same stress ranges where this high ratcheting had occurred under zero tension loading, and no significant effect of ratcheting was observed under fully reversed loading until an actual stress range equal to or greater than about 1.8 times the conventional ultimate strength was imposed.

In the loading regions of B31.7 where exceeding the $3S_m$ limit is permitted, the limits on primary stresses are still limited to S_m for membrane effects so that the mean stress available as a driving source for ratcheting is limited to $\leq 1/3$ the stress range. Thus, the zero-tension tests which have a mean stress of 1/2 the stress range would be expected to illustrate conservative ratchet effects when considering the B31.7 simplified elastic plastic cases. However, the mean stress will generally be greater than zero under B31.7 so that fully reversed tests illustrate nonconservative ratchet effects when applied to the B31.7 simplified elastic plastic cases. An appro-

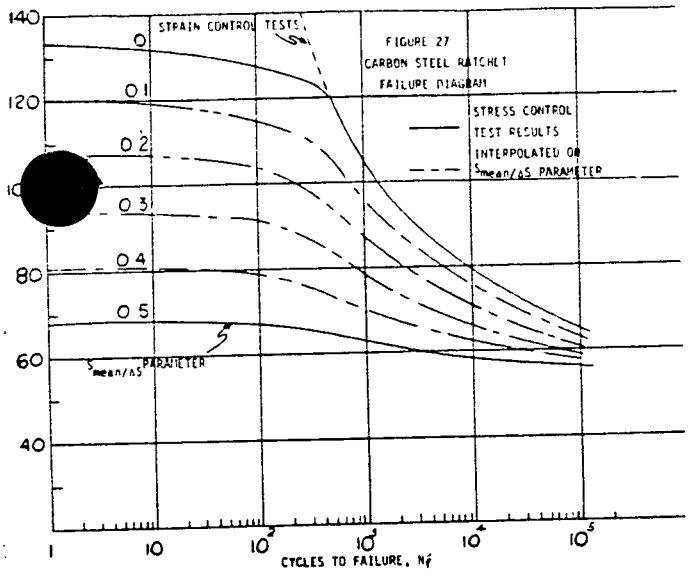

Fig.27 Carbon steel ratchet failure diagram

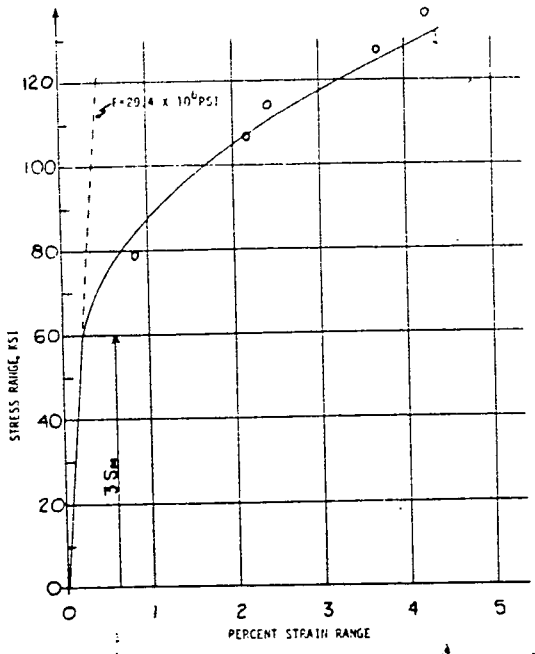

Fig.28 Benham-Ford (16) cycle stress strain data for carbon steel

priate answer can be obtained if for each material unnotched low cycle fatigue tests were performed under load control with varying amounts of mean stress ranging from 1/3 to 0 of the stress range. This could become a ratchet failure diagram where the combined effects of low cycle fatigue and ratcheting under mean stress are working to produce specimen failure.

In order to obtain a first approximation to [illegible]sults from such tests, the curves of Benham and Ford have been linearly interpolated (using the ratio of mean stress to stress range as parameter) for mild steel to produce the following ratchet failure diagram, Fig.27. The ordinate here is the true measured stress range on the specimen, and if a corresponding steady cyclic strain range were available then one could relate these stress ranges to the fictitious stress ranges of B31.7 and evaluate the effects of ratcheting on the fatigue life. This can be accomplished approximately by using the cyclic-stress strain diagram of the material under strain controlled conditions which Benham and Ford supplied in their paper for the particular mild steel, Fig.28.

Consider the case where a total nominal effective fictitious elastic calculated stress range is for example $7S_m$. This would be caused by both discontinuity displacements and applied loads. The real stress range corresponding to this $7S_m$ value (using Fig.28) is approximately 74,000 psi. Of this 74,000 psi stress range only 1.0 S_m effective stress or 20,000 psi can be applied as a mean stress under the B31.7 code rules, thus, the ratio $S_{mean}/\Delta S_{range}$ is 0.27. If the two parame[illegible] (ΔS and $S_{mean}/\Delta S$) are entered on the proposed ratchet failure diagram for uniaxial loading we find that the fatigue failure would occur at 3500 cycles. To illustrate the degrading effect due to this finite mean stress in the low cycle fatigue region causing ratcheting, we see that failure would be predicted at 20,000 cycles with no mean stress but with the same 74,000 psi stress range. This is quite a significant reduction and emphasizes that the effect of ratcheting should be controlled. If we continue and plot the ratchet failure cycles for all possible stress ranges following this same procedure the following diagram will result, Fig.29. The 1.0 S_m curve illustrates the maximum effect of mean stress. Superimposed on Fig.29 is the useful region of B31.7 where the simplified elastic-plastic analysis of B31.7 can be used without specifically considering ratcheting. The upper right corner curve bounding this region which slopes downward toward the right was established by entering the B31.7 carbon steel fatigue curve at $S_{alt} = 1/2\ K_\epsilon\ S_n$ because the K_ϵ factor is applied even for an unnotched part. With the 250 cycle limit bounding the B31.7 procedure on the right, it is seen that a large margin exists between permissible cycles and the cycles required to produce a ratchet failure even at the highest mean stress permissible under B31.7. The minimum ratio here was found to be a factor of 16.8 on cycles. For a part which involves a notch or K_f factor other than unity, the method will be even more conservative because the upper right corner of the B31.7 useful region will move to the

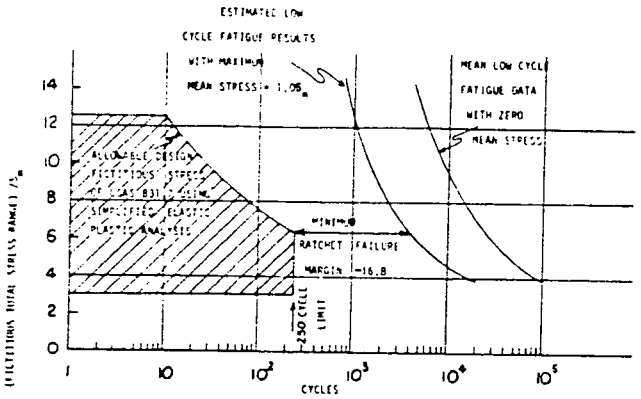

Fig.29 Estimated ratchet failure margin for carbon steel

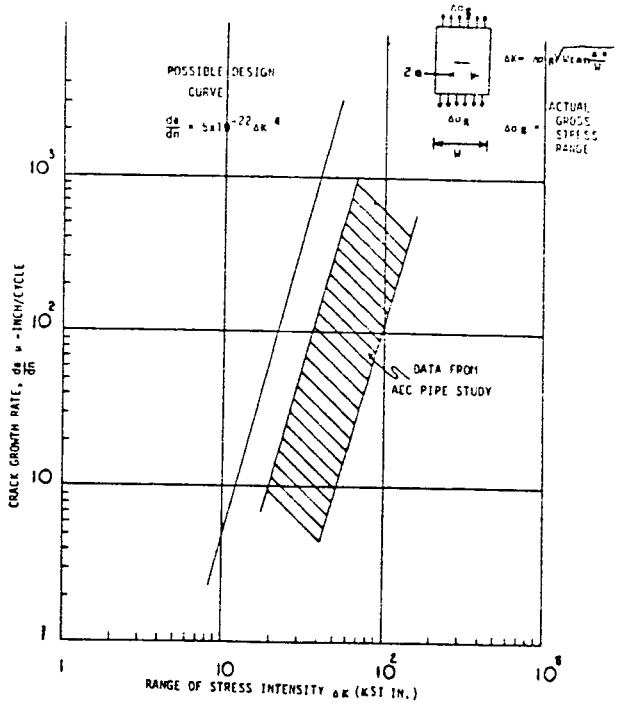

Fig.30 Crack growth computation

left. The 250 cycle limit which appears in B31.7 was chosen quite arbitrarily and it would appear from this discussion that it could have been chosen somewhat higher with little danger of a possible ratchet effect on the fatigue life. However, because actual material data concerning these effects is quite meager (only one material, carbon steel, has been discussed here) no attempt has been made here to raise this somewhat arbitrary limit. The 250 cycle limit of B31.7 is intended only to illustrate a region where ratcheting can be safely neglected and if proper account is taken of the possible ratchet effects, the simplified elastic plastic analysis of B31.7 can be extended to higher cycles of loading than 250.

IMPROVED METHODS OF LOW CYCLE FATIGUE ANALYSIS

The procedures of low cycle fatigue analysis used in ASME III and USAS B31.7 could be considerably improved if one important distinction is made. That distinction is to separate the fatigue life associated with crack initiation from that due to crack growth. The need for this separation is emphasized if one observes that crack initiation is most accurately correlated by reference to the effective multiaxial strain range while crack growth seems to depend mainly on the cyclic stress components normal to the direction of the growing crack. Thus, in pressure components the mechanisms of the crack initiation and growth appear distinctly different. It has been discussed in this paper that because of this lack of distinction it is difficult to account for a proper fatigue strength reduction factor which is related directly to elastic or plastic strain calculations. This has been a source of confusion where at one time it was proposed (12) that local strain concentrations cannot exceed the elastic stress concentration if shakedown is achieved. This concept has been clarified as was previously discussed. One reason that this confusion existed is because no distinction was made between crack initiation and crack growth. The "δ" concept illustrated by Langer (17) was an attempt to help resolve this problem, but unfortunately this concept also does not quantitatively separate crack initiation from crack growth. Since both codes—ASME III and USAS B31.7—define experimental fatigue failure as a crack which causes leakage, it will continue to be difficult to account accurately for the crack growth stage with a basic material fatigue specimen which measures principally crack initiation. The unnotched low cycle fatigue specimen presently used by ASME III and B31.7 measures chiefly crack initiation because crack initiation (about 0.010 in. length crack) usually occurs at 80 to 90 percent of the cycles to break the specimen.

Another type of materials test is needed to quantitatively account for the crack growth stage. Such tests have been in existence for several years and many possible forms of correlating the results are available. One which has been used quite extensively in the A.E.C. Pipe Rupture Study (18) being performed by General Electric is the use of the fracture mechanics stress intensity parameter ΔK. It has been shown that this parameter is capable of correlating crack growth rate under conditions of loading ranging from the early stages of crack growth where the crack dimensions are only a few mils to well past the failure stage

where the crack is through the pressure retaining member. The usual correlation appears as in Fig. 30 where the ordinate is the crack growth rate and the abscissa is the range of the fracture mechanics stress intensity factor. It is emphasized that this correlation has been tested well into the net section plastic stress region, that is, the linear elastic fracture mechanics stress intensity provides consistent correlation for crack growth well into the plastic stress region. Effects of mean stress, temperature, and geometry have been studied experimentally (19) but are generally not found to be as significant as the overall data scatter without these effects. This type correlation may be applied to any type of initiated crack provided one can obtain the proper fracture mechanics stress intensity factor. Usually for small cracks the stress intensity value can be approximated from one of the classic solutions available. The main difficulty in application to fatigue life calculations is the integration of the crack over the thickness of the pressure retaining member because as the crack progresses, through the thickness, the ΔK and, the force resultants (or equivalently the nominal stresses) through the uncracked section change. Generally, however, one can make an appropriate assumption concerning the nature of the change in the force resultant. For example, if the stress is caused by thermal or discontinuity loading, then that portion of the force resultant could be expected to diminish as the crack progresses, while that portion of the force resultant which is caused by pressure or other applied loading would be expected to remain nearly constant as the crack grows (20). In this way one can obtain approximate evaluations of the crack growth stage. It should be noted that fatigue crack growth treated in this manner automatically contains a damage accumulation process and that it is not necessary to use the Miner damage simplification. If such crack growth fatigue calculations were to become a part of the codes after sufficient simplification, evaluation and review, it would be possible to improve the analysis treatment of fillet welds in fatigue. At present, fillet welds are treated by use of a fatigue strength reduction factor of 4 or 5 when the $3S_m$ stress range requirement is met. As was discussed earlier in this paper, it is not clear whether the same 4 or 5 factor should apply when the $3S_m$ range is exceeded, and where the simplified elastic-plastic method of B31.7 is used. This is because the 4 or 5 factor is a purely empirical one which has been found to work in conjunction with the low cycle fatigue curves of ASME III (or B31.7) when the $3S_m$ range is met. This experience is missing when $3S_m$ is exceeded. In view of this, it would appear that in using the B31.7 elastic plastic method, the K_f factor should be increased for the fillet weld just as it is for the mild notches until it can be shown that such a procedure is overly conservative. If the codes were to separate the calculations of fatigue life into two parts (initiation and growth) then the problem with the fillet weld could be handled by computing fatigue life with only a crack growth stage so that resorting to an arbitrary artificial factor would be unnecessary. If for example, a design curve such as that illustrated in Fig.30 were used, then the fatigue life for the fillet weld could be computed. In order to carry out such a computation, numerous lengthy calculations may sometimes be involved, and it is often best to incrementally calculate the cycles associated with several small changes of section thickness. In this way, the appropriate changes in net section stresses, force resultants, ΔK values, and plasticity corrections, can be accounted for so that all major effects are evaluated. Numerous such calculations have been carried out in the AEC sponsored Pipe Rupture Study (21) and it has been found that a close simulation of actual metals fatigue behavior is possible using this approach. It remains to reduce these types of fatigue calculations to a simplified procedure suitable for code application.

REFERENCES

1 L. F. Coffin, Jr., "A Study of the Effects of Cyclic Thermal Stresses on a Ductile Metal," ASME Transactions, vol. 76, no. 6, August 1954, p. 931.

2 S. S. Manson, "Behavior of Materials under Conditions of Thermal Stress," Heat Transfer, Symp. Univ. Mich. Eng. Res. Inst., 1953, pp. 9-75.

3 A.R.C. Markl, "Fatigue Tests of Piping Components," Trans. ASME, 1952.

4 H. Neuber, "Theory of Stress Concentration for Shear-Strained Prismatical Bodies with Arbitrary Nonlinear Stress-Strain Law," Journal of Applied Mechanics, December 1961.

5 E. Z. Stowell, "Stress and Strain Concentration at a Circular Hole in an Infinite Plate," NACA TN-2073, February 1950.

6 E. Krempl, "Low-Cycle Fatigue Strength Reduction in Notched Flat Plates," GEAP-5410, January 1967.

7 H. F. Hardrath and L. Ohman, "A Study of Elastic and Plastic Stress Concentration Factors Due to Notches and Fillets in Flat Plates," NACA TN 2566, 1951.

8 E. E. Zwicky, "Cyclic Strain Concentration Factors with Local Plastic Flow," paper presented at the 1967 ASME Winter Annual Meeting, Pittsburgh, Pa., November 12-17, 1967.

9 H. M. Haydl, "Stress and Strain Concentration in the Plastic Range with Application to Low Cycle Fatigue," internal memorandum 257HA559, General Electric Co., Atomic Power Equipment Department.

10 Reactor Primary Coolant System Rupture Study, Quarterly Progress Report No. 10, GEAP-5554, July-September 1967.

11 S. S. Manson, "Thermal Stress and Low-Cycle Fatigue," McGraw Hill Book Company, 1966, pp. 125-149.

12 Anonymous, "Criteria of Section III of the ASME Boiler and Pressure Vessel Code for Nuclear Vessels," ASME, 1964.

13 J. D. Gilman, "Evaluation of USAS B31.7 Code Elastic-Plastic Correction Factor using GASP Computer Program on a Nozzle Transition," internal memorandum DAR 42, General Electric Co., Atomic Power Equipment Department.

14 E. Wilson, "A Digital Computer Program for the Finite Element Analysis of Solids with Nonlinear Material Properties (GASP)," July 1965.

15 D. R. Miller, "Thermal-Stress Ratchet Mechanism in Pressure Vessels," ASME Paper No. 58-A-129.

16 P. P. Benham and H. Ford, "Low Endurance Fatigue of a Mild Steel and an Aluminum Alloy," Journal of Mechanical Engineering Science, vol. 3, 1961, pp. 119-132.

17 B. F. Langer, "Design of Pressure Vessels for Low-Cycle Fatigue," Journal of Basic Engineering, vol. 84, no. 3, September 1962.

18 Reactor Primary Coolant System Rupture Study, AEC Research and Development Contract AT (04-3)-189 Project Agreement 37.

19 A. J. Brothers, Reactor Primary Coolant System Rupture Study, Quarterly Progress Report No. 3, GEAP-5082, October-December 1965, pp.6-1.

20 S. W. Tagart, Reactor Primary Coolant System Rupture Study, Quarterly Progress Report No. 6, GEAP-5279, July-September 1966, pp. 4-6 to 4-15.

21 S. A. Wilson, Reactor Primary Coolant System Rupture Study, Quarterly Progress Report No. 7, GEAP 5427, October-December 1966, pp. 3-5 to 3-10.

GHC
GCS
FIRST DRAFT
6-14-83

CRITERIA OF THE ASME BOILER AND PRESSURE VESSEL CODE FOR DESIGN BY ANALYSIS IN SECTIONS III AND VIII, DIVISION 2

I. INTRODUCTION

Section III of the ASME Boiler and Pressure Vessel Code was first published in 1963 and contained rules for the design and construction of nuclear pressure vessels. An explanation and discussion of the design by analysis concept and its origin was given in depth in the First and Second Editions of this document. The second edition was written following the 1968 Code Edition.

This third edition of the criteria document is based on the 1983 Code. Although the basic criteria has not significantly changed, there have been many revisions and additions to the Code since 1968. The 1971 Edition of Section III was expanded to include all components. Specific rules for the design of pumps, valves, piping and metal containment systems were included with the vessel rules. As an alternative to the simplified rules for these components, a detailed analysis according to the requirements of NB-3200 may be performed. Additional changes in the 1971 Edition included stress limits for emergency and faulted conditions and a simplified elastic-plastic analysis if the $3S_m$ limit on the range of primary-plus-secondary stress is exceeded. Other major changes in the Code were the addition of rules for component supports in 1973, core support structures in 1973, and concrete reactor vessels and containments (Division 2) in 1975.

CHECK DATES

Now mandatory appendices covering rules for evaluation of faulted conditions and protection against nonductile failure were published in 1973 and _____, respectively. The Section III rules do not include consideration of creep and stress rupture characteristics of materials. Therefore, there are temperature limits, generally 700 to 800'F. In _____, the first Code Case (1331) for the design of components in elevated temperature service was published. Evaluation of high cycle fatigue characteristics resulted in the extension of the fatigue curve for austentic steel, nickel-chromium-iron alloy, nickel-iron-chormium alloy, and nickel-copper alloy from 10^6 to 10^{11} cycles in 1982.

History

The design philosophy of the present Section I (Power Boilers) and Division 1 of Section VIII (Pressure Vessels) of the ASME Boiler Code requires that the wall thickness of a vessel shall be such that the maximum hoop stress does not exceed the allowable stress. It is recognized that high localized and secondary bending stresses may exist in vessels designed and fabricated in accordance with these rules. Insofar as practical, design rules for details have been written to hold such stresses at a safe level consistent with experience.

Section I and Division 1 of Section VIII do not call for a detailed stress analysis but merely set the wall thickness necessary to keep the basic hoop stress below the tabulated allowable stress. They do not require a detailed evaluation of the higher, more localized stresses which are known to exist, but instead allow for these by the safety factor and a set of design rules. Thermal stresses also do not require explicit analysis. The only reference to them is Par. UG-22 where "the effect of temperature gradients" is listed among the loadings to be considered. There is no indication of how this consideration is to be given.

The Special Committee to Review Code Stress Basis was originally established to investigate what changes in Code design philosophy might permit use of higher allowable stresses without reduction in safety. It soon became clear that one approach would be to make better use of modern methods of stress analysis. Detailed evaluation of actual stresses would permit substituting knowledge of localized stresses, and assignment of more rational margins, in place of a larger factor which really reflected lack of knowledge.

The development of analytical and experimental techniques has made it possible to determine stresses in considerable detail. When the stress picture is brought into focus, it is not reasonable to retain the same values of allowable stress for the clear detailed picture as had previously been used for the less detailed one. Neither is it sufficient merely to raise the allowable stresses to reasonable values for the peak stresses, since peak stress by itself is not an adequate criterion of safety. A calculated value of stress means little until it is associated with its location and distribution in the structure and with the type of loading which produced it. Different types of stress have different degrees of significance and must, therefore, be assigned different allowable values. For example, the average hoop stress through the thickness of the wall of a vessel due to internal pressure must be held to a lower value than the stress at the root of a

notch in the wall. Likewise, a thermal stress can often be allowed to reach a higher value than one which is produced by dead weight or pressure. Therefore the Special Committee developed a new set of design criteria which shifted the emphasis away from the use of standard configurations and toward the detailed analyses of stresses. The setting of allowable stress values required dividing stresses into categories and assigning different allowable values to different groups of categories.

The ASME Special Committee dealt with these problems partly by the knowledge and experience of individual members and partly by the results of numerous analytical and experimental investigations. The Code Committee itself does not conduct research programs, but is able to derive much useful information from the Pressure Vessel Research Committee. Among other programs PVRC has sponsored considerable work on fatigue behavior in materials and vessels. Results of these experimental programs were studied by the ASME Special Committee and formed the basis for the design methods for evaluation of fatique behavior in vessels.

The work of the Special Committee lead to the publication of Section III in 1963 and publication of Division 2, Alternative Rules for Pressure Vessels, of Section VIII in 1968. The design requirements of Division 2 consist of a text, comparable to the paragraphs on design in part UG of Division 1, and three appendices:

Appendix 4, Design Based on Stress Analysis
Appendix 5, Design Based on Fatigue Analysis
Appendix 6, Experimental Stress Analysis

These three appendices are essentially identical to the analysis requirements of Section III. They provide a means whereby one can evaluate those vessels subject to severe service stresses or which contain configurations not considered within the text, using the detailed engineering approach which modern methods of stress analysis have made possible.

Because of the prominent role played by stress analysis in designing vessels by the rules of Section III or by the appendices of Division 2, and because of the necessity to integrate the design and analysis efforts, the procedure may be termed "design by analysis." This document provides an explanation of the strength theories, stress categories, and stress limits on which these design procedures are presently based. It also provides an explanation of the methods used for determining the suitability of vessels and parts for cyclic

application of loads. This latest version includes discussions of service limits, brittle fracture criteria, ~~primary stresses for Level C and D~~, high cycle fatigue, simplified elastic-plastic fatigue analysis, thermal stress ratcheting and Class 2/3 criteria.

Strength Theories

The stress state at any point in a structure may be completely defined by giving the magnitudes and directions of the three principal stresses. The possibility of yielding must be determined by means of a strength theory. The theories most commonly used are the maximum stress theory, the maximum shear stress theory (also known as the Tresca criterion), and the distortion energy theory (also known as the octahedral shear theory and the Mises criterion). It has been known for many years that the maximum shear stress theory and the distortion energy theory are both much better than the maximum stress theory for predicting both yielding and fatigue failure in ductile metals. Section I and Division 1 of Section VII use the maximum stress theory, by implication, but Section III and Division 2 use the maximum shear theory. Most experiments show that the distortion energy theory is more accurate than the shear theory, but the shear theory was chosen because it is a little more conservative, it is easier to apply, and it offers some advantages in applications of the fatigue analysis, as will be shown later.

The maximum shear stress at a point is defined as one-half of the algebraic difference between the largest and the smallest of the three principal stresses. Thus, if the principal stresses are σ_1, σ_2, and σ_3, and $\sigma_1 > \sigma_2 > \sigma_3$ (algebraically), the maximum shear stress is $1/2\ (\sigma_1 - \sigma_3)$. The maximum shear stress theory of failure states that yielding in a component occurs when the maximum shear stress reaches a value equal to the maximum shear stress at the yield point in a tensile test. In the tensile test, at yield, $\sigma_1 = S_y$, $\sigma_2 = 0$, and $\sigma_3 = 0$; therefore the maximum shear stress is $S_y/2$. Therefore yielding in the component occurs when

$$1/2\ (\sigma_1 - \sigma_3) = 1/2\ S_y.$$

In order to avoid the unfamiliar and unnecessary operation of dividing both the calculated and the allowable stresses by two before comparing them, a new term called "equivalent intensity of combined stress" or, more briefly, "stress intensity" has been used. The stress intensity is defined as twice the

maximum shear stress and is equal to the largest algebraic difference between any two of the three principal stresses. Thus the stress intensity is directly comparable to strength values found from tensile tests. The term "stress intensity" as just defined is not to be confused with the same term from the field of fracture mechanics.

Design, Service and Test Loadings

The loads on a component are categorized as design, service or test conditions. The analysis requirements and stress limits vary with the category of loading. Primary stresses are evaluated for design, Level C and D service conditions and testing. A fatigue analysis for cyclic stresses is required for Level A and B service conditions. Since primary stresses are not evaluated for Level A and B conditions, the design conditions should include primary loads from Level A and B. The limits for Level C and D primary stresses are higher than Design on the basis that some damage is acceptable for lower probability loads. Level C stress limits are applicable to loads which have a low probability of occurrence but are included to provide assurance that no gross loss of structural integrity will result. Shutdown for repair of damage on the system is required. In addition, the total number of postulated occurrences for such events shall not cause more than 25 stress cycles having an alternating stress value greater than that allowed for 10^6 cycles. This is to preclude fatigue as a failure mode. Level D stress limits are applicable to loads associated with extremely-low-probability events whose consequences are that the integrity and operability of the component may be impaired to the extent that considerations of public health and safety are involved.

II. MODES OF FAILURE, STRESS CATEGORIES AND STRESS LIMITS

Modes of Failure

The various possible modes of failure which confront the pressure vessel designer are:

1. Excessive elastic deformation including elastic instability.
2. Excessive plastic deformation.
3. High strain - low cycle fatigue.
4. Plastic instability - incremental collapse.
5. Brittle fracture.
6. Stress rupture/creep deformation (inelastic)
7. Stress corrosion.
8. Corrosion fatigue.

In dealing with these various modes of failure, we will assume that the designer has at his disposal a picture of the state of stress within the part in question. This would be obtained either through calculation or measurements of both the mechanical and thermal stresses which could occur throughout the entire vessel during transient and steady state operations. The question one must ask is what do these numbers mean in relation to the adequacy of the design? Will they insure safe and satisfactory performance of a component? It is against these various failure modes that the pressure vessel designer must compare and interpret stress values. For example, elastic deformation and elastic instability (buckling) cannot be controlled by imposing upper limits to the calculated stress alone. One must consider, in addition, the geometry and stiffness of a component as well as properties of the material.

The plastic deformation mode of failure can, on the other hand, be controlled by imposing limits on calculated stress, but unlike the fatigue and stress corrosion modes of failure, peak stress does not tell the whole story. Careful consideration must be given to the consequences of yielding, and therefore the type of loading and the distribution of stress resulting therefrom must be carefully studied. The designer must consider, in addition to setting limits for allowable stress, some adequate and proper failure theory in order to define how the various stresses in a component react and contribute to the strength of that part.

The Code provisions intended to prevent the various possible modes of failure are as follows:

(a) Primary stress limits are provided to prevent plastic deformation and to provide a nominal factor of safety on the ductile burst pressure.

(b) Primary plus secondary stress limits are provided to prevent excessive plastic deformation leading to incremental collapse, and to validate the application of elastic analysis when performing the fatigue evaluation.

(c) A peak stress limit is provided to prevent fatigue failure as a result of cyclic loadings.

(d) Special stress limits are provided for elastic and inelastic instability.

(e) Protection against brittle fracture is provided by material selection and the nonmandatory rules of Appendix G, of Section III.

(f) Design criteria for elevated temperature service is provided in Code Case 1592.

Protection against environmental conditions such as corrosion and radiation effects are the responsibility of the designer.

Stress Categories

Different types of stress require different limits, and before establishing these limits it was necessary to choose the stress categories to which limits should be applied. The categories and sub-categories chosen were as follows:

A. Primary Stress

1. General primary membrane stress.
2. Local primary membrane stress.
3. Primary bending stress.

B. Secondary Stress

C. Peak Stress

Definitions of these terms are given in Fig. NB-3222-1 of Section III and Appendix 4, Table 4-120.1 of Section III, Division 2. The chief characterisitics of these terms may be described briefly as follows:

a. Primary Stress is a stress developed by the imposed loading which is necessary to satisfy the laws of equilibrium between external and internal forces and moments. The basic characteristic of a primary stress is that it is not self-limiting. If a primary stress exceeds the yield strength of the material through the entire thickness, the prevention of failure is entirely dependent on the strain-hardening properties of the material.

b. Secondary Stress is a stress developed by the self-constraint of a structure. It must satisfy an imposed strain pattern rather than being in equilibrium with an external load. The basic characteristic of a secondary stress is that it is self-limiting. Local yielding and minor distortions can satisfy the discontinuity conditions or thermal expansions which cause the stress to occur.

c. Peak Stress is the highest stress in the region under consideration. The basic characteristic of a peak stress that it causes no significant distortion and is objectionable mostly as a possible source of fatigue failure.

The need for dividing primary stress into membrane and bending components is that, as will be discussed later, limit design theory shows that the calculated value of a primary bending stress may be allowed to go higher than the calculated value of a primary membrane stress. The placing in the primary category of local membrane stress produced by mechanical loads, however, requires some explanation because this type of stress really has the basic characteristics of a secondary stress. It is self-limiting and when it exceeds yield, the external load will be resisted by other parts of the structure, but this shift may involve intolerable distortion and it was felt that it must be limited to a lower value than other secondary stresses, such as discontinuity bending stress and thermal stress.

Secondary stress could be divided into membrane and bending components, just as was done for primary stress, but after the removal of local membrane stress to the primary category, it appeared that all the remaining secondary stresses could be controlled by the same limit and this division was unnecessary.

Thermal stresses are never classed as primary stresses, but they appear in both of the other categories, secondary and peak. Thermal stresses which can produce distortion of the structure are placed in the secondary category and thermal stresses which result from almost complete suppression of the differential expansion, and thus cause no significant distortion, are classed as peak stresses.

A special exception to these general rules is the case of the stress due to a radial temperature gradient in a cylindrical shell. It is specifically stated that this stress may be considered a local thermal stress. In reality, the linear portion of this gradient can cause deformation, but it was the opinion of the Special Committee that this exception could be safely made.

One of the commonest types of peak stress is that produced by a notch, which might be a small hole or a fillet. The phenomenon of stress concentration is well-known and requires no further explanation here.

Many cases arise in which it is not obvious which category a stress should be placed in, and considerable judgement is required. In order to standardize this procedure and use the judgement of the writers of the Code rather than the judgement of individual designers, a table was prepared covering most of the situations which arise in pressure vessel design and specifying which category each stress must be placed in. This table appears as Fig. NB-3222-1 of Section III and Appendix 4, Table 4-120.1 of Division 2.

The grouping of the stress categories for the purpose of applying limits to the stress intensities is illustrated in Fig. NB-3222-1 of Section III and Fig. 4-130.1 of Appendix 4 of Division 2. This diagram has been called the "hopper diagram" because it provides a hopper for each stress category. The calculated stresses are made to progress through the diagram in the direction of the arrows. Whenever a rectangular box appears, the sum of all the stress components which have entered the box are used to calculate the stress intensity, which is then compared to the allowable limit, shown in the circle adjacent to the rectangle. The following points should be noted in connection with this diagram:

a. The symbols P_m, P_l, P_b, Q and F do not represent single quantities, but each represents a set of six quantities, three direct stress and three shear stress components. The addition of stresses from different categories must be performed at the component level, not after translating the stress components into a stress intensity. Similarly, the calculation of membrane stress intensity involves the averaging of stresses across a section, and this averaging must also be performed at the component level.

b. The stresses in Category Q are those parts of the total stress which are categorized as secondary, and do not include primary stresses which may also exist at the same point. It should be noted, however, that a detailed stress analysis frequently gives the combination of primary and secondary stresses directly, and this calculated value represents the total of P (or P_L) + P_b + Q and not Q alone. It is not necessary to calculate Q separately since the stress limit (to be described later) applies to the total stress intensity. Similarly, if the stress in Category F is produced by a stress concentration, the quantity F is the additional stress produced by the notch, over and above the nominal stress, but it is not necessary to calculate F separately.

Basic Stress Intensity Limits

The choice of the basic stress intensity limits for the stress categories described above was accomplished by the application of limit design theory tempered by some engineering judgement and some conservative simplifications. The principles of limit design which were used can be described briefly as follows.

The assumption is made of perfect plasticity with no strain-hardening. This means that an idealized stress-strain curve of the type shown in Fig. 1 is assumed. Allowable stresses based on perfect plasticity and limit design theory may be considered as a floor below which a vessel made of any sufficiently ductile material will be safe. The actual strain-hardening properties of specific materials will give them larger or smaller margins above this floor.

In a structure as simple as a straight bar in tension, a load producing yield stress, S_y, results in "collapse". If the bar is loaded in bending, collapse does not occur until the load has been increased by a factor known as the "shape factor" of the cross section; at that time a "plastic hinge" is formed. The shape factor for a rectangular section in bending is 1.5. When the primary stress is a rectangular section consists of a combination of bending and axial tension, the value of the limit load depends on the ratio between the tensile and bending loads. Fig. 2 shows the value of the maximum calculated stress at the outer fiber of a rectangular section which would be required to produce a plastic hinge, plotted against the average tensile stress across the section, both values expressed as multiples of the yield stress, S_y. When the average tensile stress, P_m, is zero, the failure stress for bending is 1.5 S_y. When the average tensile stress is S_y, no additional bending stress, P_b, may be applied.

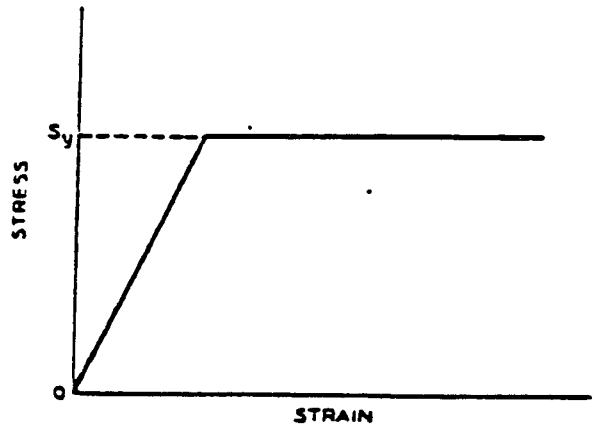

FIGURE 1. IDEALIZED STRESS-STRAIN RELATIONSHIP

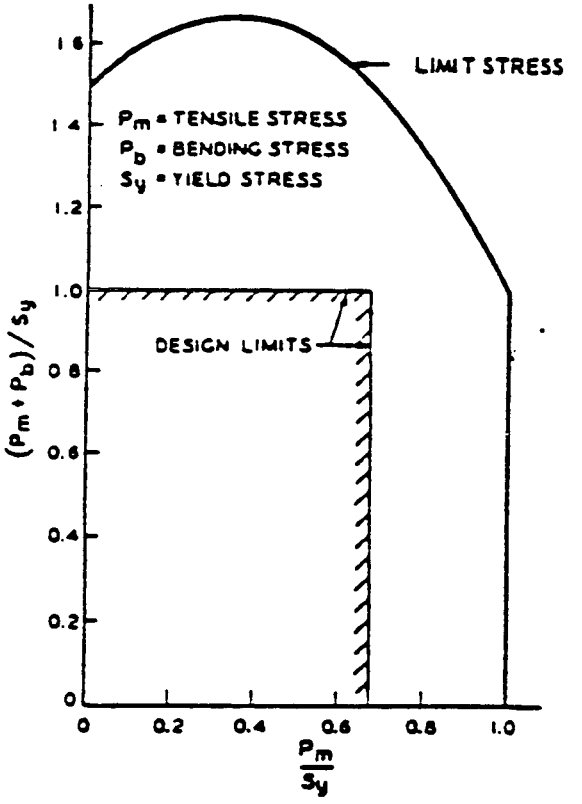

FIGURE 2. LIMIT STRESS FOR COMBINED TENSION AND BENDING (RECTANGULAR SECTION)

Figure 2 was used to choose allowable values, in terms of the yield stress, for general primary membrane stress, P_m, and primary membrane-plus-bending stress, $P_m + P_b$. It may be

seen that limiting P_m to (2/3) S_y and $P_m + P_b$ to S_y provides adequate safety. The safety factor is not constant for all combinations of tension and bending, but a design rule to provide a uniform safety factor would be needlessly complicated.

In the study of allowable secondary stresses, a calculated elastic stress range equal to twice the yield stress has a very special significance. It determines the borderline between loads which, when repetitively applied, allow the structure to "shake down" to elastic action and loads which produce plastic action each time they are applied. The theory of limit design provides rigorous proof of this statement, but the validity of the concept can easily be visualized. Consider, for example, the outer fiber of a beam which is strained in tension to a strain value , somewhat beyond the yield strain as shown in Fig. 3(a) by the path OAB. The calculated elastic stress would be $S = S_1 = E$ 1. Since we are considering the case of a secondary stress, we shall assume that the nature of the loading is such as to cycle the strain from zero to 1 and back to zero, rather than cycling the stress from zero to S_1, and back to zero. When the beam is returned to its undeflected position, Ø, the outer fiber has a residual compressive stress of magnitude $S_1 - S_y$. On any subsequent loading, this residual compression must be removed before the stress goes into tension and thus the elastic range has been increased by the quantity $S_1 - S_y$. If $S_1 = 2S_y$, the elastic range becomes $2S_y$, but if S_1 $2S_y$, the fiber yields in compression, as shown by EF in Fig. 3(b) and all subsequent cycles produce plastic strain. Therefore, $2S_y$ is the maximum value of calculated secondary elastic stress which will "shake down" to purely elastic action.

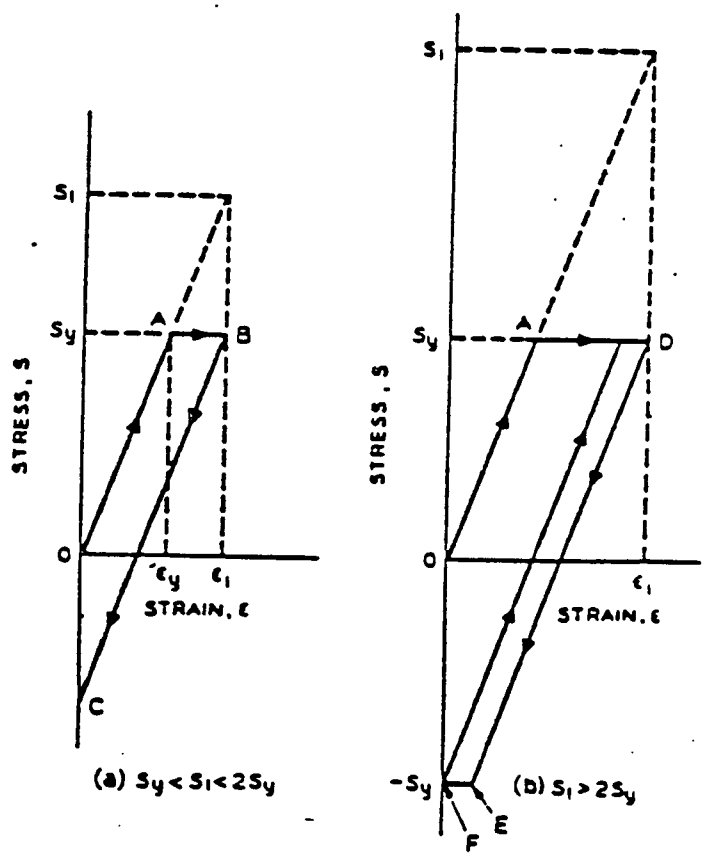

FIGURE 3. STRAIN HISTORY BEYOND YIELD

An important point to note from the foregoing discussion of primary and secondary stresses in 1.5 S_y is the failure stress for primary bending, whereas for secondary bending $2S_y$ is merely the threshold beyond which some plastic action occurs. Therefore the allowable design stress for primary bending must be reduced below $1.5S_y$ to, say, $1.0S_y$, whereas $2S_y$ is a safe design value for secondary bending since a little plastic action during overloads is tolerable. The same type of analysis shows that $2S_y$ is also a safe design value for secondary membrane tension. As described previously, local membrane stress produced by mechanical load has the characteristics of a secondary stress but has been arbitrarily placed in the primary category. In order to avoid excessive distortion, it has been assigned an allowable stress level of S_y, which is 50 percent higher than the allowable for general primary membrane stress but precludes excessive yielding.

We have now shown how the allowable stresses for the first four stress categories listed in the previous section should be related to the yield strength of the material. The last category, peak stress, is related only to fatigue, and will be discussed later. With the exception of some of the special

stress limits, the allowables in Codes are not expressed in terms of the yield strength, but rather as multiples of the tabulated value S_m, which is the allowable for general primary membrane stress. In assigning allowable stress values to a variety of materials with widely varying ductilities and widely varying strain-hardening properties, the yield strength alone is not a sufficient criterion. In order to prevent unsafe designs in materials with low ductility and in materials with high yield-to-tensile ratios, the Code has always considered both the yield strength and the ultimate tensile strength in assigning allowable stresses. This principle has not been changed in Section III or Division 2 but the chosen fractions of the mechanical properties have been increased to two-thirds yield strength and one-third ultimate strength instead of five-eighths yield strength (for ferrous materials) and one-fourth ultimate strength. The Special Committee believed that this increase was quite safe because the detailed stress analysis required eliminates the need for a large safety factor to cover unanalyzed areas. The stress intensity limits for the various categories given are such that the multiples of yield strength described above are never exceeded.

The allowable stress intensity for austenitic steels and some non-ferrous materials, at temperatures above 100 F, may exceed $(2/3)S_y$ and may reach $0.9S_y$ at temperature. Some explanation of the use of up to $0.9S_y$ for these materials as a basis for S_m is needed in view of Figure 2 because this figure would imply that loads in excess of the limit load are permitted. The explanation lies in the different nature of these materials' stress strain diagram. These materials have no well-defined yield point but have strong strain-hardening capabilities so that their yield strength is effectively raised as they are highly loaded. This means that some permanent deformation during the first loading cycle may occur, however the basic structural integrity is comparable to that obtained with ferritic materials. This is equivalent to choosing a somewhat different definition of the "design yield strength" for those materials which have no sharply defined yield point and which have strong strain-hardening characteristics. Therefore, the S_m value in the code tables, regardless of material, can be thought of as being no less than 2/3 of the "design yield strength" for the material in evaluating the primary and secondary stresses.

Table I summarizes the basic stress limits and shows the multiples of yield strength and ultimate strength which these limits do not exceed.

TABLE I. BASIC STRESS INTENSITY LIMITS

Stress Intensity	Tabulated Value	Yield Strength	Ultimate Tensile Strength
General primary membrane (P_m)	S_m	$\leq 2/3S_y$	$\leq 1/3S_u$
Local primary membrane (P_l)	$1.5S_m$	$\leq S_y$	$\leq 1/2S_u$
Primary membrane plus bending ($P_l + P_b$)	$1.5S_m$	$\leq S_y$	$\leq 1/2S_u$
Primary plus secondary ($P_l + P_b + Q$)	$3S_m$	$\leq 2S_y$	$\leq S_u$

Stresses Above Yield Strength

The primary criterion of the structural adequacy of a design, is that the stresses, as determined by calculation or experimental stress analysis, shall not exceed the specified allowable limits. It frequently happens that both the calculated stress and allowable stress exceeds the yield strength of the material. Nevertheless, unless stated specifically otherwise, it is expected that calculations be made on the assumption of elastic behavior.

Allowable stresses higher than yield appear in the values for primary-plus-secondary stress and in the fatigue curves. In the case of the former, the justification for allowing calculated stresses higher than yield is that the limits are such as to assure shake-down to elastic action after repeated loading has established a favorable pattern of residual stresses. Therefore the assumption of elastic behavior is justified because it really exists in all load cycles subsequent to shake-down.

In the case of fatigue analysis, plastic action can actually persist throughout the life of the vessel, and the justification for the specified procedure is somewhat different. Repetitive plastic action occurs only as the result of peak stresses in relatively localized regions and these regions are intimately connected to larger regions of the vessel which behave elastically. A typical example is the peak stress at the root of a notch, in a fillet, or at the edge of small hole. The material in these small regions is strain-cycled rather than stress-cycled (as will be discussed

later) and the elastic calculations give numbers which have the dimensions of stress but are really proportional to the strain. The factor of proportionality for uniaxial stress is, of course, the modulus of elasticity. The fatigue design curves have been specially designed to give numbers comparable to these fictitious calculated stresses. The curves are based on strain-cycling data and the strain values have been multiplied by the modulus of elasticity. Therefore stress intensities calculated from the familiar formulas of strength-of-materials texts are directly comparable to the allowable stress values in the fatigue curves.

Prevention Against Brittle Fracture

Pressure vessel components, made of ferritic materials, can fail in a brittle fracture mode under certain conditions. Primary characteristics of brittle fracture are that the failure will be sudden and that there will be little deformation prior to failure. The parameters that govern the brittle fracture mode are operating metal temperature, material toughness, presence of sharp defects and stress state.

Four different approaches are used in the ASME Boiler and Pressure Vessel Code to provide assurance against brittle fracture. The four approaches are 1) to require the materials to satisfy certain fracture toughness requirements (NB-2330); 2) to require non-destructive examination of components both during fabrication (NB-5000) and during operation (IWB-1000); 3) hydrostatic testing (NB-6212 and IWB-5000) and 4) analysis (NB-3211d).

Fracture toughness is the single material property that characterizes the brittle fracture behavior. Fracture toughness requirements, specified in the Code (NB-2331) are based on both transition temperature and fracture mechanics concepts. In essence, the transition temperature concept is based on the marked change in fracture behavior with increasing temperature from cleavage fracture to ductile fracture. The transition procedure is applied in design by permitting loading on the component only at temperatures that are a specified increment higher than the transition temperature. Drop weight tests (NB-2321.1) and Charpy V-Notch tests (NB-2321.2) are used to define the transition temperature. For the drop weight test, the nil-ductility transition temperature (NDT) is defined in ASTM E-208-69 as the temperature above which the specimen will sustain a specific amount of deformation without complete failure. The resulting transition temperatures can be defined for the Charpy V-Notch specimen in terms of an energy level, the amount of deformation or the fracture appearance.

Although the transition temperature procedure has the virtues of simplicity, it does not inherently have the capability of quantitatively treating the presence of flaws in structures. Linear elastic fracture mechanics (LEFM is the more quantitative approach to treating the presence of flaws. This concept (LEFM) is based on an elastic analysis of the stresses in the neighborhood of the tip of a sharp crack. It is found that the stress distributions near the crack tip are similar and the stress magnitudes all depend on a single parameter termed the stress intensity factor, designated as K_I. The subscript I designates the opening mode of displacement between crack surfaces. The stress intensity factor K_I quantifies the potential for brittle fracture in terms of the nominal tensile stress (σ) normal to the plane of the crack and the characteristic dimension such as crack depth (a) in the general form:

$$K_I = C\sigma\sqrt{a}$$

where C is a dimensionless constant dependent on crack geometry, ratio of the crack size to the size of the structural member and the type of loading (membrane, bending, etc.).

The basic premise of linear elastic fracture mechanics is that unstable propagation of an existing flaw will occur when the value of K_I attains a critical value designated a K_{IC}. K_{IC} is called the fracture toughness of the material. In the case jof ferritic materials, it has been found that the fracture toughness properties are dependent on temperature and on the loading rates imposed. Dynamic initiation fracture toughness obtained under fast or rapidly applied loading rates is designated K_{Id}. Further, in structural steels a crack arrest fracture toughness is obtained under conditions where a propagating flaw is arrested with a test specimen. The crack arrest toughness is designated K_{Ia}. Appendix G to Section III presents a K_{IR}, reference stress intensity factor as a function of temperature based on the lower bound of static K_{IC}, dynamic K_{Id}, and crack arrest K_{Ia} fracture toughness values. The derivation of the K_{IR} vs. temperature curve shown in Figure 4 is given in WRC Bulletin 175 (1) and represents all known K_{IC}, K_{Id} and K_{Ia} data for A533 grade B class 1 plates, A508 class 2 forgings and associated

weldments. No available data points for static, dynamic or arrest tests fall below the curve given in Figure G-2110.1. The value of K_{IR} at NDT represents a very conservative assumption as to the critical stress intensity vs. temperature properties of materials similar to those tested, as related to the measured NDT.

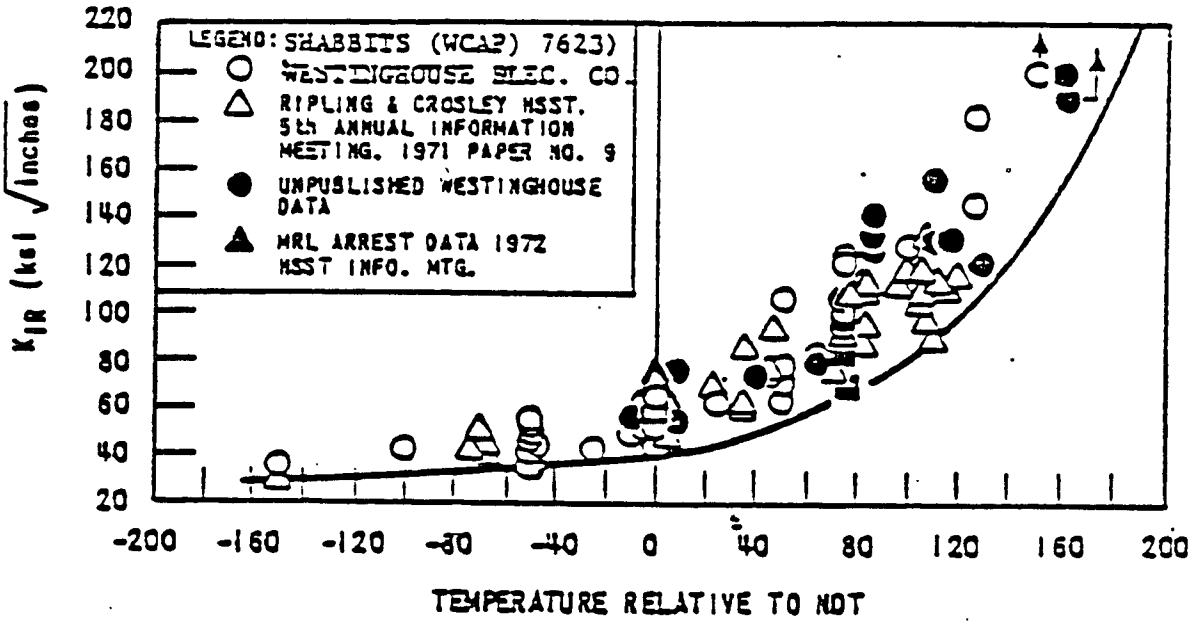

FIGURE 4 DERIVATION OF CURVE OF REFERENCE STRESS INTENSITY FACTOR (K_{IR})

The Code identifies a reference nil-ductility transition temperature RT_{NDT} (NB-2331a) to index the K_{IR} curve to the temperature scale. The reference temperature RT_{NDT} is defined (NB-2331) as the greater of the drop weight nil-ductility transition temperature or the temperature 60'F less than the 50 ft-lb (and 35 mils lateral expansion temperature) as determined from Charpy specimens oriented normal (NB-2332.2) to the rolling direction of the material. The requirements of Charpy tests at 60'F above NDT serves to weed out nontypical materials and provides assurance of adequate fracture toughness at "upper shelf" temperatures. In addition, the requirement of lateral expansion values provides protection from variation in yield strength. Measurement of lateral expansion can serve as an index of ductility.

The fourth approach, analysis for protection against brittle fracture, (NB-3211d) is based on linear elastic fracture mechanics (LEFM) discussed in the previous section. NB-3211(d) specifies that Appendix G to Section III is an acceptable procedure for non-ductile failure prevention. Appendix G is based on the principles of LEFM and incorporates the concept of postulated flaws and minimum fracture toughness in a component. G-2110 identifies the relationship which can be conservatively expected between the reference stress intensity factor K_{IR} (lower bound of K_{Ic}, K_{Id}, K_{Ia} data) and temperature which is indexed to the reference nil-ductility temperature RT_{NDT} determined per NB-2331. G-2120 give a postulated defect to be used in determining the allowable loading. It consists of a sharp surface flaw, perpendicular to the direction of maximum stress, having a depth of 1/4 of the section thickness over most of the thickness range of interest.

The assumed shape of the postulated flaw is semi-elliptic, with a length six times its depth. In sizing the postulated flaw, it was assumed that with the combination of examinations required by Section III and the volumetric examination required by Section XI, there is a low probability that a defect larger than about four times the Code allowable will escape detections. G-2200 outlines the recommended procedure for protection against nonductile failure for service level A and B operating conditions. Within G-2200, G-2214 defines methods to calculate stress intensity factors, K_I. G-2215 provides the basis for determining allowable pressure at any temperature during operating conditions. The requirements to be satisfied, and from which the allowable pressure for any assumed rate of temperature change can be determined is:

$$2K_{IM} + K_{IT} \quad K_{IR}$$

throughout the life of the component at each temperature with K_{IM} from G-2214.1, K_{IT} from G-2214.2 and K_{IR} from G-2212. The recommended safety factor of 2 on K_{IM} adds to the conservatism of the assumptions. Due to its secondary and self-releiving nature no safety factor is given for K_{IT}. G-2410 relaxes the conservatism by reducing the safety factor for K_{IM} to 1.5 during the system hydrostatic testing.

Appendix A of Section XI uses a procedure based upon the principles of linear elastic fracture mechanics for analysis of flaw indications detected during inservice inspection. While

Section III is a construction code, Section XI provides rules for the integrity of the structure during its service life. The concepts introduced in Appendix G to Section III are carried over to Appendix A of Section XI. Models for flaw analysis are given in A-2000 while material property considerations are given in A-4000. The concept of fatigue crack growth, a small flaw growing to a larger flaw, is introduced in A-4300. The K_{IR} curve of Appendix G is identified as K_{Ia} (A-4200) in Figure A-4200-1. For materials subjected to fast neutron fluence, the degradation of the material fracture toughness due to irradiation is accounted for (A-4400). The analysis of flaw indications detected during inservice inspection includes applying the anlyses to service levels C and D conditions (A-5300) as well as service level A conditions (A-5200).

Prevention against brittle fracture for ferritic Class 2 and 3 components are based on transition temperature concepts. Drop weight tests (NC 2321.1) and Charpy V-notch tests (NC 2321.2) are used to define required toughness levels with the lowest service temperature for the ferritic component materials being higher with increasing thickness of the component. This temperature increment for the components is a function of increasing thickness. The heavier sections require a larger temperature increment. Charpy V-notch tests (ND 2321) are the single transition temperature basis for Class 3 components; the temperature increment concept was similarly used. The toughness criteria used to establish the specified temperature increments considered linear elastic fracture mechanics. NC 2332 and ND specify that Appendix G to Section III is an acceptable alternate procedure for non-ductile failure prevention. More detail can be found in (1).

Design Criteria for Elevated Temperature Service

The design criteria in Section III for temperatures below the creep range are based on time-independent or tensile properties. By limiting the service temperatures for each alloy through the stresses listed in Table I-1.0, the Section III Criteria are not applied where there exists significant time-dependent phenomena such as creep and stress relaxation.

Code Cases 1331-5 (later changed to N-47) introduced design criteria for elevated temperature service for Class 1 components. Code Cases N-201 and N-253 were later developed for Class CS (Core Support Structures), and Class 2 and 3 Components, respectively. A more complete version of the design criteria for Class 1 components may be found in Reference 2 and further discussion in References 3 through 6.

III. FATIGUE ANALYSIS

One of the important innovations in Section III and Division 2 of Section VIII as compared to Section I and Division I of Section VIII, is the recognition of fatigue as a possible mode of failure and the provision of specific rules for its prevention. Fatigue has been a major consideration for many years in the design of rotating machinery and aircraft, where the expected number of cycles is in the millions and can usually be considered infinite for all practical purposes. For the case of large numbers of cycles, the primary concern is the endurance limit, which is the stress which can be applied an infinite number of times without producing failure. Similar situations may occur in reactor systems; e.g., flow induced vibration. Since the endurance limit for Anstenitic Steel, Nickel-Chromium-Iron Alloy, Nickel-Iron-Chromium Alloy and Nickel-Copper Alloy is greater than 10^6 cycles, fatigue curves are provided to 10^{11} cycles for these materials. In reactor components, however, many of the more signifcant cycles are in the range of 10^3 to 10^5. Therefore, in order to make fatigue analysis practical for pressure vessels, it was necessary to develop some new concepts not previously used in machine design [7,8].

Use of Strain-Controlled Fatigue Data

The chief difference between high-cycle fatigue and low-cycle fatigue is the fact that the former involves little or no plastic action, whereas failure in a few thousand cycles can be produced only by strains in excess of the yield strain. In the plastic region large changes in strain can be produced by small changes in stress. Fatigue damage in the plastic region has been found to be a function of plastic strain and therefore fatigue curves for use in this region should be based on tests in which strain rather than stress is the controlled variable. As a matter of convenience, the strain values used in the tests are multiplied by the elastic modulus to give a fictitious stress which is not the acutal stress applied but has the advantage of being directly comparable to stresses calculated on the assumption of elastic behavior.

The general procedure used in evaluating the strain-controlled fatigue data was to obtain a "best fit" for the quantities A and B in the equation

where
$$S = \frac{E}{4\sqrt{N}} \left(\ell_c \text{LN}\right) \frac{100}{100 - A} + B \qquad (1)$$

E = elastic modulus (psi)
N = number of cyles to failure
S = strain amplitude times elastic modulus

It is possible to estimate the fatigue properties by taking A as the percentage reduction of area in a tensile test, RA, and B as the endurance limit, S_e.

The use of strain instead of stress and the consideration of plastic action have necessitated some additional departures from the conventional methods of studying fatigue problems. It has been common practice in the past to use lower stress concentration factors for small numbers of cycles than for large numbers of cyles. This is reasonable when the allowable stresses are based on stress-fatigue data, but is not advisable when strain-fatigue data are used. Fig. 5 shows typical relationships between stress, S, and cycles-to-failure, N, from (A) strain cycling tests on unnotched specimens, (B) stress-cycling tests on unnotched specimens, and (C) stress-cycling tests on notched specimens. The ratio between

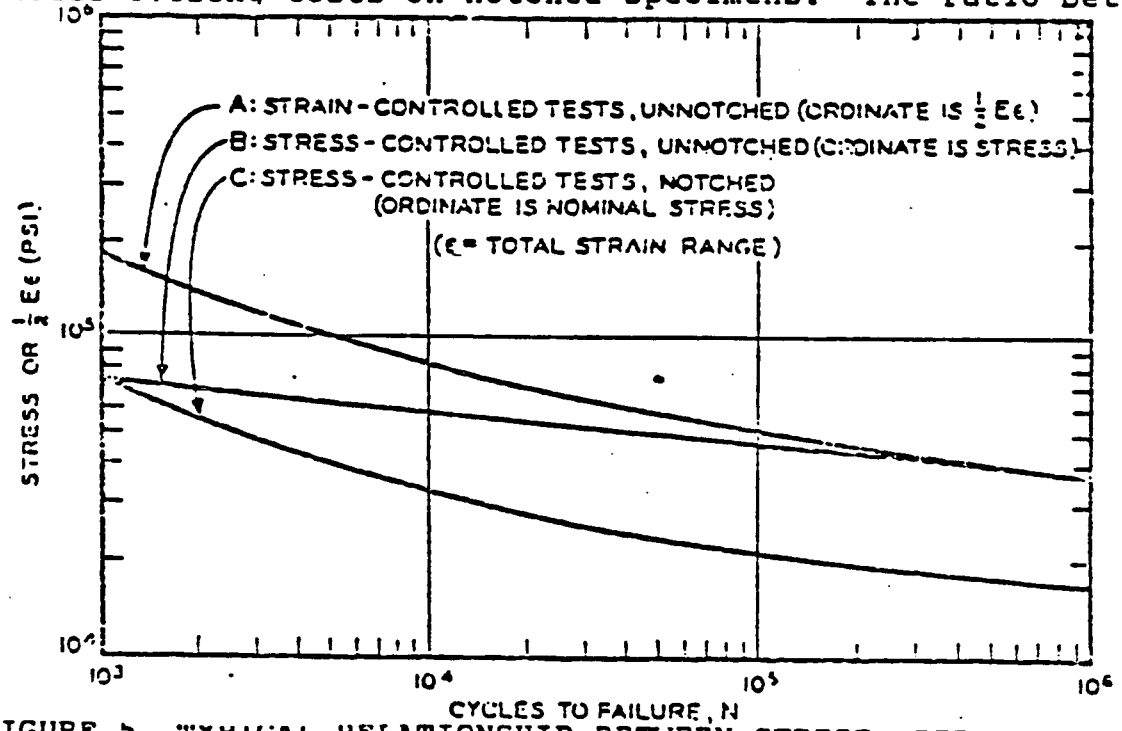

FIGURE 5. TYPICAL RELATIONSHIP BETWEEN STRESS, STRAIN, AND CYCLES-TO-FAILURE.

the ordinates of curves (B) and (C) decreases with decreasing cycles-to-failure, and this is the basis for the commonly-accepted practice of using lower values of K (stress concentration factor) for lower values of N. In (C), however, although nominal stress is the controlled parameter, the material in the root of the notch is really being strain cycled, because the surrounding material is at a lower stress and behaves elastically. Therefore it should be expected that

the ratio between curves (A) and (C) should be independent of N and equal to K. For this reason it is recommended in Section III and Division 2 of Section VIII that the same value of K be used regardless of the number of cycles involved.

The choice of an appropriate stress concentration factor is not an easy one to make. For fillets, grooves, holes, etc., of know geometry, it is safe to use the theoretical stress concentration factors found in such references as [9] and [10], even though strain concentrations can sometimes exceed the theoretical stress concentration factors. The use of the theoretical factor as a safe upper limit is justified, however, since strain concentrations significantly higher than the stress concentration only occur when gross yielding is present in the surrounding material, and this situation is prevented by the use of basic stress limits which assure shake-down to elastic action. For very sharp notches it is well known that the theoretical factors grossly overestimate the true weakening effect of the notch in the low and medium strength materials used for pressure vessels. Therefore no factor higher than 5 need ever be used for any configuration allowed by the design rules and an upper limit of 4 is specified for some specific constructions such as fillet welds and screw threads. When fatigue tests are made to find the appropriate factor for a given material and configuration, they should occur in a reasonably large number of cycles (>1000) so that the test does not involve gross yielding.

Effect of Mean Stress

Another deviation from common practice occurs in the consideration of fluctuating stress, which is a situation where the stress fluctuates around mean value different from zero, as shown in Fig. 6. The evaluation of the effects of mean stress is commonly accomplished by use of the modified Goodman diagram, as shown in Fig. 7 where mean stress is plotted as the abscissa and the amplitude (half range) of the fluctuation is plotted as the ordinate. The straight line joining the endurance limit, S_e, (where $S_N = S_e$) on the vertical axis (point E) with the ultimate strength, S_u, on the horizontal axis (point D) is a conservative approximation of the combinations of mean and alternating stress which produce failure in large numbers of cycles. A little consideration of

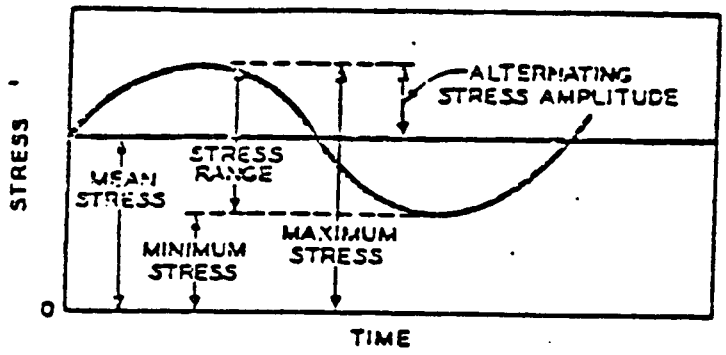

FIGURE 6. STRESS FLUCTUATION AROUND A MEAN VALUE

this diagram shows that not all points below the "failure" line, ED, are feasible. Any combination of mean and alternating stresses which results in a stress excursion above the yield strength will produce a shift in the mean stress which keeps the maximum stress during the cycle at the yield value. This shift has already been illustrated by the strain history shown in Fig. 4. The feasible combinations of mean and alternating stress are all contained within the 45 degree triangle AOB or on the vertical axis above A, where A is the yield strength on the vertical axis and B is the yield strength on the horizontal axis. Regardless of the conditions under which any test or service cycle is started, the true conditions after the application of a few cycles must fall within this region because of combinations above AB have a maximum stress above yield and there is a consequent reduction of mean stress which shifts the conditions to a point on the line AB or all the way to the vertical axis.

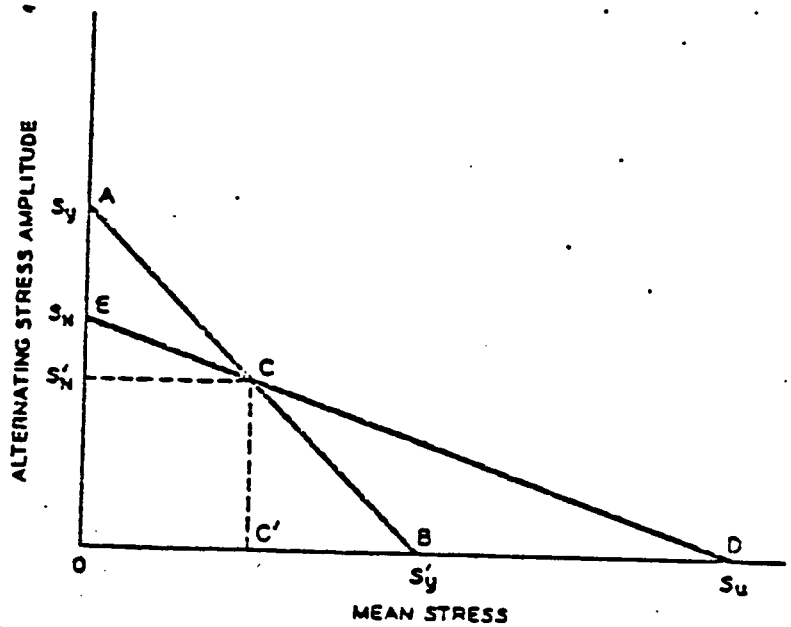

FIGURE 7. MODIFIED GOODMAN DIAGRAM

It may be seen from the foregoing discussion that the value of mean stress to be used in the fatigue evaluation is not always the value which is calculated directly from the imposed loading cycle. When the loading cycle produces calculated stresses which exceed the yield strength at any time, it is necessary to calculate an adjusted value of mean stress before completing the fatigue evaluation. The rules for calculating this adjusted value when the modified Goodman diagram is applied may be summarized as follows:

Let S'_{mean} = basic value of mean stress (calculated directly from loading cycle)

S_{mean} = adjusted value of mean stress

S_{alt} = amplitude (half range) of stress fluctuation

S_y = yield strength

If $S_{alt} + S'_{mean} \leq S_y$, $S_{mean} = S'_{mean}$

If $S_{alt} + S'_{mean} > S_y$, and $S_{alt} < S_y$, $S_{mean} = S_y - S_{alt}$ (1)

If $S_{alt} \geq S_y$, $S_{mean} = \emptyset$.

The fatigue curves are based on tests involving complete stress reversal, that is $S_{mean} = \emptyset$. Since the presence of a mean stress component detracts from the fatigue resistance of the material, it is necessary to determine the equivalent alternating stress component for zero mean stress before entering the fatigue curve. This quantity, designated S_{eq}, is the alternating stress component which produces the same fatigue damage at zero mean stress as the actual alternating stress component, S_{alt}, produces at the existing value of mean stress. It can be obtained graphically from the Goodman diagram by projecting a line as shown in Fig. 8 from S_u through the point (S_{mean}, S_{alt}) to the vertical axis. It is usually easier, however, to use the simple formula

$$S_{eq} = \frac{S_{alt}}{1 - \frac{S_{mean}}{S_u}}. \qquad (3)$$

S_{eq} is the value of stress to be used in entering the fatigue curve to find the allowable number of cycles.

The foregoing discussion of mean stress and the shift which it undergoes when yielding occurs leads to another necessary deviation from standard procedures. In applying stress concentration factors to the case of fluctuating stress, it has been the common practice to apply the factor to only the alternating component. This is not a logical procedure, however, because the material will respond in the same way to a given load regardless of whether the load will later turn out to be steady or fluctuating. It is more logical to apply the concentration factor to both the mean and the alternating component and then consider the reduction which yielding produces in the mean component. It is important to remember that the concentration factor must be applied before the adjustment for yielding is made. The following example shows that the common practice of applying the concentration factor to only the alternating component gives a rough approximation to the real situation but can sometimes be unconservative.

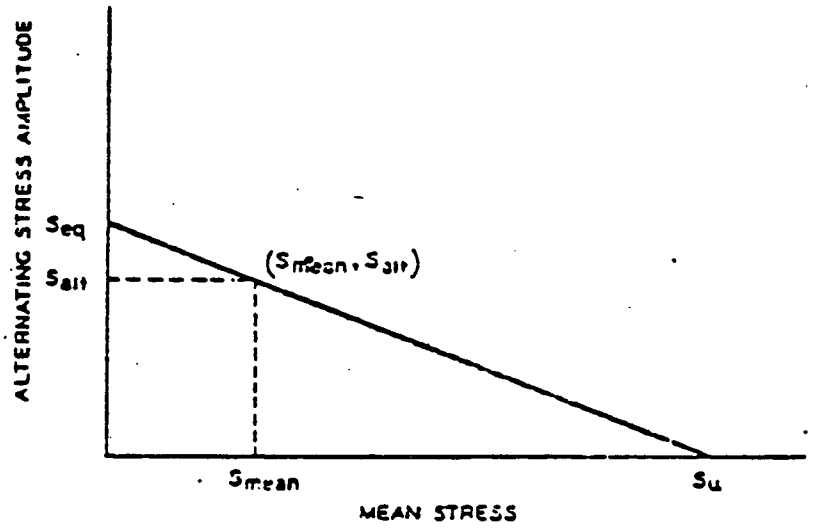

FIGURE 8. GRAPHICAL DETERMINATION OF S_{eq}.

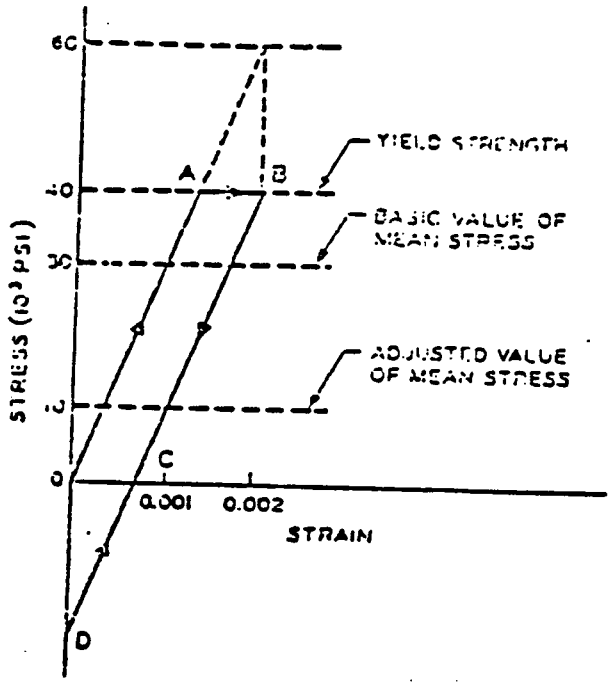

FIGURE 9. IDEALIZED STRESS VS STRAIN HISTORY

Take the case of a material with 80,000 psi tensile strength, 40,000 psi yield strength and 30 x 10^6 psi modulus made into a notched bar with a stress concentration factor of 3. The bar is cycled between nominal tensile stress values of 0 and 20,000 psi. Common practice would call S_{mean}, the mean stress, 10,000 psi and S_{alt}, the alternating component, (1/2) x 3 x 20,000 = 30,000 psi. The stress-strain history of the material at the root of the notch would be, in idealized form, as shown in Fig. 8. The calculated maximum stress, assuming elastic behavior, is 60,000 psi. The basic value of mean stress, S_{mean}, is 30,000 psi, but since $S_{alt} + S_{mean} = 60,000$ psi $> S_y$ and $S_{alt} = 30.000$,psi $< S_y$,

$$S_{mean} = S_y - S_{alt} = 40,000 - 30,000 = 10,000 \text{ psi}$$

and

$$S_{eq} = \frac{30,000}{1 - \frac{10,000}{80,000}} = 34,300 \text{ psi.}$$

It so happens that, for the case chosen, the common practice gives exactly the same results as the proposed method. Thus, the yielding during the first cycle is seen to be the justification for the common practice of ignoring the stress concentration factor when determining the mean stress component. The common practice, however, would have given the

same result regardless of the yield strength of the material, whereas the proposed method gives different mean stresses for different yield strengths. For example, if the yield strength had been 50,000 psi, S_{mean} would have been 20,000 psi and S_{eq} by the proposed method would have been 40,000 psi. The common practice would have given 34,3000 psi for S_{eq} and too large a number of cycles would have been allowed.

For parts of the structure, particularly if welding is used, the residual stress may produce a value of mean stress higher than that calculated by the procedure. Therefore it would be advisable and also much easier to adjust the fatigue curve downward enough to allow for the maximum possible effect of mean stress. It will be shown here that this adjustment is small for the case of low and medium-strength materials.

As a first step in finding the required adjustment of the fatigue curve, let us find how the mean stress affects the amplitude of alternating stress which is required to produce fatigue failure. In the modified Goodman diagram of Fig. 7 it may be seen that at zero mean stress the required amplitude for failure in N cycles is designated S_N. As the mean stress increases along OC', the required amplitude of alternating stress decreases along the line EC. If we try to increase the mean stress beyond C', yielding occurs and the mean stress reverts to C'. Therefore C' represents the highest value of mean stress which has any effect on fatigue life. Since S_N' in Fig. 7 is the alternating stress required to produce failure in N cycles when the mean stress is at C', S_N' is the value to which the point on the fatigue curve at N cycles must be adjusted if the effects of mean stress are to be ignored. From the geometry of Fig. 7, it can be shown that

$$S'_N = S_n \quad \frac{S_u - S_y}{S_u - S_N} \quad \text{for } S_N < S_y$$

When N decreases to the point where $S_N \geq S_y$, the $S_N' = S_N$ and no adjustment of this region of the curve is required.

Figures 10, 11, and 12 show the fatigue data which were used to construct the design fatigue curves for certain materials. In each case the solid line is the best-fit failure curve for zero mean stress and the dotted line is the curve adjusted in accordance with Eq. (4). A single design curve is used for carbon and low-alloy steel below 80,000 psi ultimate tensile strength because, as may be noted from Fig. 10 and 11, the adjusted curves for these classes of material were nearly identical. Fig. 12 contains data on austenitic steels and other alloys which were not available when the original design curve was published.

For the case of high-strength, heat-treated, bolting materials, the heat treatment increases the yield strength of the material much more than it increases either the ultimate strength, S_u, or the fatigue limit, S_N. Inspection of (4) shows that for such cases, S_N becomes a small fraction of S_N and thus the correction for the maximum effect of mean stress becomes unduly conservative.

Test data indicate that use of the Peterson cubic equation

$$S_{eq} = \frac{7S_a}{8 - \left(1 + \frac{S_{mean}}{S_a}\right)^3}$$

results in an improved method for high strength bolting materials, and this equation has been used in preparing design fatigue curves for such bolts [16].

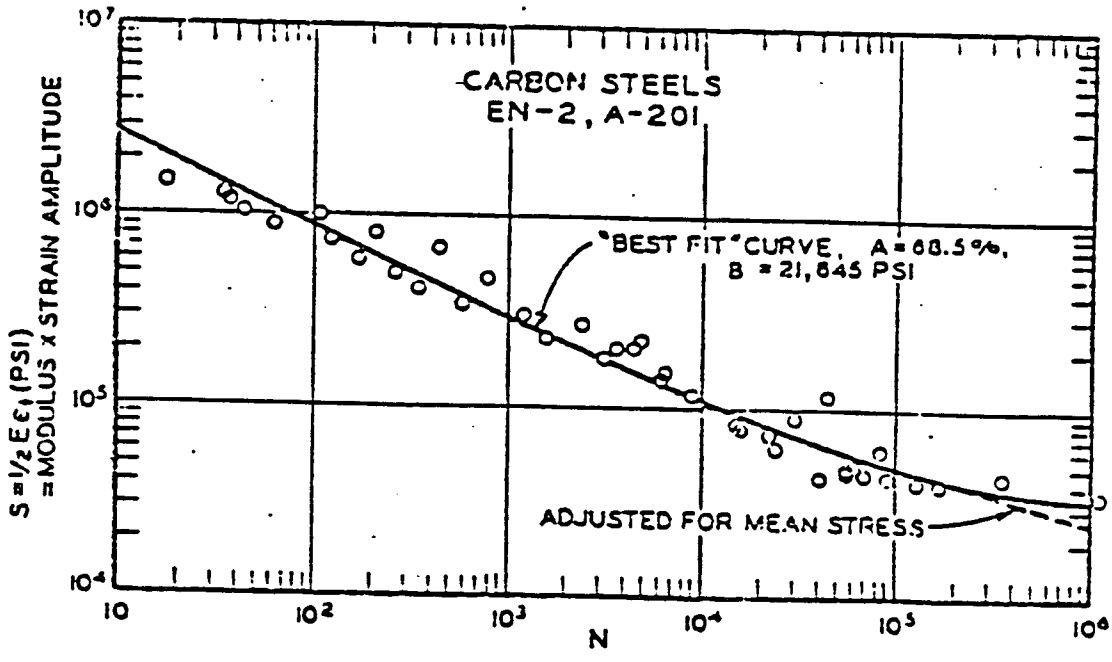

FIGURE 10. FATIGUE DATA - CARBON STEELS

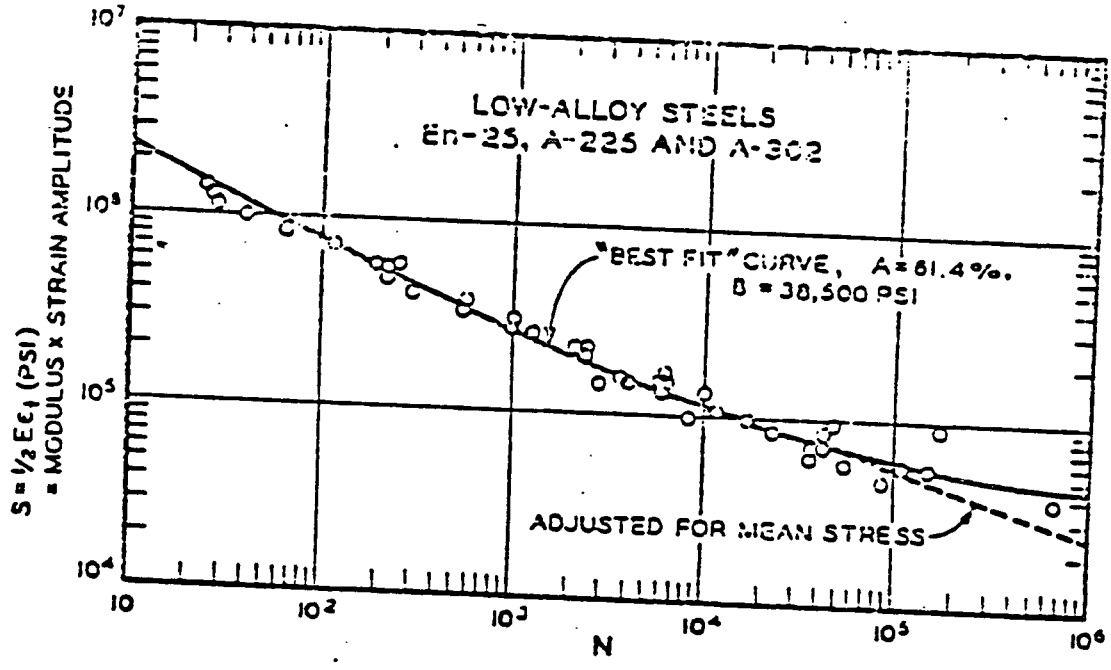

FIGURE 11. FATIGUE DATA - LOW ALLOY STEELS

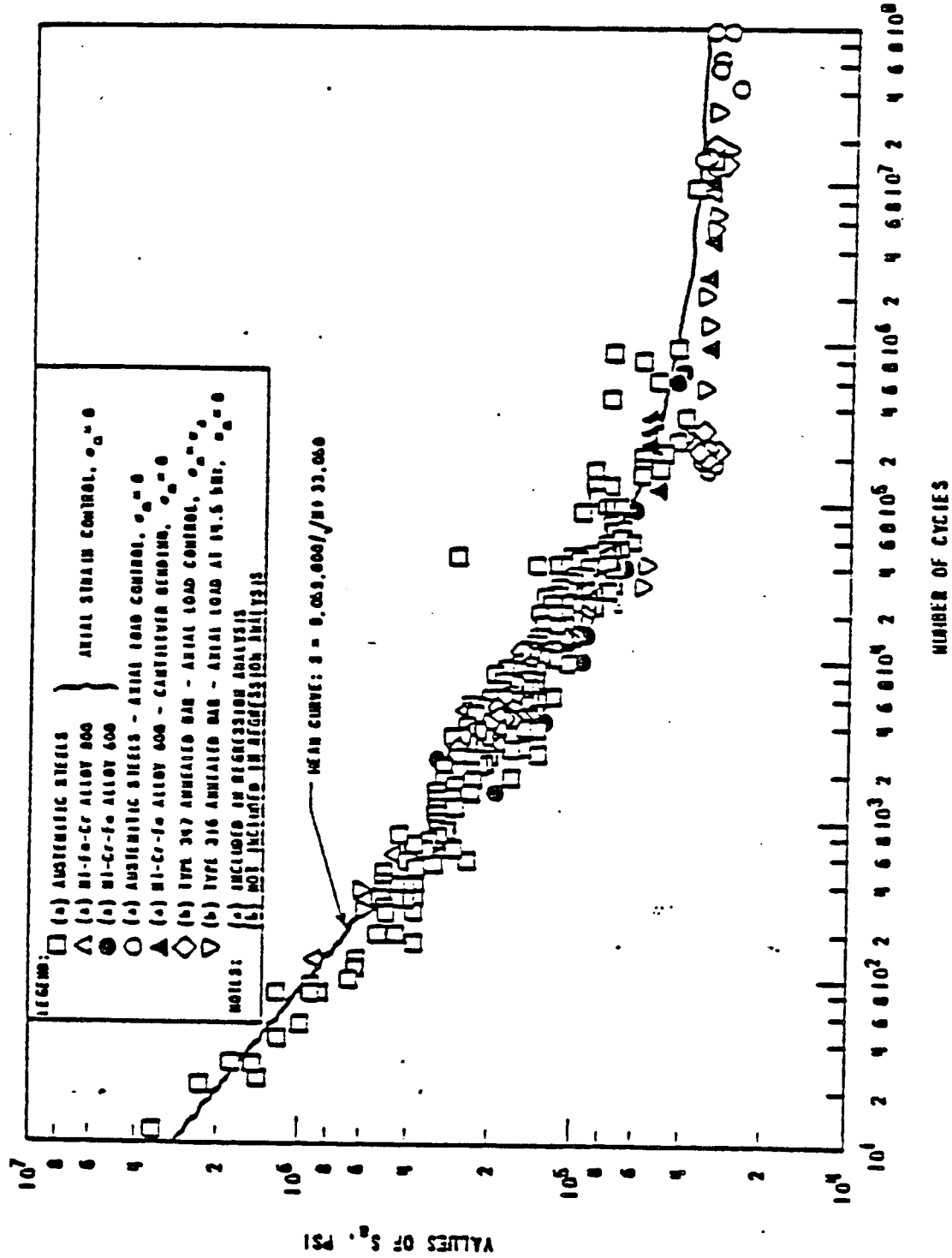

FIGURE 12. FATIGUE DATA FOR AUSTENITIC STEELS, NICKEL-IRON-CHROMIUM ALLOY 800, AND NICKEL-CHROMIUM-IRON ALLOY 600.

High Cycle Fatigue

Three fatigue curves (A, B, and C) are provided in Section III and Section VIII, Division 2 for Austinetic Steels, Nickel-Chromium-Iron Alloy, Nickel-Iron-Chromium Alloy and Nickel-Copper Alloy in the range of 10^6 to 10^{11} cycles.

Curve A is derived from the basic code equation

$$S = 9{,}159{,}000 \sqrt{N_f} + 47{,}350 \text{ psi} \qquad (6)$$

using reduction factors of 20 on cycles or 2 on stress and for a modulus of 28.3 x 10^6 psi. It is applicable for an elastic analysis when the stress ($P_L + P_B + Q$) range is less than 27,000 psi or for an inelastic analysis (independent of stress). By limiting the primary stress range, the major loading is under strain control and the residual stresses and mean strains induced by prior straining are reduced without significant damage and long life is achieved under stable inelastic strain.

Curve B is based on one-half of the average fatigue strength data for load controlled tests at 10^8 cycles. This curve is also the value of equivalent alternating stress for zero mean load in the code calculation of the reduced allowable alternating stress when mean loads are applied. Curve B is used for an elastic analysis for weld metal and heat affected zones when the major loading is strain controlled and the stress ($P_L + P_B + Q$) range is less than 27,200 psi or for an inelastic analysis.

Curve C is derived from Curve B using the maximum mean stress that can be retained under combined mean strain and alternating stress. It is applicable for an elastic analysis when the stress ($P_L + P_B + Q$) range is greater than 27,200 psi and the major loading is stress controlled. It is applicable to base metal, welds, and heat affected zones.

Procedure for Fatigue Evaluation

The step-by-step procedure for determining whether or not the fluctuation of stresses at a given point is acceptable is given in detail in Par. NB-3222.4 of Section III and Appendix 5 of Section VIII, Division 2. The procedure is based on the maximum shear stress theory of failure and consists of finding the amplitude (half full range) through which the maximum shear stress fluctuates. Just as in the case of the basic stress limits, the stress differences and stress intensities (twice maximum shear stress) are used in place of the shear stress itself.

At each point on the vessel at any given time there are three principal stresses, σ_1, σ_2, and σ_3 and three stress differences, S_{12}, S_{23}, and S_{31}. The stress intensity is the largest of the three stress differences and is usually considered to have no direction or sign, just as for the strain energy of distortion. When considering fluctuating stresses, however, this concept of non-directionality can lead to errors when the sign of the shear stress changes during the cycle.

Therefore, the range of fluctuation must be determined from the difference in the values of the six stress components σ_t, σ_l, σ_r, τ_{lt}, τ_{lr}, and τ_{rt} at any two points in time. Let prime components denote the difference between stress components at the two points in time, e.g., $\sigma'_t = \sigma_{t1} - \sigma_{t2}$. Then a set of principal stress intensity ranges (σ'_1, σ'_2, and σ'_3) is calculated from the differences in the six stress components at the two points in time (σ'_t, σ'_l, σ'_r, τ'_{lt}, τ'_{lr}, and τ'_{rt}). The alternating stress intensity, S_{alt}, is one-half of the largest absolute magnitude of the stress differences; i.e., of $S'_{12} = \sigma'_1 - \sigma'_2$, $S'_{23} = \sigma'_2 - \sigma'_3$, and $S'_{13} = \sigma'_3 - \sigma'_1$. It is recognized that the directions of the principal stresses may change between the two points in time. This feature of being able to maintain directionality and thus find the algebraic range of fluctuation is one reason why the maximum shear stress theory rather than the strain energy of distortion theory was chosen.

When the directions of the principal stresses change during the cycle (regardless of whether the stress differences change sign), the non-directional strain energy of distortion theory breaks down completely. This has been demonstrated experimentally by Findley and his associates [11] who produce fatigue failures in a rotating specimen compressed across a diameter. The load was fixed while the specimen rotated. Thus the principal stresses rotated but the strain energy of distortion remained constant. The procedure outlined in NB-3216.2 of Section III-1 and 5-110.3(b) of Section VIII, Division 2, is consistent with the results of Findley's tests and uses the range of shear stress on a fixed plane as the criterion of failure. The procedure brings in the effect of rotation of the principal stresses by considering only the changes in shear stress which occur in each plant between the two extremes of the stress cycle.

Cumulative Damage

In many cases a point on a vessel will be subjected to a variety of stress-cycles during its lifetime. Some of these cycles will have amplitudes below the endurance limit of the material and some will have amplitudes of varying amounts above

the endurance limit. The cumulative effect of these various cycles is evaluated by means of a linear damage relationship in which it is assumed that, if N cycles would produce failure at a stress level S_1, then n_1 cycles at the same stress level would use up the fraction n_1/N_1 of the total life. Failure occurs when the cumulative usage factor, which is the sum $n_1/N_1 + n_2/N_2 + n_3/N_3 + \ldots$ is equal to 1.0. Other hypotheses for estimating cumulative fatigue damage have been proposed and some have been shown to be more accurate than the linear damage assumption. Better accuracy could be obtained, however, only if the sequence of the stress cycles were known in considerable detail, and this information is not apt to be known with any certainty at the time the vessel is being designed. Tests have shown [6] that the linear assumption is quite good when cycles of large and small stress magnitude are fairly evenly distributed throughout the life of the member, and therefore this assumption was considered to cover the majority of cases with sufficient accuracy. It is of interest to not that a concentration of the larger stress cycles near the beginning of life tends to accelerate failure, whereas if the smaller stresses are applied first and followed by progressively higher stresses, the cumulative usage factor can be "coaxed" up to a value as high as 4 or 5.

When stress cycles of various frequencies are intermixed through the life of the vessel, it is important to identify correctly the range and number of repetitions of each type of cycle. It must be remembered that a small increase in stress range can produce a large decrease in fatigue life, and this relationship varies for different portions of the fatigue curve. Therefore the effect of superposing two stress amplitudes cannot be evaluated by adding the usage factors obtained from each amplitude by itself. The stresses must be added before calculating the usage factors. Consider, for example, the case of a thermal transient which occurs in a pressurized vessel. Suppose that at a given point the pressure stress is 20,000 psi tension and the added stress from the thermal transient is 70,000 psi tension. If the thermal cycle occurs 10,000 times during the design life and the vessel is pressurized 1000 times, the usage factor should be based on 1000 cycles with a range from zero to 90,000 psi and 9000 cycles with a range from 20,000 psi to 90,000 psi. Another example is given in NB-3222.4(e)(5).

Fatigue Analysis for Primary Plus Secondary Stress $> 3S_m$

One of the principal reasons for the $3S_m$ limitation on primary-plus-secondary stress is to assure shakedown to elastic action. If shakedown is not achieved, the fatigue analysis procedure becomes questionable. Cases arise in which the $3S_m$ limit is exceeded, but the application is quite safe for

limited numbers of cycles. NB-3228.3 gives a procedure for allowing primary-plus-secondary stress to exceed $3S_m$ but assuring safety by taking a penalty on the fatigue analysis. This procedure had its origin in the development of detailed stress analysis for nuclear power piping components under the former USAS B31.7 Nuclear Power Piping Code. In the process of

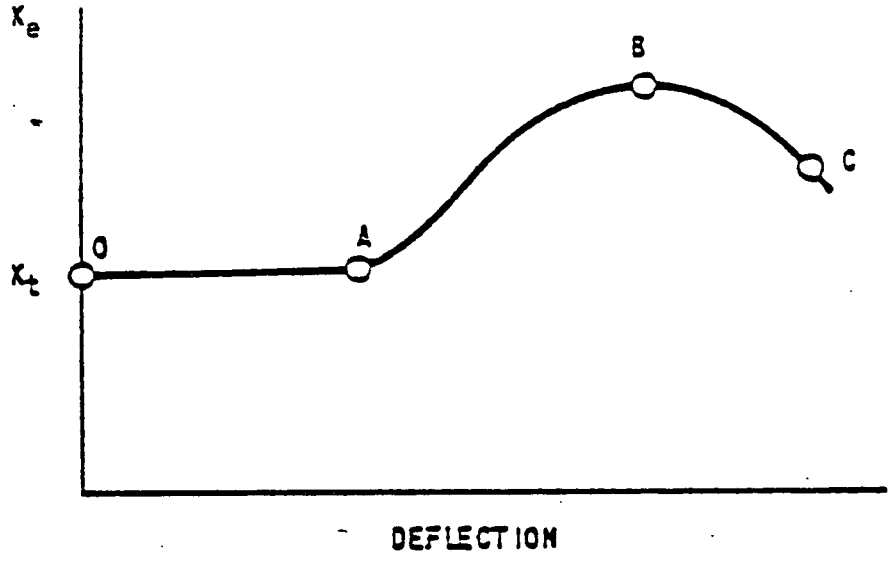

FIGURE 13

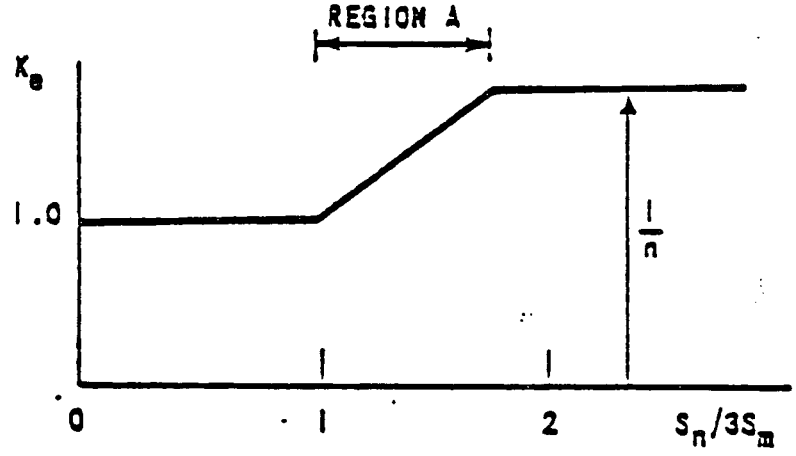

FIGURE 14

developing that code, the frequently occurring large primary-plus-secondary stresses which result in piping components gave need for a simplified procedure to evaluate these effects. A detailed procedure was implemented into the B31.7 code and referenced by ASME Paper 68-PVP-3, listed as Reference 19. This development relied on tests of notched bar specimens which measured the strain concentrating effect when the $3S_m$ limit was exceeded. Although it was generally agreed that the recommended procedures presented in this paper were safe and conservative by those who reviewed them in detail, further developments of simplified formulas occurred when the piping code was combined into III-1. Due to the complexity of the elastic-plastic behavior, no simple formula could be developed which would accurately represent the entire phenomenon.

In simple terms, the strain concentration phenomenon which occurs is illustrated by Figure 13. Here we see a plot of the peak strain concentration factor in either a notched member or a member with some other type of stress concentration. The peak strain concentration remains constant from Ø to A where the material behavior is perfectly elastic. At Point A, the strain concentration begins to exceed the elastic stress concentration, K_t, and continues to rise until some Point B is reached at which a maximum strain concentration occurs.

If deflection is continued, the strain concentration begins to drop off as shown in Point C. Langer, in Reference 20, has estimated the generalized maximum strain concentration which can occur at a point such as B. He illustrates that the strain concentration factor K_e is approximately 1/n, where n is the strain hardening exponent of the material. This maximum value of strain concentration is the basis for the assumed shape of the K_e correction factor which appears in the Code. The specific Code formula is

$$
(1) \qquad
\begin{cases}
K_e = 1.0 & (Sn < 3Sm) \\
K_e = 1.0 + \dfrac{1-n}{n(m-1)}\left(\dfrac{Sn}{3Sm} - 1\right) & (3Sm < Sn < 3mSm) \\
K_e = \dfrac{1}{n} & (Sn > 3mSn)
\end{cases}
$$

This equation quantitatively expresses this strain concentration and contains two materials terms, n and m. The m term was introduced into the formula in order to produce any desired slope on the K_e factor in region A of Figure 14. Thus, the form of equation 1 was selected in order to provide two features: 1) a maximum correction for the strain concentration of 1/n and, 2) any experimentally observed slope of the K_e correction in region A. While the strain-hardening

exponent n is easily obtained for the static case by measuring the uniform elongation at maximum load during the tensile test, such values of n may not reflect accurately the behavior which occurs in a fatigue situation. Therefore, the values of n which appear in the Code for this procedure are only approximate values of the strain-hardening exponent as compared with those from a tensile test. There is no straightforward method for measuring m without using the results of fatigue tests. The method which was used to establish the validity of the correction factor K_e supplied by equation 1 for specific m and n values was through comparison with fatigue test results. Other methods are possible, but a standard method has not been developed at the present time. Numerous fatigue tests have been run and the results of these tests have been published and have demonstrated that the correction predicted is conservative for use with the Code.

References 21 through 26 illustrate some of the sources of verifying the current elastic-plastic design formulas. For example, Figure 15 of Reference 22 (reproduced here as Figure 15) shows a direct comparison between the strain concentration factors used in the Code and the values obtained from tests on type 304 stainless steel. In the original concept of the elastic-plastic correction as presented in Reference 23, a limit of 2500 cycles is suggested below which no specific account was required to assure that ratcheting would be negligible. The current rules of III-1 have no such limitations; however, it should be noted that in NB-3223.3, Paragraph (a), a range of primary plus secondary membrane bending stress intensity excluding thermal bending stresses must always be less than 3Sm.

Paragraph (d) requires that the through wall thermal gradient effects meet the requirements of NB-3222.5 for ratcheting due to pressure and thermal effects. In addition, the values of the K_e factor drastically reduce the allowable fatigue life cycles. Satisfying these requirements provides assurance that a negligible amount of ratcheting can occur; therefore, no special requirement for limiting cycles due to ratcheting is necessary.

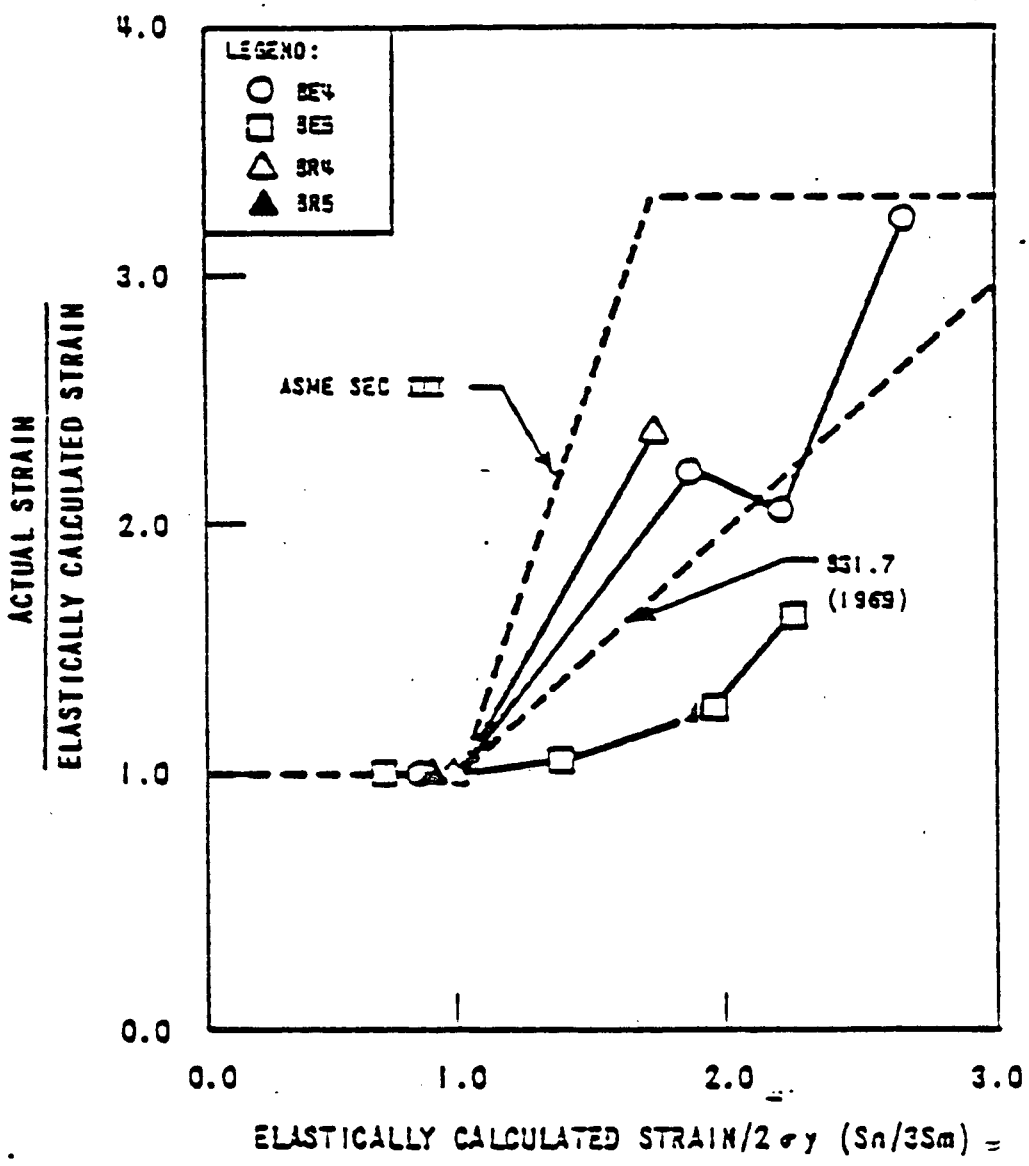

FIGURE 15. COEFFICIENT FOR MODIFYING ELASTICALLY CALCULATED STRAIN (FROM REFERENCE 22)

Exemption from Fatigue Analysis

The fatigue analysis of a vessel is quite apt to be one of the most laborious and time-consuming parts of the design procedure and this engineering effort is not warranted for vessels which are not subjected to cyclic operation. However, there is no obvious borderline between cyclic and non-cyclic operation. No operation is completely non-cyclic, since startup and shutdown is itself a cycle. Therefore, fatigue cannot be completely ignored, but NB-32222.4 (d) and AD-160 give rules which may be used to justify the by-passing of the detailed fatigue analysis for vessels in which the danger of fatigue failure is remote. The application of these rules requires only that the designer know the specified pressure fluctuations, the full range of mechanical loads, and that he have some knowledge of the temperature differences which will exist between different points in the vessel. He does not need to determine stress concentration factors or to calculate cyclic thermal stress ranges. He must, however, be sure that the basic stress limits of NB-3221 and NB-3222 or of 4-131 to 4-134 are met, which may involve some calculation of the most severe thermal stresses.

The rules for exemption from fatigue analysis are based on a set of assumptions which provide for an overall conservative design and have been proved in practice. These assumptions are:

1. The worst geometrical stress concentration factor to be considered is 2. This assumption is unconservative since K = 4 is specified for some geometrics.

2. The concentration factor of 2 occurs at a point where the nominal stress is $3S_m$, the highest allowable value of primary-plus-secondary stress. This is a conservative assumption. The net result of assumptions 1 and 2 is that the peak stress due to pressure is assumed to be $6S_m$, which appears to be a safe assumption for a good design.

3. All significant pressure cycles and thermal cycles have the same stress range as the most severe cycle. This is a highly conservative assumption. (A "significant" cycle is defined as one which produces a stress amplitude higher than the fatigue strength at 10^6 cycles).

4. The highest stress produced by a pressure cycle does not coincide with the highest stress produced by a thermal cycle. This is unconservative and must be balanced against the conservatism of assumption 3.

5. The calculated stress produced by a temperature difference ΔT between two points does not exceed $2E\alpha\Delta T$, but the peak stress is raised to $4E\alpha\Delta T$ because of the assumption that a K value of 2 is present. This assumption is conservative, as evidenced by the following examples of thermal stress:

   a. For the case of a linear thermal gradient through the thickness of a vessel wall, if the temperature difference between the inside and the outside of the wall is ΔT, the stress is

$$= \frac{E \alpha_{\lambda}^{\Delta} T}{2(1-\nu)} = .715\ E\alpha\Delta T \quad (\text{for } \nu = 0.3)$$

   b. When a vessel wall is subjected to a sudden change of temperature, ΔT, so that the temperature change only penetrates a short distance into the wall thickness, the maximum thermal stress is

$$= \frac{E\alpha\Delta T}{1-\nu} = 1.43\ E\alpha\Delta T \quad (\text{for } \nu = 0.3)$$

   c. When the average temperature of a nozzle is ΔT degrees different from that of the rigid wall to which it is attached, the upper limit to the magnitude of the discontinuity stress is

$$= 1.83\ E\alpha\Delta T \quad (\text{for } \nu = 0.3).$$

   Thus the coefficient of $E\alpha\Delta T$ is always less than the assumed value of 2.0

When the two points in the vessel whose temperatures differ by ΔT are separated from each other by more than $2\sqrt{Rt}$, there is sufficient flexibility between the two points to produce a significant reduction in thermal stress. Therefore only temperature differences between "adjacent" points need be considered.

Section VIII, Division 2 also provides the rules for exemption from fatigue analysis as does Section III and, in addition, provides even simpler and more conservative rules applicable to vessels made of materials which have a specified minimum tensile strength at room temperature not exceeding 80,000 psi.

Experimental Verification of Design Fatigue Curves

The design fatigue curves are based primarily on strain-controlled fatigue tests of small polished specimens. A best-fit to the experimental data was obtained by applying the method of least squares to the logarithms of the experimental values. The design stress values were obtained from the best-fit curves by applying a factor of two on stress or a factor of twenty on cycles, whichever was more conservative at each point. These factors were intended to cover such effects as environment, size effect, and scatter of data.

Since the original publication of the design fatigue curves in Section III, various tests and studies have been conducted to find whether or not the design curves, developed from small laboratory specimens, could be used to design components and could be used with confidence. It was found that the curves can be used safely provided two possible misapplications are avoided.

1. The designer must be careful not to apply the curves to a situation where shakedown is not achieved unless the proper fatigue correction factors described in NB-3228.3 are used.

2. The designer must be sure that the calculated stress used to enter the design curve is really the highest stress which exists in the structure.

The appropriateness of the fatigue design curves for pressure vessels has been demonstrated by tests conducted by the Pressure Vessel Research Committee [27, 29]. In these tests 12-inch diameter model vessels and 3-foot diameter full-size vessels were tested by cyclic pressurization after a comprehensive strain gage survey was made of the peak stresses. Fig. 16 shows a summary of the PVRC test results compared to the recommended design fatigue curve of Section III and Section VIII, Division 2 for carbon and low-alloy steel. It may be seen that no crack initiation was detected at any stress level below the allowable stress, and no crack progressed through a vessel wall in less than three times the allowable number of cycles. In these tests the membrane stress in the vessel walls was up to the yield stress (above Code limits) of the material and the life factor undoubtedly was reduced by lack of complete shutdown. Greater conservatism is indicated from tests in which the membrane stress was within the Code limits.

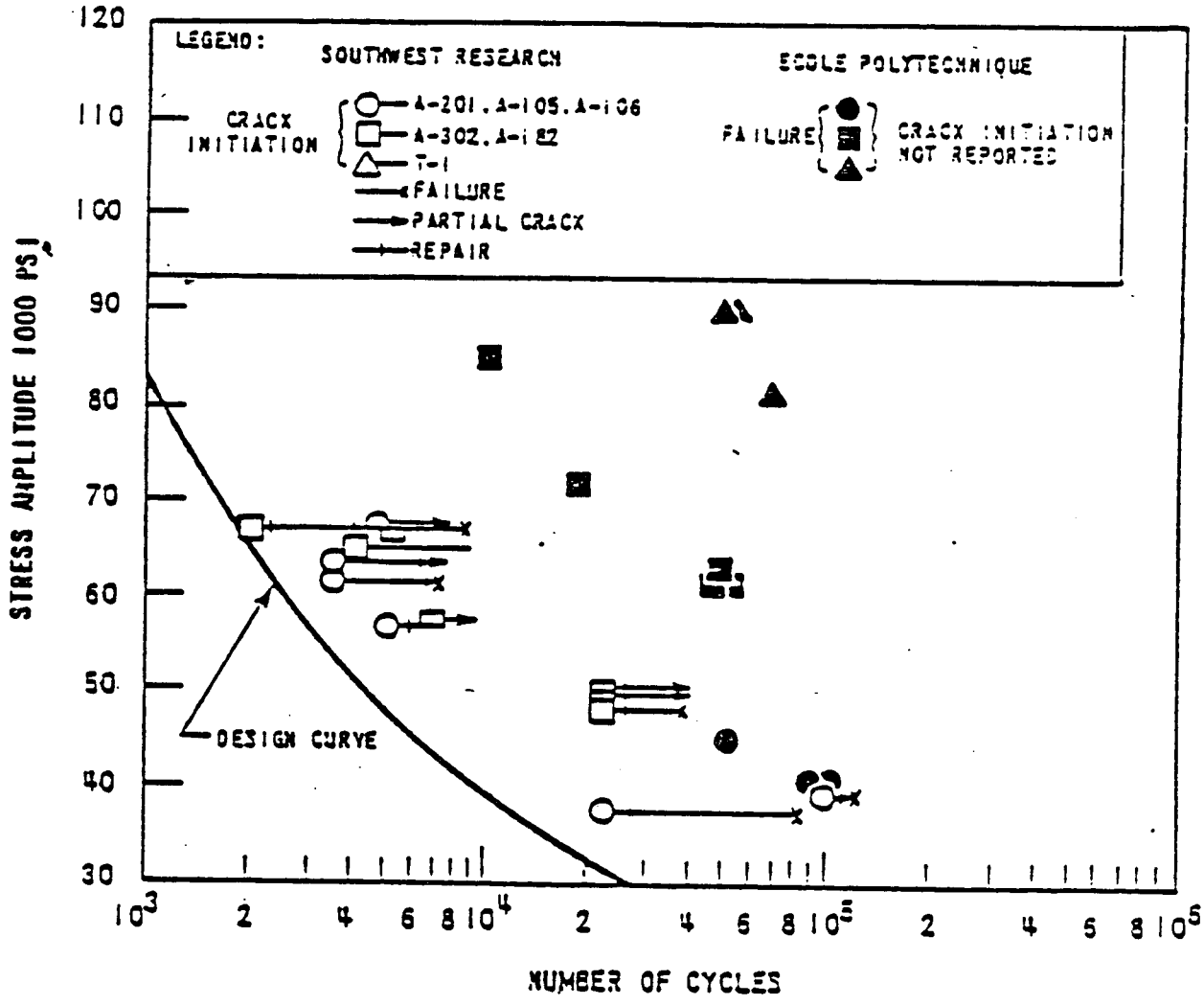

FIGURE 16. PVRC FATIGUE TESTS

Another extensive series of pressure-cycling tests was that performed by the British Welding Research Association (29) on 20-inch diameter vessels one inch thick. The primary purpose of these tests was to find the comparative fatigue strengths of various non-integral type nozzle reinforcements. Figure 17 summarizes the results. The stresses plotted here are from strain gages on the inner surface of the vessel measuring hoop stress at the crotch formed by the intersection of the nozzle opening and the vessel. In the majority of tests this crotch stress was the one which produced the final failure, and these test points plot in a narrow band closely related to the test results from plain plate specimens. In some tests, however, notably series 11, failure occurred at the periphery of a reinforcing pad, where the stress was higher than at the crotch due to the sharp change in profile at the fillet weld.

Another series of tests aimed specifically at validating the design curves for piping design is described in Reference 30. The 28 piping components tested included girth welds, elbows and tees at room temperature and 550'F. The materials were carbon steel, type 304 stainless steel and 2 1/4 CR-1 Mo steel. The test results were compared to the design procedures specified in NB-3653.6 of Section III (Simplified Elastic-Plastic Discontinuity Analysis). The overall conclusion was "that the Code rules are adequately conservative, particularly at the highest stress conditions."

The tests of References 27 through 30 indicate that the ASME design curve is a sound guide as long as the peak stress is estimated with sufficient care and at the correct location.

These factors of 2 on stress and 20 on cycles are needed to cover a variety of differences between practical components and laboratory fatigue specimens, including undetected defects. It is important to note, however, that even though all the tested components were manufactured with no more than ordinary care and good workmanship, most failures were the result of the configurations and were caused by predictable stresses, not by small defects which eluded the available inspection techniques.

FIGURE 17

A.S.M.E. DESIGN CURVE
LEGEND:
SERIES 7
SERIES 8
SERIES 8a
SERIES 9
SERIES 10
SERIES 11
SERIES 12
PLAIN PLATE
NOT FAILED
SOLID POINTS DENOTE RADIAL FAILURES AT CROTCH
OPEN POINTS DENOTE OTHER TYPES OF FAILURE
CROTCH MAX MEASURED STRESS RANGE (ton/in²)
60
40
30
20
10
0
10³ 2 4 6 8 10⁴ 2 4 6 8 10⁵ 2 4 6 8 10⁶ 2 4 6 8 10⁷
NUMBER OF PRESSURE APPLICATIONS TO FAILURE

IV. SPECIAL STRESS LIMITS

Paragraph NB-3227 of Section III contains special stress limits. These deviations from the basic stress limits are provided to cover special Service Loadings or configurations. Some of these deviations are more restrictive, and some are less restrictive, than the basic limits. In cases of conflicts the optical stress limits take precendence for the particular situations to which they apply.

The Service Loadings and Configurations addressed by the special limits include:

(a) Provisions for modifying the stress limits for Bearing Loads relative to the distance of the point of load application to a free edge (NB-3227).;
(b) Special stress limits for cross sections loaded in pure shear (NB-3227.2);
(c) Requirements to prevent progressive distortion on non-integral connections (NB-3227.3);
(d) A limit on the sum of the principal stresses (NB-3227.4);
(e) Special rules to be applied at the transition between a vessel nozzle and the attached piping (NB-3227.5);
(f) A modified Poissons` ratio value to be used when computing local thermal stresses (NB-3227.6);
(g) Special rules to be applied to welded seals such as omega and canopy seals (NB-3227.7).

The consideration with regard to bearing loads in Item (a) is that the material does not permanently deform such that bolted closures or other similar configurations can become loose during operation. The limit of 5y on the bearing stress precludes permanent deformation. The limit of 1.5 5y on the bearing stress for locations away from edges restricts permanent deformation to acceptable values due to the restraint of adjacent material.

Item (b), which addresses sections loaded in pure shear, is a modification which takes advantage of the more accurate Von Mises criterion instead of the maximum shear stress theory. In addition, the linear variation of torsional shear stress on solid circular sections is considered through the limit of Ø.85m.

The requirements for non-integral connections referred to by Item (c) reflect the concern that these connections could be disengaged as a result of progressive distortion (ratchetting). By limiting the primary plus secondary stress intensities to 5y, this potential condition is avoided since the original relationship of the mating parts is maintained on each new cycle.

Item (d) is included since the "stress intensity" limit used in the code is based upon the maximum shear stress criterion, there is no limit on the "hydrostatic" component of the stress. Therefore, the triaxial stress limit on the algebraic sum of the three principal stresses is required for completeness.

Item (e) is included to maintain an added degree of structural integrity in the vessel when subjected to external loads. Its purpose is to ensure that no yielding can be forced upon the vessel by the piping.

The requirements incorporated by the provisions of Item (f), relative to the Poisson's ratio value, recognize that when the maximum stress is calculated on an elastic basis, it may exceed the yield strength of the material. Since the limit of $3S_m$ (NB-3222.2) ensures shakedown, elastic cycling will result except in regions containing significant local structural discontinuities or local thermal stresses. Therefore, in evaluating the local thermal stress, the Code requires the use of a modified Poisson's ratio value to properly consider the total strain.

Specially designed welded seals as referenced in Item (g) are given special stress limits to recognize that they are designed as membranes with strength being provided by a separate device such as a bolted joint.

Thermal Stress Ratcheting

In addition to the Special Stress Limit just described, there are other special requirements defined in paragraph NB-3222.5 to address the problem of thermal stress ratchetting. As previously discussed, the basic stress limits of the Code for primary and secondary stress ranges are designed to cause shakedown to elastic action in a relatively few cycles. If either or both of these exceed their limiting values, then shakedown to elastic action may not take place. Instead, some increment of plastic deformation will be experienced on cycles subsequent to the initial cycle, in one of two ways. Either, (i) the magnitude of the increment of plastic deformation will decrease with each subsequent cycle, and will eventually cease; or, (ii) the magnitude of the increment of plastic deformation will remain substantially constant with each subsequent cycle, resulting in a more-or-less monotonic accumulation of plastic strain. The first of these two states is referred to as plastic strain cycling, and leads eventually to shakedown. The second of these states is referred to as ratcheting.

Miller, in a pioneering paper on the ratchet mechanism in 1959[31], used a one-dimensional elastic-perfectly-plastic model to define simple criteria for establishing the limiting values of primary and secondary stresses which determine whether shakedown to elastic action will occur. Miller showed that four "regimes" of behavior could be defined, as follows (see Figure 18).

1. Elastic Regime (no plastic yielding). In this regime all deformations resulting from loads are elastic, and no plastic action is experienced. Hence ratcheting cannot occur.

2. Shakedown Regime (plastic flow on initial cycle only). This regime is defined by the "shakedown theorem" of plasticity, which states that shakedown will occur if and only if a state of residual stress can be found such that superposition of the applied cycles of load and temperature upon this state of residual stress nowhere leads to an extension of the yield surface. It is characterized by plastic flow on the initial loading cycle, with purely elastic action taking place during each subsequent cycle.

3. Plastic Cycling Regime (plastic flow with each cycle, but no ratcheting). Plastic flow occurs on each cycle, but the magnitude of the increment of plastic strain decreases with each cycle, and finally ceases. Upon cessation of plastic strain incrementation, shakedown is achieved.

4. Ratcheting Regime (monotonic incremental distortion). Ratcheting is characterized by a monotonic plastic deformation resulting from the succesive application of cyclic loads superimposed upon a steady-state (primary) load. Plastic flow occurs as the cyclic load is applied, followed by only a partial strain reversal during unloading, resulting in a monotonic accumulation of plastic strain.

Miller and Bree[32] have shown that the boundaries of these stress regimes, utilizing the one-dimensional elastic-perfectly-plastic (Figure 18) can be defined by the following criteria.

FIGURE 18 STRESS REGIMES FOR ONE-DIMENSIONAL ELASTIC-PERFECTLY-PLASTIC MODEL

The Elastic Regime is defined by

$$\frac{\sigma_m}{\sigma_y} + \frac{\sigma_t}{\sigma_y} \leq 1$$

Where, σ_m = membrane stress developed by primary load

σ_t = thermal stress resulting from linear temperature gradient across wall thickness (see Figure I-2.3)

σ_y = yield strength of material at mean temperature

The Shakedown Regime is bounded by

$$\frac{\sigma_m}{\sigma_y} + \frac{\sigma_t}{4\sigma_y} = 1, \text{ when } \frac{\sigma_m}{\sigma_y} > 0.5$$

$$\frac{\sigma_t}{\sigma_y} = 2, \text{ when } \frac{\sigma_m}{\sigma_y} < 0.5$$

The Plastic Cycling Regime is bounded by

$$\frac{\sigma_m \sigma_t}{\sigma_{y^2}} = 1, \text{ and } \frac{\sigma_m}{\sigma_y} < 0.5$$

The Ratcheting Regime exists outside the bounds established by the criteria of the above equations. These criteria are readily verified by reference to Bree .

The Code rules are established to keep the material in the shakedown or elastic regimes for the cases of linear or parabolic temperature distributions. The Code rules are also written to consider the effects of strain hardening or strain softening, in the case of a large number of cycles.

V. CREEP AND STRESS RUPTURE

It is an observed characteristic of pressure vessel materials that in service above a certain temperature, which varies with the alloy composition, the materials undergo a continuing deformation (creep) at a rate which is strongly influenced by both stress and temperature. In order to prevent excessive deformation and possible premature rupture it is necessary to limit the allowable stresses by additional criteria on creep-rate and stress-rupture. In this creep range of temperatures these criteria may limit the allowable stress to substantially lower values than those suggested by the usual factors on short time tensile and yield strengths.

Code (ANSI B31.1), which extends into elevated temperature application, gives allowable values for the thermal stresses which are produced by expansion of piping systems and varies the allowable stresses with the number of expected cycles. However, a complete evaluation of localized and combined peak stresses and associated fatigue life assessment is not required.

As discussed herein, the Code Committee recognized that additional design considerations and rules were desired for nuclear components. These components would be exposed to severe service conditions (e.g., highly cyclic loadings, recurring severe thermal shocks) where superior reliability was required to offset potentially serious consequences of failure. These needs led to the preparation of the design rules in Section III, Division 1. Rules to account for creep, stress-rupture, or other time-independent failure modes were not included in Section III.

After rules in Section III were initially developed for low-temperature design, there was an effort to extend the rules to elevated temperature design. By 1963, the first version of Case 1331 was approved. Subsequent versions of Case 1331 appeared, but it was not until 1971 and Case 1331-5 that extensive rules and limits were given to address the additional failure modes associated with elevated temperature operation. Additions and improvements led to the -6, -7 -8 versions of Case 1331. With the further preparation of rules for use in elevated temperature construction, the Code Case for elevated temperature design was changed to Case 1592, and subsequently to N-47.

Experience in performing stress analysis of nuclear power plant components in accordance with the ASME Code Cases for elevated temperature service indicated the need for a document, similar to this one, to provide the background criteria for the rules of these Code Cases. Accordingly, in 1976, the ASME published the "Criteria for Design of Elevated Temperature Class 1 Components in Section III, Division 1, of the ASME Boiler and

Pressure Vessel Code". This publication sets forth the criteria, reasoning, and supporting data for existing rules for design of Class 1 pressure boundaries of components intended for elevated temperature service. The term elevated temperature refers to temperatures that exceed those for which allowable stress values are given in Section III. The key consideration that sets the high temperature rules apart from the Section III, Subsection NB (Class 1) design rules is creep effects. Unlike Subsection NB design rules, which primarily guard against time-independent failure modes, the elevated temperature rules are applicable for service conditions where creep and other time-dependent effects are significant.

In nonnuclear applications, the design of pressure boundary components for elevated temperature service dates back forth five years. Over those years, vessels designed by the rules of Section I (Power Boilers) and Section VIII, Division 1 (Pressure Vessels) of the ASME Code have established a record of successful elevated temperature operation.

This success is due to a combination of factors: (1) the ease of inservice inspection for such vessels has made it possible to detect incipient failure conditions before gross failure could occur, (2) the variety of operating and environmental conditions have been successfully addressed outside the Code rules by individual engineering effort, and (3) the Code design rules have required extra wall thickness for service where creep phenomena are significant.

In Section IO and Section VIII, Division 1, the design rules employ allowable stress criteria which utilize creep rate and stress-rupture properties in addition to short-term tensile strength properties. However, these Sections doe not have mandatory requirements for a detailed stress analysis but set the wall thickness necessary to keep the basic hoop stress below the tabulated allowable stress, and they rely on the design rules for details and the design factor to hold secondary bending and high localized stresses at a safe level consistent with experience. Even through these Sections employ criteria based on the average stress to provide a creep rate of 0.01% per 1000 hr and the average and minimum stress to produce rupture in 10^5 hr, it is not to be inferred that 10^5 hr (or any definite interval) is the intended design life for such construction. The foreward to the ASME Code states that the objective of its rules "is to afford reasonably certain protection of life and property and to provide a margin for deterioration in service so as to give a reasonably long safe period of usefulness". Neither Section I or Section VIII, Division 1, have mandatory requirements for a cyclic fatigue analysis.

VI. DESIGN PHILOSOPHY FOR CLASS 2 AND 3 COMPONENTS

Division 1 of Section III includes the rules for the design and construction of nuclear pressure vessels and is subdivided into nuclear code classes 1, 2 and 3. As previously described, the design requirements for Class 1 components involve the criteria of "design by analysis" where as the design requirements for Class 2 and 3 components typically involve the criteria of design by geometric rules. Essentially, these geometric rules are based on the capacity of the vessel pressure boundary to withstand non-cyclic pressure loading and permits the establishment of the maximum allowable working pressure based solely on a pressure test. The allowance for other loads is included by incorporation of a substantial factor of safety such as in the deviation of allowable stress as being the lower of 1/4 times the ultimate tensile strength or 5/8 times the yield strength. However, it is recognized that the designer may be required to provide additional design considerations for pressure vessels to be used in severe types of service, for highly cyclic operation, for service requiring superior reliability or where periodic inspection is difficult. For these situations, an alternative to these geometric rules is provided in Subarticle NC-3200 of Section III for Class 2 vessel and involves design procedures which are based on Division 2 of Section VIII. These alternative procedures, like the Class 1 rules of Section III, invoke the maximum shear stress yield criterion, but permit the evaluation of stresses by rigorous analysis, or in specific cases, the "design by formula" approach.

As discussed in Section II of this criteria document, the components of a nuclear power plant may be subjected to a wide range of loading conditions, both anticipated and postulated, the consequences of which may vary considerable with respect to their significance to plant safety. Since 1971, the Code provided a four-tiered structure of stress limits for Class 1 components against which the stresses resulting from various loading combinations may be evaluated. These four sets of stress limits were identified as service loadings A, B, C, and D. However, no comparable foundation existed in 1971 for the evaluation of Class 2 and 3 components, although the need had long been recognized. That is, Class 2 and 3 components may be subjected to loads included in Class 1 under level C or D conditions but code design criteria did not exist. Accordingly, an ASME Task Group was appointed to formulate appropriate criteria of which the recommendations are now incorporated in Section III of the code.

The Task Group noted that existing geometric rules such as those given in Section III for Class 2 and 3 vessels were simple yet practical, and would continue to serve satisfactorily when dealing with Levels A and B service limits. However, the higher combinations of loadings associated with Levels C and D service limits would call for at least a limited amount of detailed stress analysis.

Noting that the level C and D conditions may both result in at least some local permanent deformation or distortion of the pressure boundary, the Task Group recognized that standard plant operating procedures would call for the isolation of the affected component for examination, and for its repair or replacement, as warranted. It was apparent, therefore, that no consideration of the long-term effects of such conditions was justified, and that secondary stresses due to cyclic thermal loads, and the evaluation of cumulative fatigue damage, could be ignored. Hence, in handling level C and D conditions, only the primary, load-controlled stresses would have to be controlled.

Stress categories and design practices of using geometric rules for Class 2 and Class 3 components are based for the most part on the maximum normal stress theory. It was decided in general to continue to utilize the same yield criteria and related analytical methods, on the grounds that their suitability has been amply demonstrated by successful experience; notwithstanding certain theoretical deficiencies.

From these considerations, equivalence between Class 1 concepts and Class 2 and 3 concepts were developed:

Class 1	Equivalent Class 2 and 3
P_m	σ_m
P_L	σ_L
P_b	σ_b

It should be noted that P_m, P_L and P_b are stress intensities whereas σ_m, σ_L and σ_b are simply principal stresses. One notes the absence of Class 1 stress categories Q (secondary stress) and F (peak stress). These are not included because the Task Force deemed that adequate protection against fatigue is furnished by the rules existing in the code for design conditions.

The criteria established by the Task Force is illustrated by Table VI-1.

TABLE VI-1 - BASIS STRESS LIMITS FOR CLASS 2 AND CLASS 3 COMPONENTS

Service Condition	Stress Limits[a],[b]	P_{max}[c],[d]
Level A[e]	$\sigma_m \leq 1.0S$ $(\sigma_m \text{ or } \sigma_L) + \sigma_b \leq 1.65S$	1.0P
Level B[e]	$\sigma_m \leq 1.1S$ $(\sigma_m \text{ or } \sigma_L) + \sigma_b \leq 1.65S$	1.1P
Level C	$\sigma_m \leq 1.5S$ $(\sigma_m \text{ or } \sigma_L) + \sigma_b \leq 1.8S$	1.2P
Level D	$\sigma_m \leq 2.0S$ $(\sigma_m \text{ or } \sigma_L) + \sigma_b \leq 2.4S$	1.5P

Notes

a. When applied to pumps and valves, satisfaction of these limits does not assure operability or continued function.

b. For cast items, a casting quality factor of 1.0 shall be assumed in satisfying these stress limits.

c. Applies to pumps and valves only.

d. The maximum pressure shall not exceed the tabulated factors listed under P_{max} times the design pressure of the rated pressure at the applicable operating condition temperature.

e. The potential for local or general buckling shall be considered for thin-walled vessels and tanks.

For those Class 2 vessels designed in accordance with the alternate design rule of Subarticle NC-3200, Levels B, C, and D Service Limits are handled by means of a factor, "K", applied to the basic allowable stress intensity value "S_m", while both the local primary membrane stress intensity, P_L, and the primary membrane-plus-bending stress intensity, (P_m or P_L) + P_b, are limited to 1.5 "k S_m". Applicable values of "k" for each service condition are given in Table VI-2.

A comparison between the basic stress limit factors of Table VI-1, and the corresponding limits shown in Table VI-2, shows substantial agreement with the exception of the Level D limit on primary membrane-plus-bending stress intensity, which may go to (1.5) (2.0) = 3.0 S_m. While this is higher than is otherwise permitted for other Class 2 and Class 3 components, a limit of 3.0 S_m is permitted for the primary membrane-plus-bending stress intensity in Class 1 piping by the Level D condition rules of Appendix F, when the stress intensity is calculated by equation (9) of NB-3652. In equation (9), the general membrane stress is computed as the hoop stress. Provided the same basic procedure is followed for calculating the membrane-plus-bending stress intensity in applying the above rules to NC-3200, the 3.0 S_m limit appears justifiable. Alternatively, the Level D condition rules of Appendix F should be followed in their entirety; or, a reduction in the value of the "k" factor should be considered.

TABLE VI-2

STRESS INTENSITY K-FACTORS CLASS 2 VESSELS,

ALTERNATIVE DESIGN RULES

Service Condition	k
Level A	1.0
Level B	1.1
Level C	1.2
Level D	2.0

VII. SUMMARY

The design criteria of Section III and Division 2 of Section VIII differ from those of Section I and Division 1 of Section VIII in the following respects:

a. Section III and Division 2 use the maximum shear stress (Tresca) theory of failure instead of the maximum stress theory.

b. Section III and the Appendices of Division 2 require the detailed calculation and classification of all stresses and the application of different stress limits to different classes of stress, whereas Section I and Division 1 of Section VIII give formulas for minimum allowable wall thickness.

c. Section III and Division 2 require the calculation of thermal stresses and give allowable values for them, whereas Section I and Division 1 do not.

d. Section III and Division 2 consider the possibility of fatigue failure and give rules for its prevention, whereas Section I and Division 1 do not.

The stress limits for Section III and Division 2 are intended to prevent three different types of failure, as follows:

a. Bursting and gross distortion from a single application of pressure are prevented by the limits placed on primary stresses.

b. Progressive distortion is prevented by the limits placed on primary-plus-secondary stresses. These limits assure shake-down to elastic action after a few repetitions of the loading.

c. Fatigue failure is prevented by the limits placed on peak stresses.

REFERENCES

1. "PVRC Recommendations on Toughness Requirements for Ferritic Material", Welding Research Council Bulletin 175, August 1972.

2. Criteria for Design of Elevated Temperature Class 1 Components in Section III, Division 1, of the ASME B&PV Code - ASME 1976.

3. Advances in Design for Elevated Temperature Environment - ASME 1975 (Edited by S. Y. Zamrik and R. I. Jetter).

4. W. J. O'Donnell and J. Porowski, "Upper Bounds for Accumulated Strains Due to Creep Ratcheting", ASME Trans., J. of Pressure Vessel Tech., 1975.

5. M. T. Jakub, "New Rules for Construction of Section III, Class 1 Components for Elevated Temperature Service", ASME Trans., J. of Pressure Vessel Tech., August 1976.

6. R. I. Jetter, "Elevated Temperature Design of Code Components - Design Criteria", ASME Trans., J. of Pressure Vessel Tech., August 1976.

7. B. F. Langer, "Design Values for Thermal Stress in Ductile Materials," Welding J. Res. Suppl., Vol. 37, September 1958, p. 411-s.

8. B. F. Langer, "Design of Pressure Vessels for Low-Cycle Fatigue," J. Basic Eng., Vol. 84, No. 3, September 1962, p. 389.

9. R. E. Peterson, "Stress Concentration Design Factors," John Wiley and Sons, Inc., New York, N.Y., 1953.

10. R. B. Heywood, "Designing by Photoelasticity," Chapman & Hall, Ltd., London, 1952.

11. W. N. Findley, P. N. Mathur, E. Szczepanski and A. O. Temel, "Energy Versus Stress Theories for Combined Stress - A Fatigue Experiment Using a Rotating Disk," J. Basic Eng., Vol. 83, No. 1, March 1961.

12. E. E. Baldwin, G. J. Sokol, and L. F. Coffin, Jr., "Cyclic Strain Fatigue Studies on AISI Type 347 Stainless Steel, " ASTM Proc., Vol. 57, 1957, p. 567.

13. L. F. Kooistra and M. M. Lemcoe, "Low Cycle Fatigue Research on Full-Size Pressure Vessels," Welding Res. Suppl., August 1962, p. 368-s.

14. G. Welter and J. Dubuc, "Fatigue Resistance of Simulated Nozzles in Model Pressure Vessels of T-1 Steel," Welding J. Res. Suppl., August 1962, p. 368-s.

15. C. W. Lawton, "High-temperature Low-cycle Fatigue: A Summary of Industry and Code Work," Experimental Mechanics, June, 1968, p. 264.

16. A. L. Snow, and B. F. Langer, "Low-cycle Fatigue of Large Diameter Bolts," Journal of Engineering for Industry, Vol. 89, Ser. B, No. 1, Feb., 1967, p. 53.

17. R. J. Shield and D. C. Drucker, "Design of Thin-walled Torispherical and Toriconical Pressure Vessel Heads," Journal of Applied Mechanics, Vol. 28, Ser. E., June, 1962, p. 262.

18. D. R. Miller, "Thermal-stress Ratchet Mechanism in Pressure Vessels," ASME Transactions, Vol. 81, Ser. D, No. 2, 1959.

19. S. W. Tagart, "Plastic Fatigue Analysis of Pressure Components," ASME Paper 68-PVP-3, Pressure Vessels and Piping, Design and Analysis, Vol. 1, p. 209, ASME 1972.

20. B. F. Langer, "Design-Stress Basis for Pressure Vessels," Experimental Mechanics, January 1971.

21. E. C. Rodabaugh, Phase Report No. 11-2, February 1969.

22. T. Kiss and J. Heald, "Low Cycle Fatigue of Nuclear Pipe Components," ASME Paper No. 74-PVP-5, August 1974.

23. E. Kiss, J. Heald and D. A. Hale, "Low Cycle Fatigue of Notched Prototype Piping," ASME Paper No. 71-WA/PVP-4.

24. T. L. Gerber, "Effect of Constraint and Loading Mode on Low-Cycle Fatigue Crack Initiation - Comparison with Code Design Rules," GEAP-20662, October 1974.

25. T. Udoguchi, Y. Asada, "Initiation of Low Cycle Fatigue Strength of Piping Components," Second International Conference on Pressure Vessel Technology, San Antonio, Texas, October 1973.

26. Y. Ando, G. Yagawa, O. Kawaguchi, K. Okabayashi, S. Veda, and T. Nagata, "Low Cycle Fatigue Strength of Piping Components," Second International Conference on Pressure Vessel Technology, San Antonio, Texas, October 1973.

27. L. F. Kooistra and M. M. Lemcoe, "Low Cycle Fatigue Research on Full-Size Pressure Vessels," Welding Res. Suppl., July 1962, p. 297-s.

28. G. Welter and J. Dubuc, "Fatigue Resistance of Simulated Nozzles in Model Pressure Vessels of T-1 Steel," Welding J. Res. Suppl., August 1962, p. 368-s.

29. P. H. R. Lane and R. T. Rose, "Comparative Performance of Pressure Vessel Nozzles Under Pulsating Pressure," Proceedings of Institute of Mechanical Engineers, Vol. 175, 1961.

30. J. O. Heald and E. Kiss, "Low Cycle Fatigue or Prototype Pipe Components," GEAP-10763, AEC R&D Report, January 1973.

31. MILLER PAPER

32. BREE PAPER

Enclosure 3

Additional Information
to be Provided

I. Turbine Building

1. Provide a comparison of correction factors based on the wide-band solution and on the narrow-band solution for 2% damping for the following:

Direction	Elevation	Location	Node
N - S	42'	Area 2 deck (A-53)	580, 586, 611
V	35.5'	Area 6 deck (A-60)	29, 71, 86
E - W	35.5'	Area 6 deck (A-61)	29, 71, 86

2. Provide the direct generation floor spectra ordinate, using envelope input spectra and SRSS technique combining responses generated by three orthogonal earthquake motions. For example:

$$S_{1e} = (S_{11}^2 + S_{12}^2 + S_{13}^2)^{\frac{1}{2}} \text{ for direction 1.}$$

3. Provide a comparison of 2% damping floor response spectra between the Bechtel and the IMPELL uncorrected envelope spectrum at the locations specified in item 1.

II. Reactor Building

Provide the following information:
- Structure and Soil-Foundation Model
- Dynamic Properties of Fixed-Based Structure Models
- Foundation Impedance Functions and Compliance Functions in Terms of Plots and Calculation Files
- Earthquake Time Histories
- Floor response spectra of 2% and 5% damping in terms of plots and digitized data for NS, EW and vertical direction at the steam generator compartment and at the operating deck
- Comparison between Bechtel and IMPELL results for 2% damping in terms of plots and digitized data for NS, EW, and vertical direction at the steam generator compartment and at the operating deck.